



Autoreferat

1. IMIĘ I NAZWISKO.

Danuta Kaczorek

2. POSIADANE DYPLOMY, STOPNIE NAUKOWE LUB ARTYSTYCZNE – Z PODANIEM PODMIOTU NADAJĄCEGO STOPIEŃ, ROKU ICH UZYSKANIA ORAZ TYTUŁU ROZPRAWY DOKTORSKIEJ.

Magister inżynier rolnictwa w zakresie agronomii, 3.4.1996, Katedra Gleboznawstwa, Wydział Rolniczy, Szkoła Główna Gospodarstwa Wiejskiego w Warszawie, promotor: prof. dr hab. Zbigniew Czerwinski. Wpływ procesu tworzenia się rudy darniowej na akumulację metali ciężkich.

Doktor nauk rolniczych w zakresie agronomii, 7.3.2001, Wydział Rolnictwa, Szkoła Główna Gospodarstwa Wiejskiego w Warszawie, promotor: prof. dr hab. Zbigniew Czerwinski, tytuł parcy: Skład mineralogiczny i ogólna zawartość pierwiastków w glebach z poziomami rudy darniowej.

3. INFORMACJA O DOTYCHCZASOWYM ZATRUDNIENIU W JEDNOSTKACH NAUKOWYCH LUB ARTYSTYCZNYCH.

od 1.06.2019 – na stażu naukowym w Research Area 1 "Landscape Functioning" Leibniz Centre for Agricultural Landscape Research (ZALF), Müncheberg, Germany. (SGGW-urlop bezpłatny).

Od 2004 - adiunkt w Katedrze Gleboznawstwa, Wydział Rolnictwa i Biologii, SGGW 2001-2004, asystent w Katedrze Gleboznawstwa, Wydział Rolniczy, SGGW, Warszawa. 1996–2001, studia doktoranckie na Wydziale Rolniczym, SGGW, Warszawa

4. OMÓWIENIE OSIĄGNIĘĆ, O KTÓRYCH MOWA W ART. 219 UST. 1 PKT. 2 USTAWY Z DNIA 20 LIPCA 2018 R. PRAWO O SZKOLNICTWIE WYŻSZYM I NAUCE (Dz. U. z 2021 R. POZ. 478 Z PÓŹN. ZM.).

a) tytuł osiągnięcia naukowego:

Charakterystyka i przemiany fitogenicznego krzemu (fitolitów) w glebach różnych biogeosystemów.

b) Publikacje wchodzące w skład osiągnięcia naukowego:

D. Kaczorek, Sommer M. 2004. Obieg krzemu w biogeosystemach lądowych klimatu umiarkowanego. Roczniki Gleboznawcze (Soil Science Annual). T. LV No 3, 221-230.

D. Kaczorek, D. Puppe, J. Busse, M. Sommer. 2019. Effects of phytolith distribution and characteristics on extractable silicon fractions in soils under different vegetation – An exploratory study on loess. Geoderma 356/ 113917/.

M. Sommer, H. Jochheim, A. Höhn, J. Breuer, Z. Zagorski, J. Busse, D. Barkusky, K. Meier, D. Puppe, M. Wanner, and D. Kaczorek. 2013. Si cycling in a forest biogeosystem – the importance of transient state biogenic Si pools. Biogeosciences, Volume 10, No. 7, pp 4991-5007.

D. Puppe, A. Höhn, D. Kaczorek, M. Wanner, M. Wehrhan, M. Sommer. 2017. How big is the influence of biogenic silicon pools on short-term changes in water-soluble silicon in soils? Implications from a study of a 10-year-old soil–plant system. Biogeosciences, 14, 5239–5252.

Wprowadzenie w tematykę badań

Krzem jest jednym z najbardziej rozpowszechnionych pierwiastków na kuli ziemskiej. Stanowi 26% całości skorupy ziemskiej i wchodzi w skład ponad 370 minerałów skałotwórczych. Jest jednym z podstawowych składników gleb, gdyż jest składnikiem niemal wszystkich skał macierzystych. Krzem jako drugi pod względem ilościowym pierwiastek odgrywa bardzo ważną rolę w globalnym obiegu materii. Biorąc pod uwagę całościowy proces wietrzenia krzemianów, którego intensywność jest uwarunkowana zmianami klimatu, krzem istotnie wpływa na obieg węgla w środowisku. Głównym źródłem krzemu w środowiskach morskich są procesy wietrzeniowe w biogeosystemach lądowych (Wollast, McKenzie 1983;

Treguer i in. 1995, Treuguer, Pondaven 2000, Treguer 2002, Conley 2002). Rola oceanów jako magazynu węgla współdziała z globalnym obiegiem krzemu, który wykorzystywany jest do budowy komórek przez radiolarie i okrzemki, które stanowią znaczącą część morskiej biomasy. Im więcej jest osadów na dnie mórz, tym więcej węgla wyłączonego jest z obiegu materii. Największym źródłem związków krzemu dla oceanów są spływy tego pierwiastka z lądów z wodami rzek. Przeprowadzony przez Treguer i in. (1995) bilans pokazuje, że 80% krzemu w oceanach pochodzi z rzek i w ostateczności z wietrzenia krzemianów w biogeosystemach lądowych. Z tych 80% aż 20% krzemu dostarczają rzeki klimatu umiarkowanego.

W glebach związki krzemu występują pod wieloma postaciami: w minerałach pierwotnych (krzemianach i glinokrzemianach), minerałach wtórnych (głównie minerałach ilastych) oraz w minerałach własnych krzemionkowych powstałych w warunkach pedogenezy (np. wtórny kwarc, opal). Wietrzenie krzemianów jest procesem ciągłym w środowiskach glebowych, sama pedogeneza jest jednym z ważniejszych procesów tłumaczących globalny obieg krzemu. Wietrzenie chemiczne pierwotnych i wtórnych krzemianów w glebach prowadzi do uwolnienia związków krzemu do roztworu glebowego, których stężenie może wynosić od 60-120 $\mu\text{mol}\cdot\text{l}^{-1}$ (Sommer 2002). Kwasy krzemowe w roztworze glebowym występują w formie kwasów monokrzemowych, które w procesie polimeryzacji przechodzą w kwasy polikrzemowe, a następnie mogą powstawać z nich koloidy, żele, czy wytrącenia krzemionkowe. Z żeli krzemionkowych powstawać mogą wtórne glinokrzemiany (smektyt, alofany), jak i wtórne krzemionki (opal A) (Kaczorek & Sommer 2004). Wytrącenia krzemionkowe mogą również tworzyć amorficzne otoczki na powierzchni innych ziaren mineralnych występujących w glebie (Veerhoff, 1992). Pewne ilości związków krzemu mogą być wyptukiwane z gleby wraz z wodą przesiąkającą (= desilifikacja, Anderson et al., 2000; Oliva et al., 1999).

W glebach obecny jest również krzem biogeniczny, do którego zaliczamy krzem fitogeniczny (fitolity), mikrobiologiczny i protozoiczny. Wiedza na temat wielkości, właściwości i przemian tych zasobów Si w glebach jest niewielka. Jedną z biogenicznych form Si w glebach jest Si pochodzenia roślinnego (fitolity, krzem fitogeniczny) (Alexandre i in., 1997, 2011). Kwas krzemowy, który został pobrany z roztworu glebowego (aktywnie lub pasywnie), wytrąca się głównie jako amorficzna krzemionka ($\text{SiO}_2\cdot n\text{H}_2\text{O}$) na ścianach komórkowych, w świetle komórki czy w pustkach międzykomórkowych (Jones i Handreck, 1967; Piperno, 1988; Watteau i Villemin, 2001; Ma i in., 2001; Neumann, 2003). Zawartość krzemu w roślinach waha

się od 0,1 do 16% mas.-% s.m. (Raven, 1983; Sangster i Hodson, 1986; Epstein, 1994; Marschner, 1995; Datnoff i in., 2001). Wytrącenia Si (fitolity) w roślinach mogą osiągać wielkości od 100 nm (Watteau i Villemin, 2001) do 500 μm (Piperno, 1988). Fitolity to amorficzne cząsteczki krzemionki ($\text{SiO}_2 \cdot n\text{H}_2\text{O}$) mające specyficzną morfologię i dlatego można je przypisać do różnych grup taksonomicznych roślin (Piperno, 2006). Fitolity dostają się do gleby in situ poprzez opadanie liści i rozkład roślin; mogą być również dostarczane do gleby przez czynniki zewnętrzne, np. przez działalności człowieka (nawożenie organiczne, składowanie odpadów organicznych, stosowanie biowęgla) lub mogą występować jako podstawowe składniki skały macierzystej (lessy, skały osadowe) jako domieszki. Pomimo złożonych procesów, które mogą wpływać na fitolity w glebie (translokacja, rozpuszczanie, erozja), Alexandre i in. (1999) wykazali, że fitolity glebowe mogą być dobrymi markerami zmian roślinności.

Fitolity uważa się za główny składnik puli krzemionki biogenicznej w glebie, a następnie okrzemki i gąbki (Meunier i Colin, 2001; Clarke, 2003). Zawartość fitolitów w glebie mieści się w przedziale od 0,1 do 3 mas.-%. Fitolity podlegają w profilach glebowych również przemieszczaniu wywołanemu szczególnie przez bioturbację i perkolację (Alexandre i in., 1997; Fishkis i in., 2009, 2010). Dlatego istotnym jest przedstawienie, jakim przemianom i procesom podlegają fitogeniczne (fitolity) związki krzemu w glebach oraz jakie czynniki (glebotworcze) wpływają na ich formy jak i na sam proces rozpuszczenia czy transportu?

Obiekty badawcze i cele badań

Badania przeprowadzone zostały na 3 stanowiskach:

1. *Beerenbusch* to duży obszar leśny, zwany "Naturpark Stechlin-Ruppiner Land" Niemcy. Rekonstrukcja historii użytkowania terenu wykazała, że *Beerenbusch* był pokryty lasami przez co najmniej 230 lat. W celu uwzględnienia jednego z czynników wpływających na DSi (krzem rozpuszczony), tj. zawartości minerałów wietrzeniowych w glebie, zbadany został zalesiony teren z absolutną dominacją kwarcu (>95%). Określono ilościowo strumienie Si (wewnętrzne, zewnętrzne) dla okresu 4 lat i zinterpretowano eksport DSi (rozpuszczonego Si) w kategoriach źródeł lito-/pedogenicznych i biogenicznych, jak również zmian wegetacji. Postawiono tu hipotezę o minimalnym wpływie chemicznego wietrzenia krzemianów na ilość krzemu rozpuszczonego ($\text{Si}_{\text{H}_2\text{O}}$) DSi.

2. *Chicken Creek (Hühnerwasser)* reprezentuje sztuczną zlewnię w krajobrazie pogórnym zlokalizowanym w aktywnym obszarze górniczym Welzow South (kopalnia odkrywkowa węgla brunatnego) Brandenburgia, Niemcy. Chicken Creek to teren badań o zdefiniowanych warunkach początkowych i oferujący rzadką możliwość monitorowania dynamiki rozwoju gleb od samego początku. Celem niniejszych badań było:

(i) ilościowe określenie różnych pul biogenego krzemu (BSi), tj. profitycznej, pierwotniakowej, zoogenicznej i fitogenicznej puli Si, w czasie początkowego rozwoju gleb jak i ekosystemu;

(ii) analiza zmian w pulach BSi, po dekadzie rozwoju ekosystemu; oraz

(iii) ocena wpływu różnych pul BSi na Si rozpuszczalny w wodzie.

3. *Miechów*, (Małopolska, Polska), głównym kryterium wyboru miejsca badań była skała macierzysta gleb (lessy) oraz odmienne użytkowanie terenu. Wybrano następujące stanowiska: las bukowy *Fagus sylvatica* L (czystość gatunkowa 100%, wiek > 100 lat), las sosnowy *Pinus sylvestris* L (czystość gatunkowa > 70%, wiek > 100 lat), grunty orne (100-letnie pole uprawne), oraz użytki zielone (10-letnie łąki), wcześniej wykorzystywane jako grunty orne. Postawiono hipotezę, że rozmieszczenie i zbiorowiska fitolitu w glebach terenów rolniczych i leśnych są kontrolowane przez roślinność (która jest kształtowana przez użytkowanie gruntów), a bezpośredni wpływ na wyekstrahowane frakcje Si zależy głównie od cech fitolitu, tj. stopnia rozpuszczania i morfologii (proporcje morfotypów).

Metodyka badań

Oznaczanie form krzemu.

Szczawian amonowy ($\text{NH}_4\text{-Oxalat}$) zastosowano do ilościowego określenia Si zaadsorbowanego/okludowanego na pedogenicznych tlenkach i wodorotlenkach; chlorek wapnia (CaCl_2) oraz roztwór wody (H_2O) zostały wykorzystane do ekstrakcji łatwo rozpuszczalnej lub mobilnej frakcji Si, czyli frakcji $\text{Si}_{\text{CaCl}_2/\text{H}_2\text{O}}$ przyswajalnej dla roślin (Si obecny w roztworze glebowym, czyli monomeryczny kwas krzemowy (H_4SiO_4)). Tiron ($\text{C}_6\text{H}_4\text{Na}_2\text{O}_8\text{S}_2\cdot\text{H}_2\text{O}$) zastosowano do ilościowego oznaczania amorficznej frakcji Si (w tym fitogenicznego Si). Całkowitą zawartość krzemu w materiale roślinnym oznaczono stosując kwas fluorowodorowy.

Analizę składu całkowitego (Si, Al, Fe, K, Mg, Ca, Na, Ti) w próbkach glebowych wykonano metodą fluorescencji rentgenowskiej (XRF). Podstawowy skład mineralny oznaczono na próbkach proszkowych na dyfraktometrze rentgenowskim (XRD).

Fitolity izolowano z gleby metodą separacji grawimetrycznej (ekstrakcja fizyczna), zastosowano ciecz ciężką: poliwolframat sodu ($\text{Na}_6(\text{H}_2\text{W}_{12}\text{O}_{40})\cdot\text{H}_2\text{O}$) o ciężarze właściwym $2,3 \text{ g cm}^{-3}$. Utlenianie materii organicznej w próbkach glebowych przeprowadzono na mokro z wykorzystaniem 30% H_2O_2 i 65% HNO_3 . Z materiału roślinnego pozoskano fitolity spalając materię organiczną w piecu muflowym w temp 450°C . (Szczegółowe opis zastosowanych metod znajdują się w publikacjach).

Morfotypy fitolitów oraz stopień rozpuszczenia fitolitu

Do scharakteryzowania wyizolowanych fitolitów zostały użyte odpowiednio: mikroskop świetlny (Nikon eclipse LV100) i skaningowy mikroskop elektronowy (SEM; JEOL JSM6060 LV). Sześć najczęściej występujących form (morfotypów) fitolitów zostało wyliczonych przy użyciu 10 zdjęć wykonanych w mikroskopie skaningowym (SEM) (przy powiększeniu 500x) zgodnie z międzynarodową terminologią (ICPN-International Code for Phytolith Nomenclature 1.0, Madella i in., 2005). Wydzielono następujące morfotypy fitolitów: 1. naczyniowe (vascular), 2. podłużne (elongate), 3. kuliste (globular), 4. wrzecionowate (fusiform), 5. lancetowate (lanceolate), 6. krótkie komórki (short cells): bilobate, krzyżowe (cross), brodawkowate (papillae), oponkowate (rondel), siodłowe (saddle), formy fitolitów rzadko występujące lub niejednoznaczne pod względem budowy zaliczono do grupy "inne formy".

Stan rozpuszczenia fitolitów analizowano również z wykorzystaniem 10 zdjęci z SEM, użytych wcześniej do klasyfikacji morfotypów. Wszystkie policzone fitolity przypisano do jednej z trzech klas rozpuszczenia fitolitu: (i) fitolity bez wyraźnych cech rozpuszczania (gładkie; plain), (ii) fitolity wykazujące pewne wytrawianie powierzchni (porowate; rough-porous) oraz (iii) fitolity z silnymi cechami rozpuszczania (gąbczaste; cratered/spongy).

Fitolitów poddano dodatkowo analizie ich widma pierwiastkowego (mapowanie pierwiastków) w celu określenia składu całkowitego (EDX-X-Flash-Detector).

Opis uzyskanych wyników badań

Glebę w **Beerenbusch** sklasyfikowano jako Brunic Arenosol (Dystric) według WRB (2006). Wzbogacona w próchnicę wierzchnia warstwa gleby sięgała do głębokości 35 cm.

Poziom AE wskazywały na niewielką bielicość, natomiast rdzawienie doprowadziło do jasnobrązowego zabarwienia w poziomie Bw do głębokości 80 cm. Pojedyncze cienkie warstewki/otoczki ilaste w głębszych poziomach i materiale macierzystym wskazywały makroskopowo na przemieszczenie ilu (do 120 cm). W glebie przeważały frakcje piasku (>85%) z dominacją frakcji piasku średniego. W górnych 50 cm stwierdzono zawartości frakcji ilastej nie przekraczającej 3%. Gleba była odwapniona do głębokości 1,8 m. W górnej części profilu glebowego wartości pH była pomiędzy 4,3 a 4,5, w poziomach skały macierzystej wartość pH wyniosła ponad 7,0. Mineralem dominującym we wszystkich poziomach glebowych był kwarc, stwierdzono również niewielkie domieszki skaleni (ortoklaz > plagioklaz), piroksenu i kalcytu.

Wykonane badania mikromorfologiczne ujawniły bardzo mały stopień zwietrzenia krzemianów (ortoklaz, mikroklin) jak również brak oznak wytrawień na ziarnach kwarc. Przyczyną tego zjawiska mogą być otoczki żelazowo-ilaste, które chronią ziarna skaleni i kwarcu przed rozpuszczaniem. Ostatecznie stwierdzono, że wietrzenie skaleni oraz kwarcu nie miało wpływu na stężenia DSi (krzemu rozpuszczonego).

W materiale roślinnym oznaczono całkowite zawartości krzemu, najwyższe ilości Si stwierdzono w liściach buka, a następnie w korze gałęzi i drewnie pnia, łuskach pąków i kapsułkach owoców. Biorąc pod uwagę biomasę poszczególnych przedziałów roślinnych, łączna pula Si w biomasie nadziemnej wyniosła 83 kg Si ha⁻¹. Największy udział miała kora pnia (50 %), następnie liście (36 %), kora gałęzi (6 %) i drewno pnia (3 %). Pobór Si przez rośliny przyczynił się do największego wewnętrznego przepływu Si w biogeosystemie (35 kg Si ha⁻¹ rok⁻¹). Duża część transportowana była do liści (30 kg Si ha⁻¹ rok⁻¹), co czyniło jesienny opad ściółki najważniejszym składnikiem rocznego strumienia Si do gleby.

Zawartość fitolitów była najwyższa w górnych 20 cm gleby i wyniosła 140 g fitolitów m² (= 1400 kg ha⁻¹), malała wraz z głębokością w profilu glebowym (od poziomu L-8,7 g kg⁻¹ do AB-0,3 g kg⁻¹). W składzie fitolitów w poszczególnych poziomach glebowych dominowały fitolity podłużne (polilobate, fusiform) i krótko-komórkowe (bilobate, trapeziform) z niewielkim udziałem fitolitów kulistych i naczyniowych. Co zaskakujące, wyraźnie identyfikowalne fitolity buka stanowiły jedynie niewielką część w górnych centymetrach. Co więcej, formy wyizolowane ze ściółki były prawie niewykrywalne w swoim pierwotnym kształcie w glebie, nawet w górnych 2 cm. Na podstawie przedstawionych wyników można wnioskować o szybkim rozpuszczaniu fitolitów buka. Pod względem przypisanej roślinności w poziomach mineralnych poniżej 2 cm stwierdzono dominację fitolitów trawiastych.

Odpowiada to bardzo dobrze wynikom badań roślinności z 1954 roku, które wykazały, że wśród roślinności podszycia dominowały rośliny o wysokiej zawartości Si, takie jak *Calamagrostis epigejos* (2,2% Si), *Brachypodium sylvaticum* (3,1% Si) i *Agrostis capillaris* (1,4% Si). Zidentyfikowano również fitolity sosny i mchów (kuliste formy, zawierające Al). Ponieważ jednak w miejscu badań nie rosły już sosny i trawy (przynajmniej w ciągu ostatnich 30 lat), fitolity sosny i trawy wyizolowane z gleby stanowiły reliktową pulę biogenicznego Si.

W celu sprawdzenia stanu rozpuszczenia fitolitów w naszej glebie określono trzy klasy wzrastającego stopnia rozpuszczenia i policzono przyporządkowane im fitolity. Odsetek fitolitów gładkich (plain), nie wykazujących oznak rozpuszczania lub wytrawiania powierzchniowego, zmniejszył się istotnie z 69% na powierzchni gleby do 31% w poziomie AB (10-20 cm). Równocześnie wzrósł do 54% udział fitolitów wykazujących lekkie trawienie powierzchniowe (rough-porous). Fitolity silnie rozpuszczone (gąbczaste; cratered/spongy) stanowiły maksymalnie 19% w poziomie Ah (2-10 cm), ale nie wykazywały wyraźnej tendencji w zależności od głębokości.

Łącząc te wyniki z obserwacją brakujących świeżych fitolitów buka w poziomach glebowych oraz równoległym wzrostem Si rozpuszczalnego w wodzie z pulą Si fitolitu (górne 25 cm), rozpuszczanie fitogenicznego Si jest najważniejszym czynnikiem wpływającym na stężenie DSi, a tym samym na export DSi. Stosunkowo wysokich stężeń DSi (6 mg l^{-1}) oraz ilości wymywanego DSi ($12 \text{ kg Si ha}^{-1} \text{ rok}^{-1}$) nie można wyjaśnić chemicznym wietrzeniem skał ani rozpuszczaniem kwarcu. Zamiast tego, rozpuszczanie reliktovej, fitogenicznej puli Si wydaje się być głównym procesem odpowiedzialnym za obserwowane ilości DSi.

Chicken Creek.

Obszar badań Chicken Creek reprezentuje sztuczną zlewnię w krajobrazie pogórnym zlokalizowanym w aktywnym obszarze górniczym Welzow South, Brandenburgia, Niemcy. Klimat w Chicken Creek charakteryzuje się średnią temperaturą powietrza $9,6 \text{ C}$ i roczną sumą opadów 568 mm . Podstawowym składnikiem mineralnym we wszystkich frakcjach glebowych (w t_0) był kwarc (wykryto tylko niewielkie ilości skałenia K, plagioklazu), kalcyt stanowił $0,5-4,5\%$.

Do badań wykorzystaliśmy próbki pobrane krótko po wybudowaniu Chicken Creek (2005, t_0) i po okresie rozwoju ekosystemu trwającym 10 lat (2015, t_{10}). Dla t_0 (brak widocznej roślinności) założono, że biogeniczne formy krzemionkowe były jednorodnie rozmieszczone

na całym obszarze Chicken Creek (Puppe i in., 2016). Aby ocenić te różnice po dekadzie rozwoju ekosystemu, skoncentrowaliśmy się na miejscach, gdzie gatunki roślin kumulujące Si (tj. *Calamagrostis epigejos* i *Phragmites australis*), stały się dominujące (Zaplata i in., 2010).

Po 10 latach (t_{10}) rozwoju ekosystemu zasoby C_{org} wzrosły nawet 3-krotnie (396-556 g m^{-2} w górnych 5 cm) w stosunku do odpowiednich wartości w t_0 . Spowodowało to wysoki średni roczny wskaźnik sekwestracji CO_2-C wynoszący 27-32 g m^{-2} (górne 5 cm). W momencie t_0 wartości pH gleb były w zakresie od 7,9 do 8,3 po 10 latach wartości pH obniżyły się do 7,1-7,4. Stwierdzono również znaczący wzrost zawartości Si_{H_2O} w stosunku do t_0 , ilość Si_{H_2O} wynosiły od 1,5 g m^{-2} do 2,2 g m^{-2} . W t_0 średnia zawartość Si_{Tiron} w górnych 5 cm wahała się między 4,1 g kg^{-1} a 5,5 g kg^{-1} . Natomiast zawartość Si_{Tiron} po 10 latach (t_{10}) wykazała niewielki wzrost w obszarze zachodnim do 6,5 g kg^{-1} (552 g m^{-2}), natomiast po stronie wschodniej nastąpił znaczny spadek koncentracji do 2,6 g kg^{-1} .

W t_0 biogeniczny Si był reprezentowany przez fitolity (> 50%), a następnie przez okrzemki, igły gąbek i poncerzyki ameb testate. Całkowita pula biogenicznego Si wzrosła w każdym odcinku po 10 latach rozwoju ekosystemu. Całkowity BSi wykazywał silne dodatnie i statystycznie istotne korelacje z Si_{H_2O} rozpuszczalnym w wodzie. Ilości fitogenicznego Si wyniosły od 0 do 18 mg m^{-2} w t_0 i znacząco wzrosły od 12,9 mg m^{-2} do 20,7 mg m^{-2} w ciągu 10 lat. Pule Si protofitycznego (okrzemki) wynosiły od 0 do 7 mg m^{-2} w t_0 i wzrosły do średniej 47,4 mg m^{-2} w t_{10} . W t_0 nie stwierdzono obecności igieł gąbek, z jednym wyjątkiem reprezentującym wartość ekstremalną (12,7 mg m^{-2}). Po jednej dekadzie rozwoju ekosystemu pule zoogenicznego Si wzrosły do 46 mg m^{-2} (t_{10}). Również pule pierwotniakowego Si znacząco wzrosły do 11,5 mg m^{-2} w t_{10} .

Dla dwóch dominujących gatunków roślin *Calamagrostis epigejos* i *Phragmites australis*, oznaczono całkowitą zawartość krzemu, dla *C. epigejos* wynosiła ona 2,25%, natomiast dla *P. australis* 2,70%. W ściółce pod obiema trawami stwierdzono średnią zawartość Si 3,1% (*C. epigejos*) i 2,9% (*P. australis*). Z obu roślin wyizolowano również fitolity wykazując średnią zawartość fitolitów dla *C. epigejos* 0,37% i *P. australis* 0,43%. W odniesieniu do całkowitej zawartości Si w roślinach tylko 16% fitogenicznego Si było reprezentowane przez wyizolowane fitolity. Tak więc fitogeniczny Si < 5 μm stanowił około 84% całkowitej zawartości Si u *C. epigejos* i *P. australis*. Średnia zawartość ekstrahowanego fitolitu w ściółce roślinnej wynosiła dla *C. epigejos* 0,47% i *P. australis* 0,51%.

Uzyskane wyniki wskazują na silną zależność pomiędzy Si rozpuszczalnym w wodzie a całkowitą zawartością biogenicznego Si (BSi). W tym kontekście można rozważyć dwa różne łańcuchy przyczynowe: albo organizmy syntetyzujące SiO_2 są źródłem Si(OH)_4 w glebie, albo - odwrotnie - ilość Si rozpuszczalnego w wodzie w glebie jest głównym źródłem dla organizmów syntetyzujących SiO_2 , ponieważ biokrzemionka jest ograniczona przez Si(OH)_4 . Jest jednak mało prawdopodobne, że ameby testatowe wyczerpywały ilości Si(OH)_4 w tych miejscach, ponieważ odpowiednie protozoiczne pule Si są stosunkowo małe w porównaniu z fitogenicznymi.

Dekadowe zmiany Si rozpuszczalnego w wodzie w Chicken Creek są głównie zależne od biogenicznego Si; tak więc obieg Si jest kontrolowany biologicznie już na samym początku rozwoju ekosystemu. W tym kontekście fitogeniczny Si odgrywa szczególnie istotną rolę. Jednak rozwijająca się warstwa organiczna (poziom L) na powierzchni gleby tymczasowo chroni fitogeniczny Si przed rozpuszczaniem, ponieważ fitogeniczny Si jest nadal wbudowywany w elementy strukturalne roślin (tkanki). W konsekwencji dochodzi do powstania opóźniającej puli fitogenicznego Si, a uwalnianie Si do gleby jest spowolnione. Całkowita zawartość Si i fitolitu w próbkach ściółki w Chicken Creek nie różniła się od całkowitej zawartości Si i fitolitu w roślinach. Fakt ten wskazuje, że rozkład ściółki i związane z tym uwalnianie Si do gleby są procesami stosunkowo powolnymi.

Miechów

Badane gleby wytworzone na lessach, sklasyfikowane zostały jako Luvisole (buk, sosna) i Luvisole zerodowane (użytki zielone, grunty orne). Wszystkie profile glebowe zlokalizowano w odległości nie większej niż 0,5 km od siebie. Gleby miały bardzo podobny skład granulometrycznym, dominowały frakcje pyłu (>65%); frakcja ilasta stanowiła 2–25%; natomiast ilości frakcji piasku była od 2,2% (w poziomie eluwialnym gleby pod lasem sosnowym) do 10%. Zawartość węgla organicznego była najwyższa w poziomach organicznych (O): 24,9% - las bukowy, 26% - las sosnowy, 7,8% - użytek zielony. Poziomy próchniczne (A) zawierały znacznie niższe wartości C_{org} (0,8-5,0%). Gleby wykształcone pod bukiem (pH 3.5-6.1) i sosną (pH 3.4-4.1) były na ogół bardziej kwaśne w porównaniu z glebami wykształconymi pod 10-letnią łąką (pH 5.1-5.9) i gruntami ornymi (pH 5.0-6.6). Rozmieszczenie związków Fe i Al w profilach glebowych było związane z eluwialnym (E) i iluwialnym (Bt) poziomem glebowym. Najintensywniejsze pionowe przemieszczanie Fe, Al i frakcji ilastych zachodziło w

glebie pod lasem sosnowym. W glebach pod lasem bukowym i łąkach przeważała akumulacja Fe i Al w poziomie Bt. W przeszłości erozja usunęła poziomy eluwialne w glebach ornym. W związku z tym nie stwierdzono istotnych różnic w rozmieszczeniu Fe, Al w profilu glebowym. We wszystkich profilach całkowita zawartość SiO₂ była zbliżona (70-80%), jedynie w poziomach organicznych (O) zawartość SiO₂ była znacznie niższa (ok. 40%). Węglany stwierdzono w glebie pod bukiem i gruntami ornymi CaO (odpowiednio 3,5 i 2,5%). Kwarc był głównym minerałem badanych gleb; minerały poboczne oraz minerały jako domieszki to: skalenie potasowe, plagioklasy, amfibole i pirokseny.

Rozmieszczenie przyswajalnego Si (Si_{CaCl2}) w poziomach mineralnych w glebach pod lasem bukowym i sosnowym wykazał pewne podobieństwo, przy najniższej zawartości w poziomach eluwialnych (E) (5,0 mg kg⁻¹ dla sosny i 7,9 mg kg⁻¹ dla buka). Uwagę zwracał wysoki udział Si_{CaCl2} (79 mg kg⁻¹) w poziomie organicznym (O) gleby wytworzonej pod lasem bukowym, w poziomach iluwialnych (Bt) i skale macierzystej (C) zawartość Si_{CaCl2} była od 13 do 48 mg kg⁻¹. Natomiast tak dużych różnic w zawartości przyswajalnego Si nie stwierdzono w przypadku użytków zielonych (19–35 mg kg⁻¹) i gruntów ornym (22–29 mg kg⁻¹). Najwyższe stężenia krzemu amorficznego (Si_{Tironu}) wystąpiły w poziomach organicznych O (12 g kg⁻¹) i Bt pod bukiem (11 g kg⁻¹), a także w organicznym poziomie sosny (8 g kg⁻¹) i użytku zielonym (8 g kg⁻¹). Si wyekstrahowany szczawianem amonu (Si_{ox}) osiągnął najwyższe wartości w poziomach Bt (209 mg kg⁻¹ dla użytków zielonych, 87 mg kg⁻¹ dla buka i 57 mg kg⁻¹ dla sosny) w glebach uprawnych zawartość Si_{ox} rosła wraz z głębokością profilu glebowego (Ap 19, Bt 45–55, C 72–130 mg kg⁻¹). Zawartość Si_{Tiron} w badanych glebach była najwyższa w stosunku do ilości Si_{ox} czy Si_{CaCl2}.

Obecność fitolitów stwierdzono w każdym poziomie glebowym do głębokości 85 cm. Łączna masa fitolitów glebowych wyniosła 7,7 kg m⁻² dla sosny (0–75cm głębokości), 1 kg m⁻² dla buka (0-80 cm głębokości), 1 kg m⁻² dla użytków zielonych (0-85 cm głębokości) oraz 0,3 kg m⁻² dla gruntów ornym (0-70 cm głębokości). Najwyższe zawartosci fitolitów stwierdzono w glebie pod lasem sosnowym (5,5–16,0 g kg⁻¹). Ilość fitolitów pod sosną była zmienna w profilu glebowym i osiągnęła najwyższą wartość w poziomie eluwialnym (35–44 cm) 16,0 g kg⁻¹, który charakteryzuje się małą zawartością frakcji ilastej (ok. 2%). Wyższa zawartość tej frakcji w poziomie Bt (55-75 cm) mogły stanowić barierę dla dalszej translokacji fitolitów w dół, a tym samym doprowadziło to do akumulacji fitolitów powyżej tego poziomu. W pozostałych

profilach glebowych zawartość fitolitów była znacznie niższa i wyniosła między 0,01 a 2,5 g kg⁻¹ (las bukowy: 1,5–2,5 g kg⁻¹, użytki zielone: 0,01–2,4 g kg⁻¹, grunty orne: 0,15–0,52 g kg⁻¹). Ilość fitolitów na naszych stanowiskach była tego samego rzędu wielkości w porównaniu z innymi stanowiskami o podobnej roślinności (np. Blinnikov i in., 2013; Keller i in., 2012; Sommer i in., 2013). Grunty orne wykazywały najniższą zawartość fitolitów w naszym badaniu (0,15–0,52 g kg⁻¹), głównie z powodu usuwania roślin poprzez zbiory i zwiększone procesy erozyjne wynikające z uprawy gleby (Guntzer et al., 2012; Keller et al. al., 2012; Vandevenne i in., 2012).

Spośród 15 analizowanych poziomów glebowych w 11 poziomach dominowały fitolity podłużne (typowe dla roślinności trawiastej) (23–31% buk; 24–40% sosna; 22–44% użytki zielone; 21–29% grunty orne) pozostałe 3 poziomy były zdominowane przez fitolity kuliste, które najczęściej występowały w poziomach organicznych O (29% dla buka, 58% dla sosny) i próchnicznym (Ah) pod sosną (34%). W dwóch poziomach dominowały fitolity o formach krótkich: pod bukiem (26%, głębokość 30–45 cm) i sosną (32%, głębokość 35–55 cm). W poziomach organicznych obserwowano fitolity charakterystyczne dla buka (fitolity naczyniowe), procentowy ich udział wyniósł dla poziomu O pod bukiem (14%), pod sosną (2%), a w poziomie próchnicznym pod sosną (Ah, 1%). Pomimo tego, że buk na badanym terenie reprezentuje obecnie monokulturę, ilość stwierdzonych fitolitów buka (fitolitów naczyniowych) wyniosła zaledwie 14 %, a zatem około 86% fitolitów nie zostało wyraźnie przypisanych do buka. Stosunkowo dużą część fitolitów odnotowano jako „inne formy”, ponieważ ich jednoznaczna identyfikacja nie była możliwa. Poziomy organiczne (O) i próchniczne (Ah) były na ogół zdominowane (w oparciu o rozpoznawalne fitolity) przez fitolity kuliste zawierające Al, które można przypisać mchom.

Stosunkowo dużą liczbę zbiorowisk fitolitów reprezentowały fitolity, które nie były jednoznacznie przypisywalne do określonych morfotypów, a zatem zostały zapisane jako „inne formy”. W tym kontekście należy stwierdzić, że na zbiorowiska fitolitów w glebach wpływają różne procesy, takie jak fragmentacja, rozpuszczanie, translokacja itp. - czynniki, które ogólnie utrudniają uzyskanie dokładnego odzwierciedlenia (obecnej) lokalnej roślinności charakteryzowanej przez określone morfotypy fitolitu (De Rito i in., 2018). Jeśli chodzi o nasze stanowiska badawcze, „inne formy” dominowały w zbiorowiska fitolitów w próbkach gleby z gruntów ornych i 10-letnich użytków zielonych, które wcześniej były również wykorzystywane jako grunty orne. W związku z tym uprawa mechaniczna (w tym orka) mogła spowodować

mechaniczne zniszczenie fitolitów, a tym samym utrudniać ich jednoznaczną identyfikację i klasyfikację.

Badając stopień rozpuszczalności fitolitów stwierdziliśmy, że w poziomach organicznych pod bukiem (83%) i sosną (65%) dominowały formy gładkie, natomiast w pozostałych poziomach wszystkich badanych stanowisk dominowały formy szorstko-porowate (49-65%). Zawartość form gładkich generalnie zmniejszała się wraz z głębokością w profilach glebowych, czego nie obserwowano w przypadku form szorstko-porowatych czy gąbczastych. Naszą interpretację podkreślają wyniki analiz SEM dotyczących ogólnie stanu rozpuszczalności fitolitów. Gleby leśne charakteryzowały się większym udziałem fitolitów niezwiędłych (świeżych) w porównaniu z glebami rolniczymi, co wskazuje na wspomniane różnice w roślinności. Podczas gdy gleby leśne charakteryzują się (niezakłóconym) corocznym dopływem dużych ilości świeżych fitolitów poprzez opadanie ściółki, gleby rolnicze są częścią silnie zaburzonego systemu roślinno-glebowego, z którego rocznie usowane są duże ilości fitolitów. Naszą interpretację podkreślają wyniki analiz SEM dotyczących ogólnie stanu rozpuszczalności fitolitów.

Przyjmujemy ponadto, że fitolity $<5 \mu\text{m}$, które zostały odfiltrowane z ekstraktów fitolitów i tym samym nie zostały uwzględnione w grawimetrycznej kwantyfikacji zawartości fitolitów są głównym czynnikiem wpływającym na zawartość ekstrahowalnych frakcji Si w glebach. Potwierdzają to badania ekosystemu w Chicken Creek (Puppe et al. 2017) że fitolity większe niż $5 \mu\text{m}$ stanowią tylko około 16% całości zawartości Si w materiałach roślinnych *Calamagrostis epigejos* i *Phragmites australis*. Wilding i Drees (1971) wykazali, że około 72% fitolitów liściowych buka amerykańskiego (*Fagus grandifolia*) ma mniej niż $5 \mu\text{m}$. Odkrycia te wyraźnie wskazują na potencjalne znaczenie fitolitów $<5 \mu\text{m}$ w ogólnym cyklu Si. Ponadto Meunier i wsp. (2017) oraz Puppe i wsp. (2017) podkreślili znaczenie kruchych fitogenicznych struktur Si dla cyklu Si, ponieważ reprezentują kolejną ogromną i najbardziej reaktywną pulę Si w glebach.

Podsumowanie

Badania opublikowane w ramach prezentowanego cyklu artykułów naukowych dostarczyły wielu nowych i cennych wniosków dotyczących charakterystyki jak i wpływu fitolitów i fitogenicznego krzemu na obieg krzemu w środowisku glebowym. Zgodnie z oczekiwaniami, poziomy glebowe pod różną roślinnością charakteryzowały się ogólnie

różnicami w ekstrahowanych frakcjach Si, zwłaszcza w górnych poziomach glebowych. Jednak ilości fitogenicznego krzemu wbrew intuicji nie wykazały żadnych korelacji z chemicznie ekstrahowanymi frakcjami krzemu i pH gleby. Dlatego też, konieczne jest połączenie analiz mikroskopowych i metod ekstrakcji Si do badań cyklu Si w biogeosystemach, ponieważ same ekstrakcje frakcji Si nie pozwalają na wyciąganie jakichkolwiek wniosków na temat właściwości fitolitu lub interakcji między zbiornikami fitolitu a chemicznie ekstrahowanymi frakcjami Si.

Ponadto w badanych glebach dominującymi morfotypami fitolitów były fitolity podłużne i krótkie „short cell”, oba są wyznacznikami roślinności trawiastej. Fitolity charakteryzowały się różną rozpuszczalnością w glebie. Fitolity traw były bardziej odporne na rozpuszczanie w stosunku do fitolitów drzew liściastych (buk). Czynniki kontrolującymi rozpuszczanie fitolitu w glebie są: powierzchnia właściwa, zawartość glinu (Al), stan uwodnienia, wiek, szybkość biodegradacji materii organicznej i pH gleby. Stwierdzono pionowe rozmieszczenie fitolitów w poziomach glebowych na różnych stanowiskach badawczych oraz ich przemieszczanie w profilach glebowych.

Badane biogeosystemy (inicjalne, leśne, rolnicze) wykazały różnice w biogeochemicznych cyklach Si pod względem przepływu i dynamiki Si. Intensywne użytkowanie ekosystemów lądowych przez ludzi bezpośrednio wpływa na obieg krzemu, co często wiąże się z utratą (fitogenicznego) Si. W ekosystemach takich jak pola uprawne lub użytki zielone, proces akumulacji fitogenicznego krzemu w glebach jest w pewnym stopniu zahamowany poprzez zbiór plonów jak i erozję powodowaną uprawą gleby. W skali globalnej uprawy polowe pochłaniają około 35% całkowitego fitogenicznego krzemu i udział ten będzie wzrastał w ciągu najbliższych dziesięcioleci spowodowany zwiększoną produkcją rolną (Carey i Fulweiler, 2016).

Ze względu na wieloaspektowość i złożoność prezentowanej problematyki, konieczne są dalsze badania dotyczące frakcji $< 5\mu\text{m}$ fitogenicznego krzemu, która odgrywa chyba największą rolę jako źródło łatwo dostępnego Si w glebach.

Spis literatury

Alexandre, A., Meunier, J. D., Mariotti, A., Soubies, F. (1999): Late holocene paleoenvironmental record from a latosol at Salitre (southern Central Brazil). Phytolith and carbon isotope evidence. *Quaternary Res.* 51, 187–194.

Alexandre, A., Meunier, J. D., Colin, F. D., Koud, J. M. (1997): Plant impact on the biogeochemical cycle of silicon and related weathering processes. *Geochim. Cosmochim. Acta* 61, 677–682.

- Alexandre, A., Bouvet, M., Abbadie, L., 2011. The role of savannas in the terrestrial Si cycle: a case study from Lamto, Ivory Coast. *Glob. Planet. Chang.* 78, 162–169
- Anderson, S. P., Drever, J. I., Frost, C. D., Holden, P. (2000): Chemical weathering in the foreland of a retreating glacier. *Geochim. Cosmochim. Acta* 64, 1173–1189.
- Blinnikov, M.S., Bagent, M.C., Reyerson, E.P., 2013. Phytolith assemblages and opal concentrations from modern soils differentiate temperate grasslands of controlled composition on experimental plots at Cedar Creek, Minnesota. *Quat. Int.* 287, 101–113.
- Carey, J.C., Fulweiler, R.W., 2016. Human appropriation of biogenic silicon - the increasing role of agriculture. *Funct. Ecol.* 30, 1331–1339.
- Clarke, J.: The occurrence and significance of biogenic opal in the regolith, *Earth-Sci. Rev.*, 60, 175–194, 2003
- Conley 2002 Conley, D. J. (2002): Terrestrial ecosystems and the global biogeochemical silica cycle. *Global Biogeochem. Cycl.* 16, 1121–1129.
- Datnoff, L. E., Snyder, G. H., Korndörfer, G. H. (eds.) (2001): Silicon in agriculture. *Studies in Plant Science* 8, Elsevier, Amsterdam.
- De Rito, M., Honaine, M.F., Osterrieth, M., Morel, E., 2018. Silicophytoliths from a Pampean native tree community (*Celtis ehrenbergiana* community) and their representation in the soil assemblage. *Rev. Palaeobot. Palynol.* 257, 19–34.
- Epstein, E. (1994): Silicon. *Ann. Rev. Plant. Physiol. Plant. Mol. Biol.* 50, 641–664.
- Fishkis, O., Ingwersen, J., Streck, T., 2009. Phytolith transport in sandy sediment: experiments and modeling. *Geoderma* 151 (3–4), 168–178.
- Fishkis, O., Ingwersen, J., Lamers, M., Denysenko, D., Streck, T., 2010. Phytolith transport in soil: a field study using fluorescent labelling. *Geoderma* 157 (1–2), 27–36.
- Guntzer, F., Keller, C., Poulton, P.R., McGrath, S.P., Meunier, J.D., 2012. Long-term removal of wheat straw decreases soil amorphous silica at Broadbalk, Rothamsted. *Plant Soil* 352, 173–184.
- Jones, L. H. P., Handreck, K. A. (1967): Silica in soils, plants and animals. *Adv. Agron.* 19, 107–149.
- Keller, C., Guntzer, F., Barboni, D., Labreuche, J., Meunier, J.D., 2012. Impact of agriculture on the Si biogeochemical cycle: input from phytolith studies. *Compt. Rendus Geosci.* 344, 739–746.
- Ma, J. F. and Yamaji, N.: Functions and transport of silicon in plants, *Cell. Mol. Life Sci.*, 65, 3049–3057, 2008
- Marschner, 1995; Marschner, H. (1995). *Mineral nutrition of higher plants*. 2nd edn., Academic Press, San Diego
- Meunier, J. D., Colin, F., and Alarcon, C.: Biogenic silica storage in soils, *Geology*, 27, 835–838, 1999
- Meunier, J.D., Barboni, D., Anwar-ul-Haq, M., Levard, C., Chaurand, P., Vidal, V., Grauby, O., Huc, R., Laffont-Schwob, I., Rabier, J., Keller, C., 2017. Effect of phytoliths for mitigating water stress in durum wheat. *New Phytol.* 215, 229–239.
- Neumann, D. (2003): Silicon in plants, in Müller, W. E. G. (ed.): *Silicon biomineralization*. Springer Verlag, Berlin, pp. 149–162.
- Oliva, P., Viers, J., Dupre, B., Fortune, J. P., Martin, F., Braun, J. J., Nahon, D., Robain, H. (1999): The effect of organic matter on chemical weathering: Study of a small tropical watershed: Nsimi- Zoetele site, Cameroon. *Geochim. Cosmochim. Acta* 63, 4013–4035.
- Piperno, D., 2006. R.: *Phytoliths: A Comprehensive Guide for Archaeologists and Paleoecologists*. Alta Mira Press, Lanham, MD.
- Piperno, D. R. (1988): *Phytoliths. An archaeological and geological perspective*. Academic Press, London

- Puppe, D., Hohn, A., Kaczorek, D., Wanner, M., Wehrhan, M., Sommer, M., 2017. How big is the influence of biogenic silicon pools on short-term changes in water-soluble silicon in soils? Implications from a study of a 10-year-old soil-plant system. *Biogeosciences* 14, 5239–5252.
- Raven, J. A. (1983): The transport and function of silicon in plants. *Biol. Rev.* 58, 179–207.
- Sangster, A. G., Hodson, M. J. (1986): Silica in higher plants, in: Ciba Foundation Symposium 121. J. Wiley & Sons, Chichester, pp. 90–111.
- Sommer, M., Kaczorek, D., Kuzyakov, Y., Breuer, J., 2006. Silicon pools and fluxes in soils and landscapes – a review. *J. Plant Nutr. Soil Sci.* 169, 310–329.
- Sommer, M., Jochheim, H., Hohn, A., Breuer, J., Zagorski, Z., Busse, J., Barkusky, D., Meier, K., Puppe, D., Wanner, M., Kaczorek, D., 2013. Si cycling in a forest biogeosystem– the importance of transient state biogenic Si pools. *Biogeosciences* 10, 4991–5007.
- Tréguer, P. J. and De La Rocha, C. L.: The world ocean silica cycle, *Ann. Rev. Mar. Sci.*, 5, 477–501, 2013.
- Treuguer, Pondaven 2000, Tréguer, P. J. and De La Rocha, C. L.: The world ocean silica cycle, *Ann. Rev. Mar. Sci.*, 5, 477–501, 2013.
- Tréguer, P. and Pondaven, P.: Global change: silica control of carbo dioxide, *Nature*, 406, 358–359, 2000
- Vandevenne, F., Struyf, E., Clymans, W., Meire, P., 2012. Agricultural silica harvest: have humans created a new loop in the global silica cycle? *Front. Ecol. Environ.* 10, 243–248.
- Vandevenne, F., Struyf, E., Clymans, W., Meire, P., 2012. Agricultural silica harvest: have humans created a new loop in the global silica cycle? *Front. Ecol. Environ.* 10, 243–248.
- Veerhoff, M. (1992): Silicatverwitterung und Veränderung des Tonmineralbestandes in Waldböden als Folge von Versauerungsvorgängen. *Bonner Bodenkundliche Abhandlungen* 8, 1–249.
- Watteau, F. and Villemin, G.: Ultrastructural study of the biogeochemical cycle of silicon in the soil and litter of a temperate forest, *Eur. J. Soil Sci.*, 52, 385–396, 2001.
- Wilding, L. P. and Drees, L. R.: Biogenic opal in Ohio soils, *Soil Sci. Soc. Am. J.*, 35, 1004–1010, 1971.
- Wollast, R., McKenzie, F. T. (1983): The global cycle of silica, in Aston, S. R. (ed.): *Silicon geochemistry and biochemistry*. Academic Press, San Diego, pp. 39–76.
- WRB-World reference base for soil resources, *World Soil Resources Reports*, 103, p. 128, Rome, FAO, 2006.
- Zaplata, M. K., Fischer, A., and Winter, S.: Vegetation dynamics, in: *Ecosystem development 2*, edited by: Schaaf, W., Biemelt, D., Hüttl, R. F., Brandenburg University of Technology Cottbus- Senftenberg, Germany, 2010

Inne osiągnięcia naukowe

Zastosowanie mikromorfologii w badaniach biogenicznej krzemionki

Mikromorfologia jest potężnym narzędziem stosowanym dla lepszego zrozumienia procesów genezy gleb. Analizy mikroszlifów glebowych o nienaruszonej strukturze dają wgląd w mikrostrukturę gleby in situ. Obserwacja w mikroskopie świetlnym pozwala na odróżnienie lito- i pedogenicznych form mineralnych, dostarcza informacji o składnikach również tych

większych od 2mm, materii organicznej, systemie porów glebowych, formach agregatów glebowych i aktywności mikrofauny glebowej.

Badania mikromorfologiczne pozwoliły wydzielić następujące formy biogenicznej krzemionki: fitolity, okrzemki, ameby, igły gąbek (Kaczorek et al. 2018). Analizując biokrzemionkę może uzyskać wgląd w aktualne i przeszłe warunki pedogenezy oraz ujawnić trendy ewolucyjne poszczególnych gleb lub całych krajobrazów. Biogeniczna krzemionka występuje najczęściej w powierzchniowych poziomach gleb, wynika to z tego, że fitolity dostają się do gleby z masą roślinną, natomiast dla amebby glebowych, okrzemek i gąbek poziomy glebowe z materią organiczną są naturalnym środowiskiem ich życia. Igły gąbek i okrzemki mogą być dostarczane do gleby również przez nawożenie gleb. Stosując metody chemiczne lub fizyczne do identyfikacji i izolacji fitolitów, ameb czy okrzemek narażamy nasze obiekty badawcze na uszkodzenia mechaniczne. W pracy Kaczorek 2009, przeprowadziłam badanie mikrosondą na mikroszlifach i uzyskałam bardzo ciekawe formy fitolitów (podłużne, rozetowe) oraz pojedyncze osobniki amebby glebowych. W innej pracy Ehrmann et al 2013 z powodzeniem zastosowaliśmy mikroszlify do ilościowego określenia puli amebby glebowych w różnych poziomach glebowych pochodzących z 31 ekosystemów leśnych. Proste liczenie na mikroszlifach przy użyciu mikroskopu świetlnego dało gęstości amebby porównywalne z wcześniej podawanymi wartościami (tj. od $0,1 \times 10^8$ do $11,5 \times 10^8$ osobników m^{-2}). Opis in situ amebby, oparty na analizie mikroszlifu, wykazał stosunkowo równomierne mikrorozmieszczenie przestrzenne w organicznych poziomach glebowych, w poziomach mineralnych nie stwierdzono skupisk amebby testate. Badania mikromorfologiczne w połączeniu z różnymi zaawansowanymi technikami pomiarowymi (SEM-EDX) dają ogromne możliwości badawcze procesów i zjawisk zachodzących w naszych glebach.

Kaczorek D. 2009. Identyfikacja biogenicznego krzemu w glebach z wykorzystaniem badań w mikroskopie świetlnym oraz badań mikrosonda. Roczniki Gleboznawcze tom LX No 4, 42-49.

O. Ehrmann, D. Puppe, M. Wanner, D. Kaczorek, M. Sommer. Testate amoebae in 31 mature forest ecosystems– Densities and micro-distribution in soils. European Journal of Protistology. 48: 161-168, 2012

Kaczorek, D., Vrydaghs, L., Devos, Y., Peto, A´. & Effland, W.R., 2018. Biogenic siliceous features. In Stoops, G., Marcelino, V. & Mees, F. (eds.), Interpretation of Micromorphological Features of Soils and Regoliths. Second Edition. Elsevier, Amsterdam, pp. 157-176.

Krzem- inne aspekty badawcze

Moje zainteresowania krzemem sięgają roku 2004, w którym opublikowałam wraz z kolegą M. Sommerem (ZALF) swoją pierwszą pracę problemowo/przeglądową na temat krzemu w glebach (Kaczorek & Sommer 2004), potem pojawiły się kolejne prace Sommer et al 2006, Conley et al 2006 jako początek współpracy z naukowcami z Niemiec, Danii i Francji. Zebrana wiedza w opublikowanych wspólnie pracach poruszała kwestie krzemu w aspekcie globalnym, ekosystemów morski, lądowych: leśnych i rolniczych. Moje zainteresowania dotyczyły krzemu w środowisku glebowym. W tamtym czasie wiedza na temat zasobów i przemian krzemu w glebie była niewystarczająca, zwłaszcza w porównaniu z innymi pierwiastkami, takimi jak Fe, Ca, N, itp. Z perspektywy gleboznawczej istniało wiele pytań dotyczących różnych form krzemu w glebach, np. form amorficznych, w tym biogenicznych, ich stabilności i dynamiki w zależności od różnych czynników glebotwórczych (skały macierzystej, pH gleby, rodzaju roślinności).

Pierwsze wspólne badania dotyczyły metod chemicznych ekstrakcji amorficznych związków krzemu (ASi) z gleb (Saccone 2007) jak również formy krzemu dostępnej dla roślin (Höhn 2008). Przeprowadzone badania dały jednoznaczny wynik, że metody z alkalicznymi ekstrahentami są bardziej wydajne niż metody w których zastosowano ekstrahenty o niskim pH (4,5).

W pracy Steinhöfel et al 2011 przedstawiono pierwsze badania dotyczące izotopów krzemu w glebach. Uzyskane wyniki badań wykazały, że ablacja laserem femtosekundowym UV MC ICP-MS stanowi narzędzie do scharakteryzowania sygnatury izotopowej krzemu głównych puli krzemowych pozostawionych po wietrzeniu i transporcie krzemu, które zmieniły glebę. Opal biogeniczny w postaci fitolitów wykazał ujemną sygnaturę izotopową Si wynoszącą około -0,4‰.

W związku z tym, że krzem zwiększa odporność roślin na różne stresy abiotyczne i biotyczne, jest on obecnie zaliczany do substancji korzystnych dla roślin. Poprzez intensyfikację rolnictwa człowiek ma bezpośredni wpływ na obieg krzemu w skali globalnej. Eksport Si powodowany zabieraniem plonów z pól prowadzi do strat Si w glebach rolniczych. Przeprowadzone badania na długoletnich doświadczeniach polowych oceniające wpływ różnych dawek nawożenia azotowo-fosforowo-potasowego (NPK) oraz nawożenia organicznego (zwrotu słomy) na wielkość eksportu krzemu z gleby, pokazały że recykling słomy

zapobiega desylikacji krzemu z gleby a tym samym jest on łatwym źródłem Si dla roślin uprawnych (Puppe et al. 2021).

Przez prawie 20 lat prowadzonych badań nad krzemem udało się odpowiedzieć na wiele pytań dotyczących form krzemu w środowisku glebowym oraz jego funkcji w systemie gleba-roślina (Schaller et al 2021). Człowiek w znacznym stopniu zakłóca naturalny obieg Si w ekosystemach, a tym samym wpływa na niektóre właściwości gleby (magazynowanie wody, dostępność składników odżywczych i stabilność mikroagregatów)(Schaller et al 2021). Aby uzyskać całościowy obraz wpływu Si na poziomie ekosystemu oraz wyjaśnić wzajemne oddziaływanie czynników abiotycznych i biotycznych w obiegu Si, potrzebne są dalsze badania łączące takie dziedziny nauki jak: gleboznawstwo, ekologię, fizjologię roślin oraz mikrobiologię (Kratz et al 2021).

Sommer M., Kaczorek D., Kuzyakov Y., Breuer J. 2006. Silicon pools and fluxes in soils and landscapes: A review. *Journal of Plant Nutrition and Soil Science* 169: 296-314.

Conley D. J., Sommer M., Meunier J. D., Kaczorek D., Saccone L., 2006: The Silicon Cycle. Human Perturbations and Impacts on Aquatic Systems. 3. Silicon in the Terrestrial Biogeosphere. *SCOPE* 66, pp 13-28.

Saccone L., D.J., Conley, E. Koning, D. Sauer, M. Sommer, D. Kaczorek, S. W., Blecker, E. F. Kelly. 2007. Assessing the extraction and quantification of amorphous silica (ASi) in soils and grassland ecosystems. *European Journal of Soil Science*, 58, 1446-1459,

Höhn A., Sommer M., Kaczorek D., Schalitz G., Breuer J. 2008. Silicon fractions in Histosols and Gleysols of a temperate grassland site. *Journal of Plant Nutrition and Soil Science* 171, 409-418

G. Steinhöfel, J. Breuer, F. von Blanckenburg, I. Horn, D. Kaczorek, M. Sommer. 2011. Micrometer silicon isotope diagnostics of soils by UV femtosecond laser ablation. *Chemical Geology*. 286: 280-289

D. Puppe, D. Kaczorek, J. Schaller, D. Barkusky, M. Sommer. 2021. Crop straw recycling prevents anthropogenic desilication of agricultural soil–plant systems in the temperate zone – Results from a long-term field experiment in NE Germany. *Geoderma* 403 115187

J. Schaller, D. Puppe, D. Kaczorek, R. Ellerbrock, M. Sommer. Silicon Cycling in Soils Revisited *Plants*, 10, 295.

O. Katz, D. Puppe, D. Kaczorek, N. B. Prakash, J. Schaller. 2021. Silicon in the Soil–Plant Continuum: Intricate Feedback Mechanisms within Ecosystems. *Plants* 2021, 10, 652

Ruda darniowych – właściwości i charakterystyka mikromorfologiczna

Tworząca się w wyniku procesów oksydacyjno - redukcyjnych ruda darniowa ma specyficzne właściwości fizyczne, chemiczne oraz interesującą budowę mikromorfologiczną. Rudy darniowe występują powszechnie na terenach nizinnych i w dolinach rzecznych, praktycznie na terenie całej Polski. Źródłem żelaza dla tworzących się wytrąceń żelazowych, konkrecji i rud darniowych są procesy wietrzeniowe pierwotnych minerałów skał macierzystych gleb, uwolnione związki żelaza ulegają przemieszczaniu/wymywaniu w profilu glebowym i w następstwie procesów oksydacyjnych-redukcyjnych wytrącają się. Żelazo może być przenoszone z wodami gruntowymi na duże odległości gdzie w strefie utleniania następuje jego wytrącanie i akumulacja. Makromorfologicznie możemy wydzielić kilka rodzajów rud darniowych: miękką rudę darniową, formę konkrecyjną (agregatową), odnianą blokową i masywne poziom (warstwy) rudy darniowej.

Rudy darniowe składają się głównie z tlenków żelaza (20-50% Fe), manganu (0,2-1% Mn), a także zawierają duże zawartości związków fosforu (2-4% P) i węgla organicznego (1-10%). Skład mineralogiczny rud darniowych jest bardzo złożony i heterogenny: getyt i ferrihydryt występują w profilach o naturalnym układzie poziomów i niezmiennych stosunkach wodnych, gdzie poziom wód gruntowych ulega znacznym wahaniom w ciągu całego roku, natomiast w strefie redukcyjnej profilu glebowego, przy znacznej zawartości substancji organicznej oraz fosforu, tworzą się: wiwianit i syderyt. Getyt, ferrihydryt, wiwianit oraz syderyt mogą występować w tych samych poziomach, co świadczy o zachodzących zmianach potencjału oksydacyjno-redukcyjnego.

Mikromorfologia rud darniowych jest bardzo ciekawa (Kaczorek Sommer 2003, Kaczorek & Zagorski 2007), gdyż wyjaśnia sam proces jej powstawania. W masywnych poziomach rudy darniowej mamy mikrostrukturę, porowatą, czasami masywną. Masę podstawową stanowią wodorotlenki żelaza (ferrihydryt), natomiast kanaliki i wolne przestrzenie wypełniają: krystalicznie igiełkowy getyt jak i izotropowe (amorficzne) wodorotlenki żelaza, o różnej intensywności barwy. W wielu miejscach pory wypełnione są kilkoma warstwami (coating) amorficznych związków żelaza, świadczy to o ciągłym napływie żelaza z wodą gruntową i jego utlenianiem i wytrącaniem. Konkrecyjna (agregatowa) ruda darniowa powstała w wyniku działalności człowieka, który poprzez melioracje gleb jak i uprawę rolniczą zaburzył naturalny

proces tworzenia się rud darniowych. Ta odmiana rudy darniowej posiada mikrostrukturę agregatową, zawiera więcej krystalicznego getytu, w formie promieniście włóknistego goethytu w porach i kanałach (coatings). Spotyka się czasami kilka generacji krystalicznego getytu. Większe ilości krystalicznego getytu można wytłumaczyć lepszym napowietrzeniem gleby jak i niższym poziomem wody gruntowej.

Miękka ruda darniowa ma mikrostrukturę gąbczastą (vughs), oprócz getytu, ferrihydrytu występuje również krystaliczny wiwianit i syderyt. Na getycie widoczne są często impregnaty manganowe. Ten typ rudy darniowej tworzy się w poziomach o charakterze redukcyjnym w obecności materii organicznej.

Ze względu na tak dużą zawartość żelaza, w trakcie lub po uformowaniu się rud darniowych może dochodzić do akumulacji metali ciężkich. Przyczyną takiej akumulacji może być specyficzne powinowactwo metali ciężkich do wodorotlenków żelaza w połączeniu z dużą powierzchnią właściwą tlenków. Aby zbadać czy nasze rudy darniowe zawierają metale ciężkie, przeprowadziłam w Instytucie Gleboznawstwa w Bonn analizę frakcjonowaną form metali ciężkich, glinu i fosforu (Kaczorek et al. 2009). Wyniki badań wykazały, że zawartość Cr, Co, Ni, Zn, Cd i Pb nie przekracza wartości naturalnych dla gleb piaszczystych. Jedynie całkowita zawartość Mn była nieco wyższa. Najwyższe zawartości wszystkich metali ciężkich uzyskano we frakcjach tlenku żelaza V (okludowanej w niekrystalicznych i słabo krystalicznych tlenkach Fe) i VI (okludowanej w krystalicznych tlenkach Fe). Wyniki wskazują na wyraźną zależność pomiędzy zawartością Fe a ilością Zn i Pb oraz P. Frakcje rozpuszczalne w wodzie oraz dostępne dla roślin były w większości przypadków poniżej granicy wykrywalności. Biorąc pod uwagę obecną sytuację w badanych tu krajobrazach z glebami glejowymi zawierającymi rudy darniowe, można uznać, że zawartość metali ciężkich w rudach darniowych nie stanowi zagrożenia dla zdrowia ludzi i zwierząt.

Ruda darniowa : orsztyń (Ortstein) badania porównawcze

Do tej pory termin orsztyń (Ortstein) był często używany zamiennie z rudą darniową. Dlatego też przeprowadziliśmy badania porównawcze rudy darniowej i orsztyń w celu opracowania archetypów obu utwardzonych poziomów (utworów) (Kaczorek et al. 2004). Ruda darniowa posiadała mikrostrukturę porowatą składającą się prawie wyłącznie z wodorotlenków żelaza, podczas gdy orsztyń charakteryzował się mikrostrukturą mostkową

widoczną między ziarnami kwarcu. Wyraźne różnice pomiędzy tymi dwoma utworami odnotowano w składzie chemicznym i morfologii otoczek (coatings), a także rodzaju materii organicznej. Jediną cechą wspólną był mikroszkielet, który składał się w obu utworach z kwarcu. Również analizy chemiczne wykazały wyraźne różnice pomiędzy utwardzonymi poziomami. Ruda darniowa charakteryzował się znacznie wyższą zawartością pierwiastków wrażliwych na redoks (Fe, Mn), fosforu, jak również wyższym pH i niższą zawartością mobilnego Al w porównaniu z orsztyнем. Ponadto orsztyн często wykazywał wyższą zawartość organicznie związanego żelaza i glinu. Na podstawie dodatkowych obserwacji dotyczących rzeźby terenu i poziomu wód gruntowych stwierdzono, że powstawanie orsztyну związane jest z procesami bielnicowania, a rudy darniowej z procesami glejowymi.

Kaczorek D., Sommer M. 2003. Micromorphology, chemistry and mineralogy of bog iron ores from Poland. Catena 54, 393-402

Kaczorek D., Z. Zagórski. 2007. Micromorphological characteristics of the Bsm horizon in soils with bog iron ore. Polish Journal of Soil Science, Vol. XL, No. 1, 81-87.

Kaczorek D., Brümmer G., Sommer M. 2009. Content and Binding Forms of Heavy Metals, Aluminium and Phosphorus in Bog Iron Ores from. JEQ. 38: 1109-1119

Kaczorek D., Sommer M., Andruschkewitsch I., Oktaba L., Czerwiński Z., Stahr K. 2004. A comparative micromorphological and chemical study of "Raseneisenstein (bog iron ore) and "Ortstein". Geoderma 121, 83-94.

5. INFORMACJA O WYKAZYWANIU SIĘ ISTOTNĄ AKTYWNOŚCIĄ NAUKOWĄ ALBO ARTYSTYCZNĄ REALIZOWANA W WIĘCEJ NIŻ JEDNEJ UCZELNI, INSTYTUCJI NAUKOWEJ LUB INSTYTUCJI KULTURY, W SZCZEGÓLNOŚCI ZAGRANICZNEJ.

Od roku 2007 posiadam status „scientific visitor” w Centrum Badań Krajobrazu Rolniczego im. Leibniza (ZALF, Müncheberg, Niemcy). Badając zagadnienia krzemu (biogenicznego) w środowisku glebowym brałam udział w realizacji następujących projektów:

- DFG project – PAK 179 “Multiscale analysis of Si cycling in terrestrial biogeosystems”. (2007-2012)

- DFG project - "Spatiotemporal dynamics of biogenic Si pools in initial soils and their relevance for desilication" (SO 302/7-1). (2013-2016)
- DFG project - PU 626/2-1 "Biogenic Silicon in Agricultural Landscapes (BiSiAL) – Quantification, Qualitative Characterization, and Importance for Si Balances of Agricultural Biogeosystems". (2019-2020)
- Reduction of environmental and climate impacts of agricultural crop production through the use of an optimized topsoil deepening technique (2020-2022).

W latach 1998-2004 współpracowałam z Uniwersytetem w Hohenheim, Stuttgart, Niemcy. W tym czasie odbyłam dwa staże naukowe w Instytucie Gleboznawstwa i Oceny Gruntów. Efektem naszej współpracy są wspólne publikacje naukowe z zakresu badań nad przemianami związków żelaza w glebie, rudą darniową i orsztynem.

6. INFORMACJA O OSIĄGNIĘCIACH DYDAKTYCZNYCH, ORGANIZACYJNYCH ORAZ POPULARYZUJĄCYCH NAUKĘ LUB SZTUKĘ.

Przedmioty dydaktyczne prowadzone od 2001 roku na SGGW w Warszawie:
Gleboznawstwo (ćwiczenia), kierunek: rolnictwo, biologia, ochrona środowiska, ogrodnictwo, inżynieria środowiskowa.

Zajęcia terenowe prowadzone od 2001 roku na SGGW w Warszawie ze studentami studiów dziennych i zaocznych na Wydziałach: Rolnictwa i Biologii, Inżynierii Środowiska, Ogrodnictwa, Międzywydziałowym Studium Ochrony Środowiska

W Instytucie ZALF prowadziłam zajęcia z mikromorfolgii gleb dla studentów Uniwersytetu Poczdamskiego (2018).

W 2002 roku byłam „opiekunem Roku” dla pierwszego roku studiów na Wydziale Rolniczym.

2.12.2021

Danuta Kacwał

(podpis wnioskodawcy)



Leibniz Centre for
Agricultural Landscape Research
(ZALF)

Leibniz Centre for Agricultural Landscape Research (ZALF)
Eberswalder Straße 84, 15374 Müncheberg, Germany

Univ.-Prof. Dr. habil. Michael Sommer

Co-Head RA1 "Landscape Functioning"
Head WG "Landscape Pedology"
Head WG "Si Biogeochemistry"

T 0049 33432 82 - 282
F 0049 33432 82 - 280
E sommer@zalf.de

To whom it may refer

Eberswalder Straße 84
15374 Müncheberg
Germany
www.zalf.de

November 19, 2021

Declaration of co-authorships

I hereby declare that in the work: M. Sommer, H. Jochheim, A. Höhn, J. Breuer, Z. Zagorski, J. Busse, D. Barkusky, K. Meier, D. Puppe, M. Wanner, and D. Kaczorek, 2013 "**Si cycling in a forest biogeosystem – the importance of transient state biogenic Si pools**", Biogeosciences, Volume 10, No. 7, pp 4991-5007, my individual contribution consisted of: definition of research concepts, selection of research object, research methods; formulation of the main research goals; interpretation of research results; preparation of graphs, tables and figures, writing the final version of the manuscript.

Dr. Hubert Jochheim is currently retired, I as project manager declare that in the publication: M. Sommer, H. Jochheim, A. Höhn, J. Breuer, Z. Zagorski, J. Busse, D. Barkusky, K. Meier, D. Puppe, M. Wanner, and D. Kaczorek, 2013 "**Si cycling in a forest biogeosystem – the importance of transient state biogenic Si pools**", Biogeosciences, Volume 10, No. 7, pp 4991-5007, his individual contribution consisted of calculation and modeling of Si fluxes, partial preparation of the text of the publication.

Dr. Axel Höhn is now retired, I as project manager declare that in the publication: M. Sommer, H. Jochheim, A. Höhn, J. Breuer, Z. Zagorski, J. Busse, D. Barkusky, K. Meier, D. Puppe, M. Wanner, and D. Kaczorek, 2013 "**Si cycling in a forest biogeosystem – the importance of transient state biogenic Si pools**", Biogeosciences, Volume 10, No. 7, pp 4991-5007, his individual contribution consisted of taking soil samples and preparing them for research, performing and / or supervising analyzes of basic soil properties, analyzes of various forms of silicon, analysis of soil material in a scanning microscope, preparation of tables with results, interpretation of results, participation in the preparation of the text of the manuscript.

I hereby declare that in the work: D. Puppe, A. Höhn, D. Kaczorek, M. Wanner, M. Wehrhan, M. Sommer, 2017, "**How big is the influence of biogenic silicon pools on short-term changes in water-soluble silicon in soils? Implications from a study of a 10-year-old soil-plant system**", Biogeosciences, 14,

Scientific Director: Prof. Dr. Frank Ewert
Administrative Director: Martin Jank
Register of Associations VR 35 35, District court Frankfurt/Oder



Volksbank Fürstenwalde
IBAN DE72 1709 2404 0000 7700 00
BIC GENODEF1FW1
UST-ID DE811417184

5239–5252, my individual contribution consisted of creating a work concept, interpretation of research results and fund raising.

I hereby declare that in the work: D. Kaczorek, D. Puppe, J. Busse, M. Sommer, 2019 "**Effects of phytolith distribution and characteristics on extractable silicon fractions in soils under different vegetation – An exploratory study on loess**". Geoderma 356, my individual contribution consisted in the participation of result interpretation.

I hereby declare that in the work: D. Kaczorek, Sommer M., 2004 "**Silicon cycle in terrestrial biogeosystems of temperate climate**". Roczniki Gleboznawcze. T. LV No 3, 221-230, my individual contribution consisted of creating a work concept, collecting literature, preparing drawings.

Kind regards

A handwritten signature in blue ink, appearing to read 'Michael Sommer', with a large loop at the beginning and a long horizontal stroke at the end.

(Univ.-Prof. Dr. habil. Michael Sommer)

Marc Wehrhan

Research Area "Landscape Functioning"

Working Group "Landscape Pedology"

Leibniz-Centre for Agricultural Landscape Research (ZALF) e.V.

Eberswalder Str. 84

15374 Müncheberg

Germany

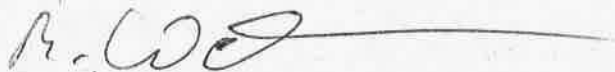
Tel.: + 49 33432 82109

E-mail: wehrhan@zalf.de

Müncheberg 22.11.2021

Declaration of co-authorship

I hereby declare that in the work: D. Puppe, A. Höhn, D. Kaczorek, M. Wanner, M. Wehrhan, M. Sommer, 2017, "How big is the influence of biogenic silicon pools on short-term changes in water-soluble silicon in soils? Implications from a study of a 10-year-old soil-plant system", *Biogeosciences*, 14, 5239–5252, my individual contribution consisted of determination and calculation of the average biomass for two plant species (*C. epigejos* and *P. australis*) on the Chicken Creek study plot, interpretation of results.



Dr. Daniel Puppe

Research Area "Landscape Functioning"

Working Group "Si-Biogeochemistry"

Leibniz-Centre for Agricultural Landscape Research (ZALF)

Eberswalder Str. 84

15374 Müncheberg

Germany

Tel.: + 49 33432 824077

Email: daniel.puppe@zalf.de

Müncheberg, 18.11.2021

Declaration of co-authorship

I hereby declare that in the work: M. Sommer, H. Jochheim, A. Höhn, J. Breuer, Z. Zagorski, J. Busse, D. Barkusky, K. Meier, D. Puppe, M. Warner, and D. Kaczorek, 2013 "Si cycling in a forest biogeosystem – the importance of transient state biogenic Si pools", Biogeosciences, Volume 10, No. 7, pp 4991-5007, my individual contribution consisted of enumeration of testate amoebae, interpretation of research results, and preparation of the manuscript text referring to testate amoebae.



D. Puppe

Dr. Daniel Puppe

Research Area "Landscape Functioning"

Working Group "Si-Biogeochemistry"

Leibniz-Centre for Agricultural Landscape Research (ZALF)

Eberswalder Str. 84

15374 Müncheberg

Germany

Tel.: + 49 33432 824077

Email: daniel.puppe@zalf.de

Müncheberg, 18.11.2021

Declaration of co-authorship

I hereby declare that in the work: D. Puppe, A. Höhn, D. Kaczorek, M. Wanner, M. Wehrhan, M. Sommer, 2017, "How big is the influence of biogenic silicon pools on short-term changes in water-soluble silicon in soils? Implications from a study of a 10-year-old soil-plant system", *Biogeosciences*, 14, 5239–5252, my individual contribution consisted of collecting soil samples, performing soil analyses, and leading the writing of the paper.



.....
D. Puppe

Dr. Daniel Puppe

Research Area "Landscape Functioning"

Working Group "Si-Biogeochemistry"

Leibniz-Centre for Agricultural Landscape Research (ZALF)

Eberswalder Str. 84

15374 Müncheberg

Germany

Tel.: + 49 33432 824077

E-mail: daniel.puppe@zalf.de

Müncheberg, 24.11.2021

Declaration of co-authorship

Due to the fact that Dr. Axel Höhn is retired I, as the first author of the published article, declare that his participation in the work: D. Puppe, A. Höhn, D. Kaczorek, M. Wanner, M. Wehrhan, M. Sommer, 2017, "How big is the influence of biogenic silicon pools on short-term changes in water-soluble silicon in soils? Implications from a study of a 10-year-old soil-plant system", Biogeosciences, 14, 5239–5252, comprised the following: collection of soil and plant samples, chemical analyses of silicon in soils and plants, and interpretation of corresponding results.



D. Puppe

Dr. Daniel Puppe

Research Area "Landscape Functioning"

Working Group "Si-Biogeochemistry"

Leibniz-Centre for Agricultural Landscape Research (ZALF)

Eberswalder Str. 84

15374 Müncheberg

Germany

Tel.: + 49 33432 824077

Email: daniel.puppe@zalf.de

Müncheberg, 18.11.2021

Declaration of co-authorship

I hereby declare that in the work: D. Kaczorek, D. Puppe, J. Busse, M. Sommer, 2019 "Effects of phytolith distribution and characteristics on extractable silicon fractions in soils under different vegetation – An exploratory study on loess". Geoderma 356/ 113917/2019, my individual contribution consisted of measuring phytolith surface roughness parameters, performing statistical analyses, interpreting the corresponding results, and writing the manuscript together with Danuta Kaczorek.



.....
D. Puppe

Kristin Meier
Research Platform „Data Analysis and Simulation“
Working Group: Research Data Management (Service)
Leibniz-Centre for Agricultural Landscape Research (ZALF) e.V.
Eberswalder Str. 84
15374 Müncheberg
Germany
T +49 33432 82 4086
kristin.meier@zalf.de

Müncheberg 20.11.2021

Declaration of co-authorship

I hereby declare that in the work: M. Sommer, H. Jochheim, A. Höhn, J. Breuer, Z. Zagorski, J. Busse, D. Barkusky, K. Meier, D. Puppe, M. Wanner, and D. Kaczorek, 2013 “Si cycling in a forest biogeosystem – the importance of transient state biogenic Si pools”, Biogeosciences, Volume 10, No. 7, pp 4991-5007, my individual contribution consisted of collecting and processing information on the history of use of the studied area over the last 250 years.



.....
signature

Dr Dietmar Barkusky
Working Group: Experimental Station Müncheberg (Service)
Experimental Infrastructure Platform
Leibniz Centre for Agricultural Landscape Research (ZALF)
Eberswalder Straße 84
15374 Müncheberg
T +49 33432 82 168
dbarkusky@zalf.de

Müncheberg 23.11.2021

Declaration of co-authorship

I hereby declare that in the work: M. Sommer, H. Jochheim, A. Höhn, J. Breuer, Z. Zagorski, J. Busse, D. Barkusky, K. Meier, D. Puppe, M. Wanner, and D. Kaczorek, 2013 "Si cycling in a forest biogeosystem – the importance of transient state biogenic Si pools", Biogeosciences, Volume 10, No. 7, pp 4991-5007, my individual contribution consisted of monitoring and management of the research object.



apl. Prof. PD Dr. rer. nat. habil. Manfred Wanner
Brandenburg University of Technology Cottbus-Senftenberg,
Dept. Ecology,
LG 2C, Room 217
Konrad-Wachsmann-Allee 6,
03013 Cottbus, Germany
T+49 0355 69 2738
e-mail: wanner@b-tu.de

Cottbus 19 Nov 2021

Declaration of co-authorship

I hereby declare that in the work: D. Puppe, A. Höhn, D. Kaczorek, M. Wanner, M. Wehrhan, M. Sommer, 2017, "How big is the influence of biogenic silicon pools on short-term changes in water-soluble silicon in soils? Implications from a study of a 10-year-old soil-plant system", Biogeosciences, 14, 5239–5252, my individual contribution consisted of analysis of testate amoebae, interpretation of research results.



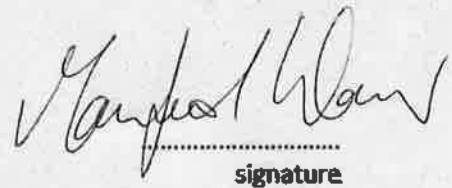
signature

apl. Prof. PD Dr. rer. nat. habil. Manfred Wanner
Brandenburg University of Technology Cottbus-Senftenberg,
Dept. Ecology,
LG 2C, Room 217
Konrad-Wachsmann-Allee 6,
03013 Cottbus, Germany
T+49 0355 69 2738
e-mail: wanner@b-tu.de

Cottbus 19 Nov 2021

Declaration of co-authorship

I hereby declare that in the work: M. Sommer, H. Jochheim, A. Höhn, J. Breuer, Z. Zagorski, J. Busse, D. Barkusky, K. Meier, D. Puppe, M. Wanner, and D. Kaczorek, 2013 "Si cycling in a forest biogeosystem – the importance of transient state biogenic Si pools", Biogeosciences, Volume 10, No. 7, pp 4991-5007, my individual contribution consisted of analysis of testate amoebae, interpretation of research results.




.....
signature

Warszawa , dn. 18.11.2021.]

Dr hab. Zbigniew Zagórski prof. SGGW
Katedra Gleboznawstwa SGGW
ul. Nowoursynowska 195
02-776 Warszawa
0225932611
zbigniew_zagorski@sggw.edu.pl

Oświadczenie o współautorstwie

Niniejszym oświadczam, że w pracy: „Si cycling in a forest biogeosystem – the importance of transient state biogenic Si pools. Biogeosciences, Volume 10, No. 7, pp 4991-5007, 2013” mój indywidualny udział w jej powstaniu polegał na: odpowiednie przygotowaniu próbek glebowych analizy oraz analiza mineralogiczna próbek glebowych metodą dyfrakcji rentgenowskiej (XRD), interpretacja otrzymanych wyników badań.



.....
Podpis

Jacqueline Busse
Research Area "Landscape Functioning"
Working Groups "Landscape Pedology"
Leibniz-Centre for Agricultural Landscape Research (ZALF) e.V.
Eberswalder Str. 84
15374 Müncheberg
Germany
Tel.: + 49 33432 82269
E-mail: jbusse@zalf.de

Müncheberg 22.11.2021

Declaration of co-authorship

I hereby declare that in the works:

1. M. Sommer, H. Jochheim, A. Höhn, J. Bréuer, Z. Zagorski, J. Busse, D. Barkusky, K. Meier, D. Puppe, M. Wanner, and D. Kaczorek, 2013 "Si cycling in a forest biogeosystem – the importance of transient state biogenic Si pools", *Biogeosciences*, Volume 10, No. 7, pp 4991-5007, my individual contribution consisted of taking all phytolith images under a scanning microscope (SEM), performing elemental composition analysis of isolated phytoliths using a microprobe (SEM-EDX)
2. D. Kaczorek, D. Puppe, J. Busse, M. Sommer, 2019 "Effects of phytolith distribution and characteristics on extractable silicon fractions in soils under different vegetation – An exploratory study on loess". *Geoderma* 356/ 113917/2019, my individual contribution consisted of taking all phytolith images under a scanning microscope (SEM), performing elemental composition analysis of isolated phytoliths using a microprobe (SEM-EDX).

Jacqueline Busse

Dr. Marion Tauschke
Administratorin
Research Area 1 "Landscape Functioning"
Leibniz Centre for Agricultural Landscape Research (ZALF)
Eberswalder Straße 84
15374 Müncheberg
T +49 (0)33432 82-249
F +49 (0)33432 82-343
E-Mail: mtauschke@zalf.de

Müncheberg 2.12.2021

Attestation

I hereby certify that, with effect from 1 June 2019, Dr Danuta Kaczorek is conducting research at ZALF in the following two projects:

1. 2019-2022 Reduction of environmental and climate impacts of agricultural crop production through the use of an optimized topsoil deepening technique. Research Area 1 "Landscape Functioning" WG: Landscape Pedology, Leibniz Centre for Agricultural Landscape Research.
2. 2018-2022 (DFG) under grant PU 626/2-1 (Biogenic Silicon in Agricultural Landscapes (BiSiAL) – Quantification, Qualitative Characterization, and Importance for Si Balances of Agricultural Biogeosystems). Research Area 1 "Landscape Functioning" WG: Silicon Biogeochemistry, Leibniz Centre for Agricultural Landscape Research

Dr. Danuta Kaczorek's research internship in Zalf will end on May 31, 2022.

M. Tauschke

**Leibniz-Centre for Agricultural
Landscape Research (ZALF) e.V.**
Research Area 1
"Landscape Functioning"
Eberswalder Straße 84, D - 15374 Müncheberg, Germany
Fon: +49 (0)33432-82 282 / 82 240 Fax: +49 (0)33432-82 280

ARTYKUŁ PROBLEMOWY

DANUTA KACZOREK¹, MICHAEL SOMMER²

OBIEG KRZEMU W BIOGEOSYSTEMACH LĄDOWYCH KLIMATU UMIARKOWANEGO

SILICON CYCLE IN TERRESTRIAL BIOGEOSYSTEMS OF TEMPERATE CLIMATE

¹Zakład Gleboznawstwa, Katedra Nauk o Środowisku Glebowym, SGGW, Warszawa, Polska; ²ZALF – Centre for Agricultural Landscape and Land Use Research, Institute of Soil Landscape Research, Muencheberg, Germany

Abstract: Silica triggers global carbon cycle through Si-C coupling in diatom biomass production of the oceans. The greatest Si source for the oceans are the continents, where weathering of silicates and subsequent leaching of Si via soil solution is the ultimate Si source for the ocean. Here we summarize the actual knowledge of the most important pools, transformations and fluxes of the Si cycle in the terrestrial biogeosystems. Principally, weathering and subsequent release of Si may lead to (i) secondarily bound Si in newly formed aluminium silicates, (ii) amorphous silica precipitation on surfaces of other minerals, (iii) plant uptake and subsequent re-translocation to soils (e.g. as phytoliths in litterfall) or (iv) final removal from soils (desilification). The research carried out hitherto focused on the participation of silicon in weathering processes. There are, however, only few investigations on the characteristics and controls of the low-crystalline almost pure silicon compounds formed during pedogenesis.

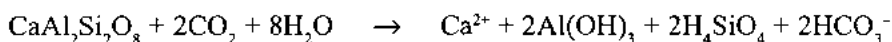
Słowa kluczowe: krzem, procesy glebotwórcze, desilifikacja, fitolity.

Key words: silicon, soil processes, desilification, phytoliths.

WSTĘP

Krzem jest jednym z najbardziej rozpowszechnionych na kuli ziemskiej pierwiastków. Stanowi 26% całości skorupy ziemskiej i wchodzi w skład ponad 370 minerałów skałotwórczych. Ponadto jest jednym z podstawowych składników gleb, gdyż jest elementem niemal wszystkich skał macierzystych gleb. Krzem jako drugi pod względem ilościowym pierwiastek skorupy ziemskiej odgrywa bardzo ważną rolę w globalnym obiegu materii. Głównym źródłem krzemu w środowiskach morskich są procesy

wietrzenia w *biogeosystemach lądowych* [Wollast, McKenzie 1983; Tréguer i in. 1995, Treuguer, Pondaven 2000, Treguer 2002, Conley 2002]. Z jednej strony biorąc pod uwagę całościowy proces wietrzenia krzemianów, którego intensywność jest uwarunkowana zmianami klimatu, krzem istotnie wpływa na obieg węgla w środowisku. W procesie wietrzenia anortytu do gibbsytu pewna ilość CO₂ zostaje zatrzymana w roztworze glebowym.



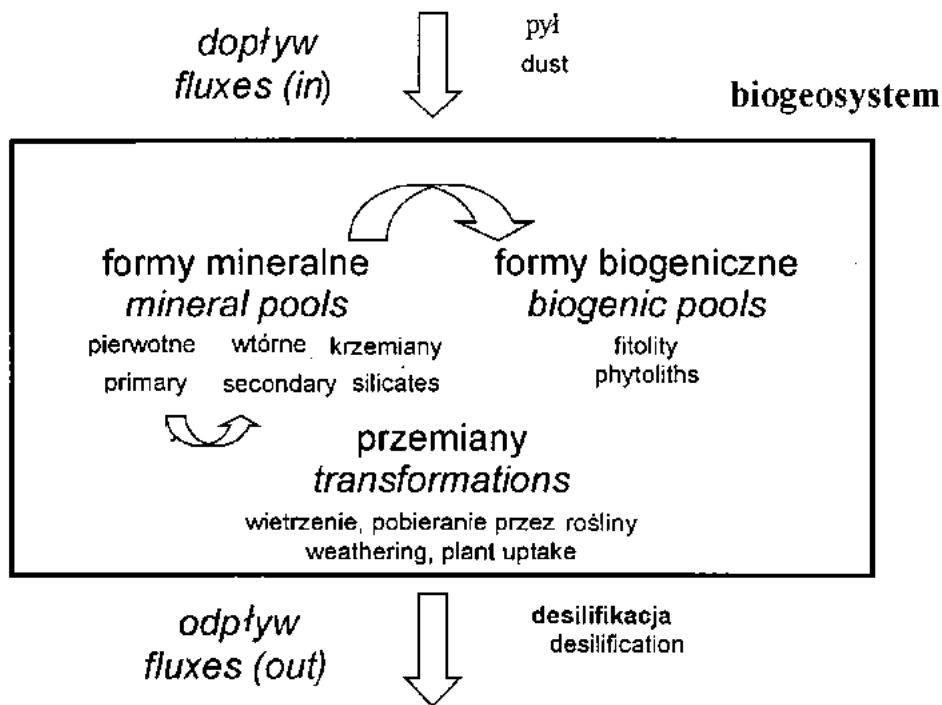
W dalszej kolejności następuje jego unieruchomienie w postaci węglanu wapnia lub magnezu w środowisku morskim [Berner 1995]. Można powiedzieć, że procesy wietrzenia krzemianów biorą udział w regulacji (buforowaniu) koncentracji CO₂ w atmosferze. Z drugiej strony rola oceanów jako magazynu węgla współdziała z globalnym obiegiem krzemu, który wykorzystywany jest do budowy komórek przez radiolarie i okrzemki, które stanowią znaczącą część morskiej biomasy. Im więcej jest osadów na dnie mórz, tym więcej węgla wyłączonego jest z obiegu materii. Największym źródłem związków krzemu dla oceanów są spływy tego pierwiastka z lądów z wodami rzek. Przeprowadzony przez Treguer i in. [1995] bilans pokazuje, że 80% krzemu w oceanach pochodzi z rzek i w ostateczności z wietrzenia krzemianów w biogeosystemach lądowych. Z tych 80% aż 20% krzemu dostarczają rzeki klimatu umiarkowanego. Dlatego ważne jest przedstawienie, jakim przemianom i procesom podlegają związki krzemu w glebach oraz jakie czynniki wpływają na formy przenoszonych związków krzemu (wolnego i biogenicznego), jak i na sam proces transportu [Conley 2002].

Artykuł przedstawia krótki opis obiegu krzemu w środowisku, jak również zwraca uwagę na pewne aspekty związane z przemianami krzemu w biogeosystemach lądowych, na które nie ma do tej pory odpowiedzi, a które są zdaniem autorów ważne dla lepszego zrozumienia całości zachodzących przemian.

FORMY I FUNKCJE KRZEMU W GLEBACH

W biogeosystemach lądowych klimatu umiarkowanego związki krzemu zgromadzone są w części mineralnej (*mineral pools*), którą dzielimy na pierwotną (krzemiany i glinokrzemiany) i wtórną (minerały ilaste, minerały własne krzemu powstałe w warunkach glebowych, np. wtórny kwarc, opal). Związki krzemu są gromadzone również w części biogenicznej (*biogenic pools*), są to fitolity, resztki organiczne i mikroorganizmy, które pod wpływem różnych czynników środowiska ulegają wietrzeniu i innym przemianom (*weathering, plant uptake*) w danym biogeosystemie. Pewne jednak ilości krzemu zostają wymyte z gleby (desilifikacja) i z przesiąkającą wodą opuszczają biogeosystem lądowy (*fluxes out*). W pewnych przypadkach może nastąpić dopływ związków krzemu do biogeosystemu (nawiewy pyłów z innych obszarów, np. pustyń), jednak proces ten w biogeosystemach klimatu umiarkowanego na ogół nie zachodzi na większą skalę (rys. 1).

Pierwotnym źródłem różnorodnych form krzemu w glebach są procesy wietrzeniowe pierwotnych i wtórnych krzemianów i glinokrzemianów [White, Brantley 1995]. Skały, zawierające w swoim składzie minerały bogate w związki krzemu i szklivo, pod wpływem różnych czynników środowiska ulegają wietrzeniu, co prowadzi do powstawania wtórnych minerałów krzemu o różnym stopniu krystalizacji, a także bezpostaciowego opalu i wolnej krzemionki (H₄SiO₄), która przechodzi do roztworu glebowego.



RYSUNEK 1. Krzem w biogeosystemach lądowych
 FIGURE 1. Si in terrestrial biogeosystems

Krzem w roztworze glebowym

Kwasy krzemowe znajdujące się w roztworze glebowym mogą występować w postaci kwasów monokrzemowych (kwas ortokrzemowy – H_4SiO_4 i metakrzemowy – H_2SiO_3) oraz kwasów polikrzemowych [Drees i in. 1989]. Te pierwsze zbudowane są z jednego atomu krzemu, atomów tlenu i wodoru. Kwas ortokrzemowy odgrywa bardzo dużą rolę w procesie dostępności pewnych pierwiastków dla roślin. Badania przeprowadzone przez Hall i Morrison [1906] wykazały wyraźną interakcję między jonami fosforu i jonami krzemu znajdującymi się w roztworze glebowym. W wyniku nawożenia gleby nawozami krzemowymi (amorficzna krzemionka lub żel krzemionkowy) wzrastał w glebie udział dostępnego dla roślin fosforu [Brogowski 2000, Gladkova 1982; Matichenkov, Ammosova 1996]. Odwrotne oddziaływanie krzemu stwierdzono w stosunku do jonów glinu. Badania laboratoryjne, jak i polowe wykazały, że nawożenie gleby odpowiednimi formami krzemu redukuje toksyczne działanie ruchomego glinu w glebach. Po pierwsze aktywna krzemionka podnosi wartość pH gleby [Lindsay 1979], po drugie kwas monokrzemowy jest adsorbowany przez wodorotlenki glinu, co osłabia mobilność glinu, a tym samym podwyższa tolerancję roślin na obecność ruchomego Al^{3+} [Panov i in. 1982]. Kwas monokrzemowy wiąże również metale ciężkie (Cd, Pb, Zn, Hg i inne) tworząc z nimi rozpuszczalne, lecz złożone związki oraz słabo rozpuszczalne krzemiany [Lindsay 1979], przez co zmniejsza mobilność tych metali w glebach oraz ich dostępność dla roślin.

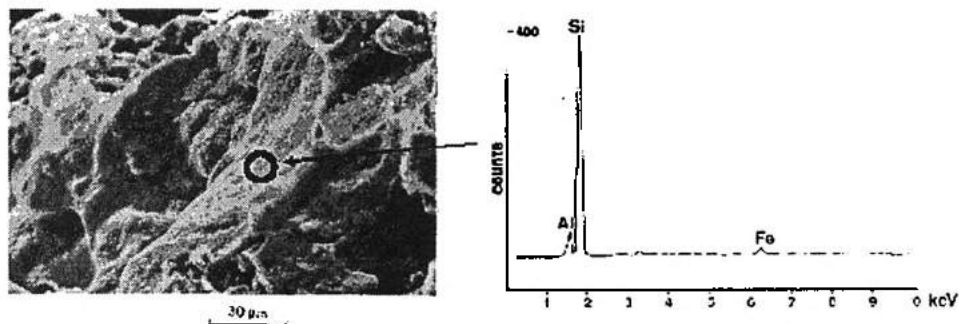
Kwasy monokrzemowe przechodzą w kwasy polikrzemowe, które też są integralną częścią roztworu glebowego [Drees i in. 1989]. Zbudowane są z dwóch lub więcej atomów krzemu, mogą występować w różnych formach, np. łańcuchy, rozgałęzienia

lub formy kuliste. W glebie, kwasy polikrzemowe oddziałują na właściwości fizyczne gleby [Dracheva 1975]. Są zdolne do tworzenia mostków krzemowych między cząsteczkami glebowymi, dzięki czemu wpływają na strukturę gleby [Dracheva 1975]. W glebie w fazie ciekłej występują również liczne połączenia kompleksowe między kwasami krzemowymi a organiczną i nieorganiczną częścią gleby [Matichenkov, Snyder 1996].

Krzem w fazie stałej gleby (części mineralnej)

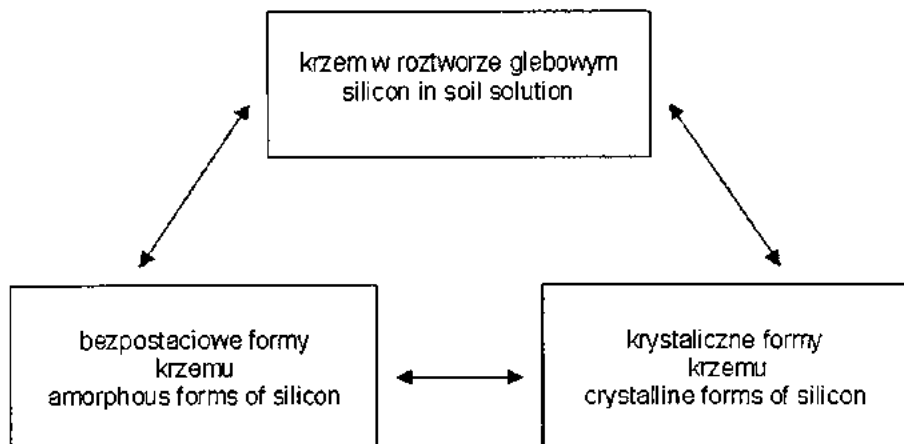
Kwasy krzemowe i polikrzemowe przechodzą w żele krzemionkowe, a te następnie w fazę stałą gleby, w której mogą występować jako minerały o różnym stopniu krystalizacji [Monger, Kelly 2002]. Do form krystalicznych zaliczamy minerały ilaste, wtórny kwarc. Do form bezpostaciowych należą minerały pochodzenia biologicznego (opal A, fitolity, bogate w Si szczątki roślinne i mikroorganizmy) i opal pochodzenia abiotycznego [Matichenkov, Bocharnikova 2001]. Ponadto w glebie powstaje szereg minerałów o strukturze nieuporządkowanej lub słabo uporządkowanej, takich jak: allofany, proto-imogolit oraz imogolit. Krystobalit można zaliczyć do minerałów kryptokrystalicznych.

Takie czynniki, jak: pH gleby, temperatura, obecność związków humusowych, mikroorganizmów, mają wpływ na powstawanie wtórnych minerałów krzemu w środowisku glebowym [Monger, Kelly 2002, Drees i in. 1989, Dove 1995, Gerard i in. 2002]. W wyniku zakwaszania środowiska glebowego minerały ilaste ulegają rozpadowi stając się jednocześnie następnym źródłem wolnej krzemionki [Veerhoff 1992, Frank 1993]. Wolna krzemionka osadza się w pewnych warunkach na ziarnach minerałów tworząc amorficzne skorupki i otoczki krzemionkowe [Veerhoff M. i Bruemmer G. W. 1993] (rys. 2). W procesie bielcowania związki krzemu i związki glinu znajdujące się w roztworze glebowym w odpowiednim stosunku (Al:Si ok. 2) mogą tworzyć nowe minerały, takie jak: imogolit [Lundstroem i in. 2000; Gustafsson i in. 1995; Anderson i in. 1997, 2000], proto-imogolit [Taylor 1988; Buurman, Van Reeuwijk 1984] i allofany [Farmer 1984, Farmer, Fraser 1982, Wada 1989]. Zjawisko to zachodzi w głębszych poziomach profilu glebowego, gdzie ilość substancji humusowych jest niewielka, a tym samym związki glinu nie tworzą z nimi stałych kompleksów, tylko ze znajdującymi się



RYSunEK 2. Amorficzna krzemionka na powierzchni minerału (po lewej) w poziomie Bt gleby płowej, EDX (po prawej); wg Veerhoffa M. i Bruemmera G. W. [1993]

FIGURE 2. Amorphous silica on mineral surfaces (left) of a loess-Luvisol Bwt horizon, energy dispersive X-ray spectrometry (EDX) (right); after Veerhoff and Bruemmer G. W. [1993]



RYSUNEK 3. Przemiany form krzemu w glebach
FIGURE 3. Transformation of silica forms in soils

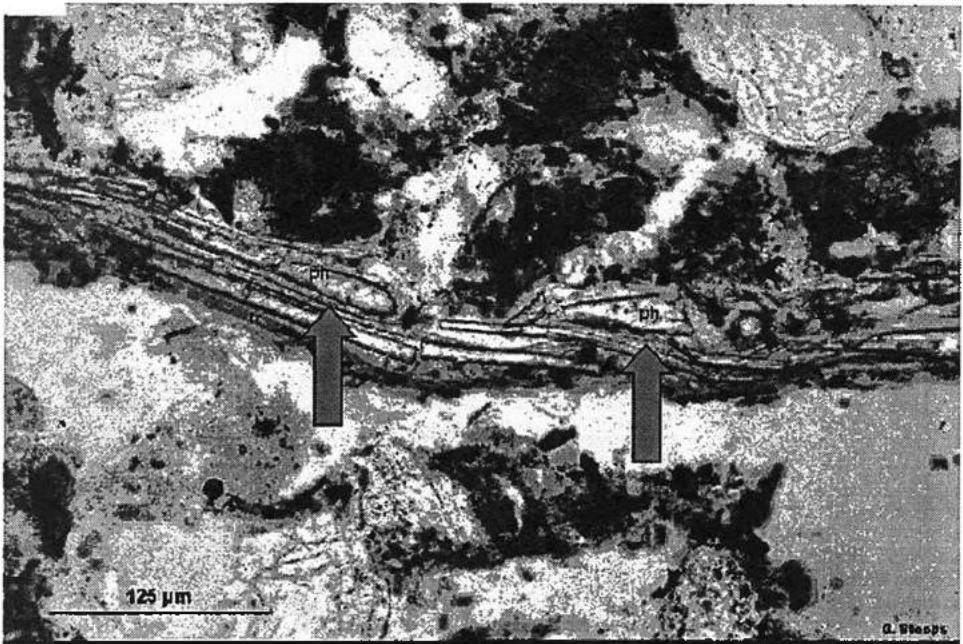
w roztworze glebowym związkami krzemu. Związki humusowe blokują powstawanie imogolitu, dlatego też w powierzchniowych poziomach gleb nie spotyka się tego minerału. Wyżej wymienione minerały możemy zaliczyć do minerałów glinowo-krzemowych.

Do krzemianów ubogich w związki glinu zaliczamy krystobalit i wtórny kwarc. Krystobalit jest minerałem skał wulkanicznych i powszechnie występuje w glebach wytworzonych z tychże skał. W innych glebach jego obecność nie została potwierdzona [Drees i in. 1989]. Jedynie w procesie diagenety opalu A (forma abiotyczna) przechodzi w krystobalit, a ten we wtórny kwarc. Wtórny kwarc może również powstawać z opalu (forma niebiotyczna) znajdującego się w scementowanych poziomach glebowych (np. duripan, orsztyń) lub powstaje bezpośrednio z żelu krzemionkowego omijając pozostałe fazy [Drees i in. 1989; Monger, Kelly 2002].

W wyniku ciągłych procesów zachodzących w środowisku glebowym różne formy krzemu (krystaliczne, bezipostaciowe oraz formy występujące w roztworze glebowym) mogą przechodzić jedne w drugie (rys. 3).

Krzem pochodzenia roślinnego

Krzem znajdujący się w roztworze glebowym może być włączony w wewnętrzny obieg materii danego biogeosystemu [Lucas 2001] (rys. 1). Jest on w formie H_4SiO_4 pobierany biernie przez rośliny wraz z wodą, a następnie odkładany w komórkach i tkankach roślinnych [Kaufman i in. 1981]. Efektem tego procesu jest obecność w suchej masie roślinnej pewnej ilości krzemu, która może wynosić od 0,1 do 10% [Danoff i in. 2001, Epstein 1994, Raven 1983]. Badania składu opadu liści i igieł w lasach występujących na glebach brunatnych wykazały, że zawartość Si w liściach buka wynosi od 0,1 mol Si · kg s.m.⁻¹, w igłach świerka waha się od 0,07 do 0,35 mol Si · kg s.m.⁻¹ [Ellenberg i in. 1986]. W przypadku igieł świerka istnieje istotna zależność między ilością krzemu a wiekiem igieł; im starsze igły, tym zawartość Si jest wyższa. Roczny opad listowia dostarcza do gleby od 760 mol · ha⁻¹ · r⁻¹ (buk) do 1900 mol · ha⁻¹ · r⁻¹ (świerk) krzemu. Nieco niższe nagromadzenie w ściółce (1400 mol · ha⁻¹ · r⁻¹) stwierdził Bartoli [1983], natomiast Prusinkiewicz i in. [1974] ustalili, że zwrot Si do gleby piaskowej



RYSUNEK 4. Fitolity (patrz strzałki) w powierzchniowych poziomach gleby, zdjęcie pochodzi z pracy Stoopsa [2003] (za przyzwoleniem Soil Science Society of America)
 FIGURE 4. Phytoliths (arrow) in topsoils, photo by Stoops [2003] (by courtesy of the Soil Science Society of America)

z opadem roślinnym mieści się w przedziale od $1400 \text{ mol} \cdot \text{ha}^{-1} \cdot \text{r}^{-1}$ (w borze mieszanym) do $2400 \text{ mol} \cdot \text{ha}^{-1} \cdot \text{r}^{-1}$ (w lesie świeżym). Jakie ilości krzemu przejdą do roztworu glebowego, a następnie zostaną ponownie pobrane, zależy od intensywności rozkładu biologicznego ściółki oraz od formy biogenicznej samego krzemu. Pewna część krzemu będzie w formie fitolitów (rys. 4), a tym samym nastąpi jego czasowe unieruchomienie [Bartoli 1985, Drees i in. 1989, Meunier i in. 1999, Meunier, Colin 2001, Watteau, Villemin 2001]. Ilość fitolitów w glebie w poziomach genetycznych wynosi od 0,1 do 5,0%, a niekiedy nawet więcej [Wilding, Drees 1971, Alexandre i in. 1997, Clarke 2003]. Tylko nieliczne badania uwzględniają to ważne czasowe zatrzymanie krzemu w glebie, brak jest natomiast opracowań dotyczących tego zjawiska w różnych glebach.

Desilifikacja

Pewna jednak ilość amorficznych form krzemu głównie w postaci kwasów krzemowych ulega wymyciu z profilu glebowego przez wodę przesiąkającą, proces ten nazywany jest odkrzemianowaniem gleby (desilifikacją) (rys. 1). Desilifikacja w wielu glebach zachodzi w dużym natężeniu we wszystkich strefach klimatycznych Ziemi. W glebach jeszcze słabo rozwiniętych klimatu subarktycznego ilość wymywanego krzemu ($500\text{--}1200 \text{ mol Si} \cdot \text{ha}^{-1} \cdot \text{r}^{-1}$) [Anderson i in. 1997, 2000] jest równie wysoka jak w glebach dobrze wykształconych występujących w klimacie tropikalnym ($700 \text{ mol} \cdot \text{ha}^{-1} \cdot \text{r}^{-1}$) [Oliva i in. 1999]. Wielkość desilifikacji zależy od charakteru skały macierzystej gleb, klimatu, jak również od wieku materiału glebowego oraz od intensywności przebiegu samych procesów glebotwórczych. Roczne wymywanie Si z

gleby w klimacie umiarkowanym jest prawie na podobnym poziomie co w glebach pozostałych klimatów. W glebach stagnoglejowych jest ono najwyższe i wynosi 950–1670 mol Si · ha⁻¹ · r⁻¹ [Meesenburg, Mueller 1992; Heyn 1989], w glebach bielcowych wynosi 880–1090 mol Si · ha⁻¹ · r⁻¹, a w glebach brunatnych – 320–590 mol Si · ha⁻¹ · r⁻¹ [Armbruster 1998; Heyn 1989]. W podobnych warunkach klimatycznych i petrograficznych istnieje ilościowy związek między wiekiem gleby a wielkością desilifikacji [Anderson i in. 2000, White 1995]. Niejasne jest natomiast, czy istnieje jakaś hierarchia czynników kierujących procesem desilifikacji.

Czynniki glebowe wpływające na ilość wolnego krzemu w glebach

Do najważniejszych czynników wpływających na ilość pedogenicznych form krzemu w glebach należą:

Rodzaj skały macierzystej – petrograficzne właściwości skał, np. zawartość łatwo wietrzejących minerałów, wydatnie wpływają na jakość procesów wietrzeniowych i, w konsekwencji, na rodzaj i ilość związków krzemu w glebach [Bluth, Kump 1994; White 1995].

Odczyn gleby (pH) – zgodnie z zasadą równowagi chemicznej, procesy wietrzeniowe i mobilność krzemu powinny być związane z pH roztworu glebowego. pH znacząco wpływa na dysocjację H₄SiO₄, zdysocjowany kwas łatwiej migruje, lecz forma niezdisocjowanego kwasu, o ile jego stężenie nie przekracza granicy rozpuszczalności, także podlega wymyciu [Dove 1995].

Warunki redoks (Eh) – poziomy glebowe podlegające naprzemiennym procesom redukcji i utleniania żelaza wykazują wyższe koncentracje niekryształicznych form krzemu w porównaniu z poziomami glebowymi, w których nie zachodzą reakcje redoks [Sommer 2002]. Powstałe żele żelaza i krzemionki są niestabilne podczas warunków beztlenowych oraz w wyniku utleniania żelaza (Fe³⁺). Wówczas krzem uwalniany jest do roztworu glebowego [Morris, Fletcher 1987]. Innym mechanizmem może być tzw. “ferroliza” [Van Ranst, De Coninck 2002, Rueckert 1992, Eağub, Blume 1982, Brinkmann 1970, 1979] polegająca na rozpadzie minerałów ilastych na skutek naprzemiennych warunków utleniania i redukcji i towarzyszących im zmianom pH.

Rodzaj roślinności – niektóre rośliny, np. trawy, skrzypy pobierają większe niż inne rośliny ilości krzemu i w konsekwencji dostarczają więcej krzemu do gleb po obumarciu [Raven 1983; Epstein 1994; Datnoff i in. 2001]. Zatem rodzaj roślinności i sposób wykorzystania gleby może mieć kluczowe znaczenie dla obiegu biogenicznej krzemionki i w dalszej kolejności dla zawartości fitolitów w glebie.

PODSUMOWANIE

Liczne badania nad obiegiem krzemionki w środowisku naturalnym miały na celu poznanie różnych niekryształicznych postaci krzemu w celu określenia stężenia krzemu w roztworach [Conley 2002]. Mimo tego ilości amorficznej krzemionki (w tym fitolitów), jak również jej przeobrażenia/przemieszczenia należą wciąż do mało poznanych zjawisk

w gleboznawstwie. Tak się dzieje również w przypadku badań przeprowadzanych na obszarze Polski. Dlatego należałoby się zastanowić, jakie czynniki, procesy i właściwości wpływają na zawartość i aktywność amorficznej krzemionki w glebach.

Postawione zadanie wymaga zastanowienia się nad szeregiem zagadnień:

1. Czy gleby o różnym pochodzeniu mają różne zawartości amorficznych związków krzemu i w jaki sposób te wartości zależą od czynników i procesów glebotwórczych?
2. Jaka metodę chemiczną należy zastosować do wyekstrahowania niekryształicznych związków krzemu?
3. Jakie ilości amorficznego krzemu pochodzenia roślinnego (fitolity) są magazynowane w poziomach glebowych w zależności od rodzaju roślinności i warunków sprzyjających wietrzeniu?
4. Co powoduje migrację związków krzemu z powierzchniowych poziomów glebowych do poziomów głębszych, a w niektórych przypadkach nawet akumulację tych związków w głębszych poziomach?

LITERATURA

- ALEXANDRE A., MEUNIER J.D., COLIN F., KOUD J.M. 1997: Plant impact on the biogeochemical cycle of silicon and related weathering processes. *Geochim. et Cosmochim. Acta* **61**: 677–682.
- ANDERSON S.P., DREVER J.I., FROST C.D., HOLDEN P. 2000: Chemical weathering in the foreland of a retreating glacier. *Geochim. et Cosmochim. Acta* **64**: 1173–1189.
- ANDERSON S.P., DREVER J.I., HUPHREY N.F. 1997: Chemical weathering in glacial environments. *Geology* **25**: 399–402.
- ARMBRUSTER M. 1998: Zeitliche Dynamik der Wasser- und Elementflüsse in Waldoekosystemen. *Freiburger Bodenkundliche Abhandlungen* **38**: 301 ss.
- BARTOLI F. 1983: The biogeochemical cycle of silicon in two temperate forest ecosystems. *Ecol. Bull.* **35**: 469–476.
- BARTOLI F. 1985: Crystallochemistry and surface properties of biogenic opal. *J. Soil Sci.* **36**: 335–350.
- BERNER R.A. 1995: Chemical weathering and its effect on atmospheric CO₂ and climate. W: A.F. White i S.L. Brantley (eds.): Chemical weathering rates of silicate minerals. Mineralogical Society of America, Washington, DC. *Reviews of Mineralogy* **31**: 565–583.
- BLUTH, G.J.S., KUMP L.R. 1994: Lithologic and climatologic controls of river chemistry. *Geochim. et Cosmochim. Acta* **58**: 2341–2359.
- BIRNKMAN, R. 1970: Ferrololysis, a hydromorphic soil forming process. *Geoderma* **3**: 199–206.
- BRINKMAN, R. 1979: Ferrololysis, a soil forming process in hydromorphic conditions. Center for Agricultural Publishing and Documentation, Wageningen: 105 ss.
- BROGOWSKI, Z. 2000: Krzem w glebie i jego rola w żywieniu roślin. *Post. Nauk Rol.* **6**: 9–16.
- BUURMAN P., VAN REEUWIJK L.P. 1984: Proto-imogolit and the process of podzol formation: a critical note. *J. Soil Sci.* **35**: 447–452.
- CLARKE J. 2003: The occurrence and significance of biogenic opal in the regolith. *Earth-Science Reviews* **60**: 175–194.
- CONLEY D.J. 2002: Terrestrial ecosystems and the global biogeochemical silica cycle. *Global Biogeochemical Cycles* **16**: 1121–1129.
- DATNOFF L.E., SNYDER G.H., KORNDÖRFER G.H. (eds) 2001: Silicon in agriculture. Studies in Plant Science 8, Elsevier, Amsterdam: 403 ss.
- DOVE P.M. 1995: Kinetic and thermodynamic controls on silica reactivity in weathering environments. W: A.F. White & S.L. Brantley (eds): Chemical weathering rates of silicate minerals. Mineralogical Society of America, Washington, DC. *Reviews of Mineralogy* **31**: 236–290.

- DRACHEVA L.V. 1975: The study of silicic acid condition in model and technological solutions and surface waters. Avtoref. Can. Diss. Moscow. MITHT.
- DREES L.R., WILDING L.P., SMECK N.E., SANKAYI A.L. 1989: Silica in soils: Quartz and disordered silica polymorphs. W: J.B. Dixon, S.B. Weed. Minerals in soil environment. SSSA. Madison: 913-974.
- EAQUB M., BLUME H.-P. 1982: Genesis of a so-called ferrolysed soil of Bangladesh. *Z. Pflanzenernähr. Bodenk.* **145**: 470-482.
- EPSTEIN E. 1994: The anomaly of silicon in plant biology. *Proc. Natl. Acad. Sci. USA* **91**: 11-17.
- ELLENBERG H., MAYER R., SCHAERMANN J. 1986: Oekosystemforschung-Ergebnisse des Sollingprojekts 1966-1986. Verlag Eugen Ulm, Stuttgart.
- FARMER V.C. 1984: Distribution of allophane and organic matter in podzol B horizons: reply to Buurman & Van Reeuwijk. *J. Soil Sci.* **35**: 453-458.
- FARMER V.C., FRASER A.R. 1982: Chemical and colloidal stability of soils in the Al_2O_3 - Fe_2O_3 - H_2O system: their role in podzolization. *J. Soil Sci.* **33**: 737-742.
- FRANK U. 1993: Chemisch-mineralogische Reaktion von Waldböden auf anthropogene Sauerbelastungen und ihre Auswirkung auf den Kationen-Antagonismus im System Boden-Pflanze. Dissertation vom Fachbereich Biologie der Universität Oldenburg.
- GLADKOVA K.F. 1982: The role of silicon in phosphate plant nutrition. *Agrochemistry* **2**: 133-150.
- GERARD F., FRANCOIS M., RANGER J. 2002: Processes controlling silica concentration in leaching and capillary soil solution of an acidic brown forest soil (Rhône, France). *Geoderma* **107**: 197-226.
- GUSTAFSSON J.P., BHATTACHERYA P., BAIN D.C., FRASER A.R., McHARDY W.J. 1995: Podzolisation mechanisms and synthesis of imogolite in northern Scandinavia. *Geoderma* **66**: 167-184.
- HALL A.D., MORRISON C.G.T. 1906: On the function of silica in the nutrition of cereals. *Proc. Royal Soc. London Ser. B* **77**: 455-465.
- HEYN B. 1989: Elementflüsse und Elementbilanzen in Waldökosystemen der Baerhalde - Suedschwarzwald. Freiburger Bodenkundliche Abhandlungen, **23**: 199 ss.
- KAUFMAN P.B., DAYANANDAN P., TAKEOKA Y., BIGELOW W.C., JONES J.D., ILLER R. 1981: Silica in shoots of higher plants. W: Silicon and Siliceous Structures in Biological Systems: 409-449.
- LINDSAY, W.L. 1979: Chemical equilibria in soils. Jon Wiley & Sons, New York.
- LUCAS Y. 2001: The role of plants in controlling rates and products of weathering: importance of biological pumping. *Annu. Rev. Earth Planet. Sci.* **29**: 135-163.
- LUNDSTROEM U.S., VAN BREEMEN N., BAIN D. 2000: The podzolisation process. A review. *Geoderma* **94**: 91-107
- MATICHENKOV V.V., AMMOSSOVA Y.M. 1996: Effect of amorphous silica on soil properties of sod-podzolic soil. *Eurasian Soil Sci.* **28**: 87-90.
- MATICHENKOV V.V., BOCHARNIKOVA E.A. 2001: The relationship between silicon and soil physical and chemical properties. *Silicon in Agriculture*: 209-219.
- MATICHENKOV V.V., SNYDER G.H. 1996: The mobile silicon compounds in some South Florida soils. *Eurasian Soil Sci.* **12**: 1165-1180.
- MEESBURG H., MUELLER H.E. 1992: Stimulation des Stofftransportes im Sickerwasser, Interflow und Bachwasser basenarmer Einzugsgebiete der Nordschwarzwaldes. Abschlussbericht PWAB-Projekt PW 89.076. Freiburg: 149 ss.
- MONGER C. H., KELLY E. F. 2002: Silica Minerals. Soil Mineralogy with Environmental Applications. SSSA, Madison: 611-636.
- MEUNIER J.D., COLIN F. 2001: Phytoliths: application in earth sciences and human history. Balkema Publishers, Lisse: 378 ss.
- MEUNIER J.D., COLIN F., ALARCON C. 1999: Biogenic silica storage in soils. *Geology* **27**: 835-838.
- MORRIS R.C., FLETCHER A.B. 1987: Increased solubility of quartz following ferrous-ferric iron reactions. *Nature* **330**: 558-561.
- OLIVA P., VIERS J., DUPRE B., FORTUNE J.P., MARTIN F., BRAUN J.J., NAHON D., ROBAIN H. 1999: The effect of organic matter on chemical weathering: study of a small tropical watershed: Nsimi-Zoetele site, Cameroon. *Geochim. et Cosmochim. Acta* **63**: 4013-4035.

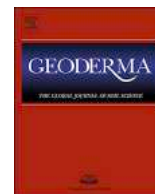
- PRUSINKIEWICZ Z., DZIADOWIEC H., JAKUBUSEK M. 1974: Zwrot do gleby pierwiastków – biogenów z opadem roślinnym w lesie liściastym i mieszanym na luźnych glebach piaskowych. *Rocz. Glebozn.* **25**, 3: 237–245.
- PANOV N.P., GONCHAROVA N.A., RADIONOVA L.P. 1982: The role of amorphous silicic acid in solonetz soil processes. *Vestnik Agr. Sci.* **11**: 18–32.
- RAVEN J.A. 1983: The transport and function of silicon in plants. *Biol. Rev.* **58**: 179–207.
- RUECKERT E. 1992: Naßbleichung und Tonzerstörung durch Ferrollysis in Stauwasserböden Baden-Württembergs? Stuttgart-Hohenheim, *Hohenheimer Bodenkundliche Hefte* **3**: 178.
- SOMMER M. 2002: Biogeochemie bewaldeter Einzugsgebiete und ihr pedogenetischer Kontext. Stuttgart-Hohenheim *Hohenheimer Bodenkundliche Hefte* **66**.
- STOOPS G. 2003: Guidelines for Analysis and Description of Soil and Regolith Thin Sections. *Soil Sci. Soc. Amer., Inc.* Madison, Wisconsin, USA.
- TAYLOR R.M. 1988: Proposed Mechanism for the Formation of Soluble Si-Al and Fe(III)-Al Hydroxy Complexes in Soils. *Geoderma* **42**: 65–77.
- TRÉGUER P. 2002: Silica and the cycle of carbon in the ocean. *C.R. Geoscience* **334**: 3–11.
- TRÉGUER P., NELSON D.M., VAN BENNEKORN A.J., DEMASTER D.J., LEYNAERT A., QUÉGUINER B. 1995: The silica balance in the world ocean: a reestimate. *Science* **268**: 375–379.
- TRÉGUER P., PONDAVEN P. 2000: Silica control of carbon dioxide. *Nature* **406**: 358–359.
- VAN RANST E., DE CONINCK F. 2002: Evaluation of ferrollysis in soil formation. *Europ. J. Soil Sci.* **53**: 513–519.
- VEERHOFF M., BRUEMMER G. W. 1993: Bildung schlechtkristalliner bis amorpher Verwitterungsprodukte in stark bis extrem versauerten Waldböden. *Z. Pflanzenernähr. Bodenk.* **156**: 11–17.
- WADA K. 1989: Allophane and Imogolite. W: J.B. Dixon, S.B. Weed. Minerals in soil environment. SSSA, Madison:1051–1087.
- WATTEAU F., VILLEMIN G. 2001: Ultrastructural study of the biogeochemical cycle of silicon in the soil and litter of a temperate forest. *European J. Soil Sci.* **52**: 385–396.
- WHITE A.F. 1995: Chemical weathering rates of silicate minerals in soils. W: A.F. White & S.L. Brantley (eds.): Chemical weathering rates of silicate minerals. Mineralogical Society of America, Washington, DC. *Reviews of Mineralogy* **31**: 407–461.
- WHITE A.F., BRANTLEY S.L. 1995: Chemical weathering rates of silicate minerals: an overview. W: A.F. White & S.L. Brantley (eds.): Chemical weathering rates of silicate minerals. Mineralogical Society of America, Washington, DC. *Reviews of Mineralogy* **31**: 1–22.
- WILDING L.P., DREES L.R. 1971: Biogenic Opal in Ohio Soils. *Soil Sci. Soc. Amer. Proc.* **35**: 1004–1010.
- WOLLAST R., MCKENZIE F.T. 1983: The global cycle of silica. W: S.R. Aston (ed.) Silicon geochemistry and biochemistry. Academic Press, San Diego: 39–76.

dr Danuta Kaczorek

Zakład Gleboznawstwa, Katedra Nauk o Środowisku Glebowym SGGW

ul Nowoursynowska 159, 02-776 Warszawa

E-mail: kaczorek@delta.sggw.waw.pl.



Effects of phytolith distribution and characteristics on extractable silicon fractions in soils under different vegetation – An exploratory study on loess

Danuta Kaczorek^{a,b}, Daniel Puppe^{a,*}, Jacqueline Busse^a, Michael Sommer^{a,c}

^a Leibniz Centre for Agricultural Landscape Research (ZALF), 15374 Müncheberg, Germany

^b Department of Soil Environment Sciences, Warsaw University of Life Sciences (SGGW), 02-776 Warsaw, Poland

^c University of Potsdam, Institute of Environmental Science and Geography, 14476 Potsdam, Germany

ARTICLE INFO

Handling Editor: Ingrid Kögel-Knabner

Keywords:

Phytolith dissolution

Phytolith morphotypes

Si extraction

Surface roughness parameters

Si cycling

ABSTRACT

The significance of phytoliths for the control of silicon (Si) fluxes from terrestrial to aquatic ecosystems has been recognized as a key factor. Humankind actively influences Si fluxes by intensified land use, i.e., agriculture and forestry, on a global scale. We hypothesized phytolith distribution and assemblages in soils of agricultural and forestry sites to be controlled by vegetation (which is directed by land use) with direct effects on extractable Si fractions driven mainly by phytolith characteristics, i.e., dissolution status (dissolution signs) and morphology (morphotype proportions). To test our hypothesis we combined different chemical extraction methods (calcium chloride, ammonium oxalate, Tiron) for the quantification of different Si fractions (plant available Si, Si adsorbed to/occluded in pedogenic oxides/hydroxides, amorphous Si) and microscopic techniques (light microscopy, confocal laser scanning microscopy, scanning electron microscopy) for detailed analyses of phytoliths extracted using gravimetric separation (physical extraction) from exemplary loess soils of agricultural (arable land and grassland/meadow) and forestry (beech and pine) sites in Poland. We found differences in dissolution signs, morphotype proportions, and vertical distribution of phytoliths in soil horizons per site. In general, dominant morphotypes of assignable phytoliths in the studied soil profiles were elongate phytoliths and short cells, both of which are typical for grass-dominated vegetation. However, the organic layers of forest soils were dominated by globular phytoliths, which are typical indicators for mosses. As expected soil horizons under different vegetation generally were characterized by differences in extractable Si fractions, especially in the upper soil horizons. However, phytogenic Si pools counter-intuitively showed no correlations with chemically extracted Si fractions and soil pH at all. Our findings indicate that it is necessary to combine microscopic analyses and Si extraction techniques for examinations of Si cycling in biogeosystems, because extractions of Si fractions alone do not allow drawing any conclusions about phytolith characteristics or interactions between phytolith pools and chemically extractable Si fractions and do not necessarily reflect phytogenic Si pool quantities in soils and vice versa.

1. Introduction

Silicon (Si) is the main component of soils developed from loess containing up to 80% of quartz. Si compounds in soils generally exhibit a great variability regarding their appearance (crystalline, poorly crystalline, amorphous, adsorbed, liquid) and are subject to continuous transformations (e.g., dissolution, precipitation, sorption processes) (e.g., Markewitz and Richter, 1998; Street-Perrott and Barker, 2008). Pedogenesis (affected by climate, organisms (soil flora and fauna, vegetation), relief, parent material, and time) directly influences these transformations (Sommer et al., 2006; Cornelis and Delvaux, 2016). One of the most active forms of Si in soils (next to Si adsorbed to clay

mineral surfaces) is Si of plant origin (phytoliths) (Alexandre et al., 1997, 2011; Blinnikov et al., 2013; Borrelli et al., 2010; De Rito et al., 2018). Phytoliths are amorphous silica particles ($\text{SiO}_2 \cdot n\text{H}_2\text{O}$) formed in living plants within cells (i.e., in the cell wall and the cell lumen) (Sangster et al., 2001; Hodson, 2016). They have a specific morphology and therefore may be ascribed to various taxonomic groups of plants (Piperno, 2006). Next to 'classic' phytoliths (i.e., durable 'plant stones' that can be frequently found in most soils), Si depositions in plants can be found in intercellular spaces or in an extracellular (cuticular) layer forming very fragile silica structures (Sangster et al., 2001; Hodson, 2016). Phytoliths enter the soil in situ via leaf fall and/or plant decay; they may also be supplied to soil by external factors, e.g., by human

* Corresponding author.

E-mail address: daniel.puppe@zalf.de (D. Puppe).

<https://doi.org/10.1016/j.geoderma.2019.113917>

Received 29 April 2019; Received in revised form 6 August 2019; Accepted 16 August 2019

Available online 04 September 2019

0016-7061/ © 2019 Elsevier B.V. All rights reserved.

activities (organic fertilization, storage of organic waste, biochar application), or may occur as primary components of the soil parent rock (loess, sedimentary rocks) as admixtures.

It has been shown that phytoliths are characterized by a variable solubility in soils. The factors which control phytolith dissolution in soils are: specific surface area, aluminium (Al) content, hydration state, age, rate of organic matter biodegradation, soil pH, and soil buffering capacity (Bartoli and Wilding, 1980; Cabanes and Shahack-Gross, 2015; Fraysse et al., 2006, 2009; Li et al., 2019; Nguyen et al., 2018; Osterrieth et al., 2015; Puppe and Leue, 2018). These factors are variable for different phytoliths and seem to depend mainly on phytolith morphotypes (i.e., phytolith geometry), although some earlier studies ascribed differences in phytolith dissolution to phytolith origin and in field observations grass phytoliths appeared to be less soluble compared to tree phytoliths, for example (Wilding and Drees 1974). However, laboratory studies did not confirm these findings but indicated that dissolution rates of phytoliths from different plants (larch, elm, horse-tail, fern, and different grasses) seem to be quite similar (Fraysse et al., 2009).

Phytoliths in soil profiles also are subject to translocation driven especially by bioturbation and percolation (Alexandre et al., 1997; Fishkis et al., 2009, 2010). Phytoliths represent a huge pool of relatively soluble silica in terrestrial ecosystems, and thus one of the main sources of Si in aqueous ecosystems (Struyf et al., 2009). In this context, different ecosystems show differences in biogeochemical Si cycling regarding Si fluxes (inputs, outputs) and Si dynamics (turnover rates) (e.g., Bartoli, 1983; Clymans et al., 2011; Cornelis et al., 2010, 2011; Sommer et al., 2013). Unfortunately, many studies on Si cycling focus on Si fraction extractions alone and do not include detailed phytolith analyses due to the fact that these analyses are very time-consuming. However, especially alkaline extraction is known to unselectively extract amorphous Si in general, i.e., it has to be considered that not only biogenic silica (in most soils mainly phytoliths next to other biogenic silica structures, see Puppe et al., 2015), but also non-biogenic (minerogenic or microcrystalline) Si forms are extracted (e.g., Saccone et al., 2007; Georgiadis et al., 2014; Li et al., 2019). In this context, the DeMaster-correction-method has been commonly used to quantify biogenic silica/phytolith contents in soils, but this technique has also been questioned recently (Meunier et al., 2014; Li et al., 2019). For a deeper understanding of the role of (different) phytoliths (next to fragile phytogetic Si structures) and their characteristics for Si cycling detailed phytolith analyses (next to chemical Si fraction extractions) are needed. Sommer et al. (2013), for example, showed the significance of phytolith morphology and dissolution status for fluxes of dissolved Si and Si cycling in a beech forest. Meunier et al. (2017) as well as Puppe et al. (2017) emphasized the importance of fragile phytogetic Si structures for Si cycling as they seem to represent a huge, most reactive Si pool in soils.

Intense usage of terrestrial ecosystems by humans (forestry, agriculture) has been recognized to directly influence Si cycling, often associated with a loss of (phytogetic) Si (i.e., anthropogenic desilication) (Struyf et al., 2010; Vandevenne et al., 2015). In dynamic farming landscapes such as arable fields or grasslands (meadows, pastures), the process of phytogetic Si accumulation (especially cereal grasses of the family Poaceae or Gramineae are known as Si accumulators) and corresponding removal of Si through harvesting is intense and may attain large scales (Clymans et al., 2011; Carey and Fulweiler, 2012). Meunier et al. (2008) estimated that harvesting of field crops can lead to a loss of up to 100 kg phytogetic Si/ha/year. On a global scale, field crops synthesize about 35% of total phytogetic Si and this proportion is going to increase within the next decades caused by increased agricultural production (Carey and Fulweiler, 2016). Despite this awareness, the mechanisms and processes of anthropogenic desilication under different vegetation directed by land use and the biological control of Si fluxes by phytoliths are still poorly understood (Street-Perrott and Barker, 2008).

We hypothesized phytolith distribution and assemblages to be controlled by vegetation with direct effects on extractable Si fractions driven mainly by phytolith characteristics, i.e., dissolution status (dissolution signs) and morphology (morphotype proportions). To test our hypothesis we combined different chemical extraction methods, i.e., (i) calcium chloride (plant available Si), (ii) ammonium oxalate (Si adsorbed to/occluded in pedogenic oxides/hydroxides), and (iii) Tiron (amorphous Si incl. phytoliths), and microscopic techniques (light microscopy, confocal laser scanning microscopy, scanning electron microscopy) for detailed analyses of interactions between these chemically extractable Si fractions and phytoliths extracted using gravimetric separation (physical extraction). For chemical Si fraction extractions as well as for physical phytolith extractions we used samples from soils of agricultural (arable land and grassland/meadow) and forestry (beech and pine) sites in Poland. Due to the fact that all four sites exhibit soils developed from loess we expected our results to directly reflect the influence of vegetation on phytolith distribution, phytolith assemblages, and extractable Si fractions. The results of our study will be helpful for a better understanding of Si cycling under different vegetation in general and the influence of phytoliths and their characteristics on extractable Si fractions in particular.

2. Materials and methods

2.1. Study sites and soil sampling

The studied soils were located in the Miechów area (50°25'32"N, 19°59'42"E) in the Małopolskie voivodship, Poland. The parent rocks of the studied soils were loess. The average annual temperature for the study area was 7 °C and the total annual precipitation was 610 mm. The main criterion used for selection of the study sites was the different vegetation/land use under which the studied soils were formed. The following sites were selected: (i) beech forest *Fagus sylvatica* L (species purity 100%, age > 100 years), (ii) pine forest *Pinus sylvestris* L (species purity > 70%, age > 100 years), (iii) arable land (100-year-old cultivated field), and (iv) a young grassland/meadow (10-year-old meadow), previously used as arable land. Regarding arable land the farming method was extensive, with 3-year crop rotation comprising 2-year tillage of cereals (wheat, oat), and root crop (fodder beet, potato) in the third year. Organic fertilizer in the form of manure was applied in each third year. Based on pedological evaluation a representative soil profile (width: approx. 100 cm) down to the parent material (beech 140 cm, pine 185 cm, grassland/meadow 185 cm, and arable land 160 cm depth) was excavated for detailed soil and phytolith analyses at every site.

All soil profiles were located at a distance not exceeding 0.5 km from each other and samples were collected per occurring layer/horizon (bulk samples of about 1–2 kg per layer/horizon, each taken along the total profile width) in every soil profile. The soils were classified as Luvisol (beech, pine) and eroded Luvisol (grassland/meadow, arable land). We assumed phytoliths of the current vegetation to categorically dominate phytolith assemblages in the analysed soils, and thus reflect recent land use, because the proportion of phytoliths of previous vegetation has been continuously decreased with time (output of phytoliths vs. input of recent phytoliths for > 100 years). In fact, soils under grassland/meadow and arable land showed signs of erosion (truncated profiles) indicating that the former phytolith pool (forests) was removed towards depositional areas to a great extent.

Bulk densities were separately determined by volumetric soil sampling using soil cores with a volume of 100 cm³ each per field replicate and horizon.

2.2. Soil analyses

Bulk soil samples were air dried, gently crushed and sieved at 2 mm to separate the fine earth fraction (< 2 mm) from gravel (> 2 mm).

Different independent soil sample aliquots of the fine earth fraction were used for subsequent soil analyses. The particle size distribution of the fine earth was determined by a combined wet sieving ($> 63 \mu\text{m}$) and pipette ($< 63 \mu\text{m}$) method (DIN ISO 11277, 1998). Pre-treatment for particle size analysis was done by wet oxidation of organic matter using H_2O_2 (10 vol%) at 80°C and dispersion by shaking the sample end over end for 16 h with a 0.01 M $\text{Na}_4\text{P}_2\text{O}_7$ -solution (Schlichting et al., 1995). Soil pH was measured using a glass electrode in 1 M KCl suspensions at a soil to solution ratio of 1:2.5. For total carbon and nitrogen analyses (C_t and N_t) the fine earth ($< 2 \text{ mm}$) was finely powdered in a disc mill. Subsequently, C_t and N_t were determined by dry combustion using an elemental analyser (CNS TruSpec, Leco Instruments). Carbonate (CaCO_3) content was measured with a multi-phase analyser (RC612, Leco Instruments). Organic carbon (C_{org}) concentrations were calculated by subtraction ($\text{C}_t - \text{CaCO}_3$) in case CaCO_3 was present. In all other cases C_t equals C_{org} .

Pedogenic oxides were characterized by dithionite extractable iron (Fe_d) and manganese (Mn_d) analysed after Mehra and Jackson (1960) and ammonium oxalate-soluble Fe (Fe_{ox}), Si (Si_{ox}), and Al (Al_{ox}) according to Schwertmann (1964) (see Schlichting et al., 1995). Si_{ox} was used for the quantification of Si adsorbed to/occluded in pedogenic oxides/hydroxides (Georgiadis et al., 2013). Calcium chloride (CaCl_2) was used to extract (by application of Cl^- to replace adsorbed Si) the easily soluble or mobile Si fraction, i.e., the plant available Si fraction (Si present in the soil solution, i.e., monomeric silicic acid (H_4SiO_4) in most soils). Two-gram samples of soils were placed in 50 mL plastic centrifuge tubes along with 20 mL 0.01 M CaCl_2 solution. Samples were agitated continuously on a reciprocating shaker for 16 h. The extraction method followed the procedure described by de Lima Rodrigues et al. (2003) and developed by Haysom and Chapman (1975). The procedure for the Tiron extraction for the quantification of the amorphous Si fraction (incl. phytogenic Si) was based on the method of Kendrick and Graham (2004). These authors used the Tiron ($\text{C}_6\text{H}_4\text{Na}_2\text{O}_8\text{S}_2\text{H}_2\text{O}$) extraction developed from Biermans and Baert (1977) and modified by Kodama and Ross (1991), i.e., extraction in a 80°C water bath for 1 h. Element concentrations in the extracts were determined by ICP-OES (ICP-iCAP 6300 Duo, Thermo Fisher Scientific Inc.) using internal standards. To avoid Si contaminations, only plastic equipment was used during the entire procedure.

Total element analysis (Si, Al, Fe, K, Mg, Ca, Na, Ti) was performed with X-ray fluorescence (XRF) using a Siemens X-ray spectrometer (Model SRS 200, Cr-K α radiation). Basic mineral composition was determined on powder samples in an X-ray diffractometer (BRUKER-AXS D5005 with Co-K α radiation). Soil sample preparations as well as analyses were conducted following standard laboratory protocols using internal standards (institutional Central Laboratory) for permanent verification of predefined method precision. All soil analyses were performed at the minimum of two lab replicates.

2.3. Phytolith separation from soils and microscopic analyses

Phytoliths were extracted using gravimetric separation (physical extraction) from 10 g of dry soil material ($< 2 \text{ mm}$) of all occurring soil horizons (incl. parent material horizons) in four steps: (1.) oxidation of organic matter using H_2O_2 (30%), HNO_3 (65%), HClO_4 (70%) at 80°C until reaction subsides, (2.) dissolution of carbonates and Fe oxides by boiling the sample in HCl (10%) for 15 min, (3.) removal of the $\leq 2 \mu\text{m}$ granulometric fraction: dispersion of remaining solid phase of step 2 with 2% sodium hexametaphosphate solution (6–12 h), centrifugation at 1000 rpm for 2–3 min, and subsequent decantation, (4.) separations of the phytoliths: shaking of remaining solid phase of step 3 with 30 mL of sodium polytungstate $\text{Na}_6(\text{H}_2\text{W}_{12}\text{O}_{40})\cdot\text{H}_2\text{O}$ (density of 2.3 g cm^{-3}), centrifugation at 3000 rpm for 10 min, carefully pipetting the supernatant, and filtering by $5 \mu\text{m}$ Teflon filter. This step was repeated three times. The filter residue was washed with distilled water, bulked, dried at 105°C , and weighed (Alexandre et al., 1997). Physical phytolith

extraction per sample was performed in triplicate.

A light microscope (Nikon eclipse LV100) and a scanning electron microscope (SEM; JEOL JSM6060 LV) were used to check purity of phytolith samples and to characterize the isolated phytoliths, respectively. For scanning electron microscopy phytoliths were placed on Al-stubs, fixed by adhesive tape, coated with a minimal amount of gold-palladium, and micrographs were taken randomly. The six most common forms/morphotypes (1. vascular, 2. elongate, 3. globular, 4. fusiform, 5. lanceolate, 6. short cells: bilobate, cross, papillae, rondel, saddle) (see Fig. 1) were enumerated using 10 SEM-micrographs (magnification $500\times$) per sample (i.e., per horizon at each site) following the international terminology (ICPN-International Code for Phytolith Nomenclature 1.0) (Madella et al., 2005); rarely occurring or ambiguous phytolith forms were recorded as ‘other forms’. Identification of phytoliths was critically checked against phytolith references (e.g., Golyeva, 2001; Peto, 2013; Piperno, 2006). Phytolith dissolution status was also analysed using the 10 SEM-micrographs previously used for morphotype classification. All counted phytoliths (minimum: 32 (arable land), maximum: 966 (pine forest)) were assigned to one of three classes of phytolith dissolution: (i) phytoliths with no obvious dissolution features (plain), (ii) phytoliths showing some surface etching (rough-porous), and (iii) phytoliths with strong dissolution features (cratered/spongy) (see Fig. 2) (Sommer et al., 2013). Phytolith samples were additionally analysed on their element spectrum (element mapping) (see Fig. 3) by Hitachi S-2700 device, EDX-X-Flash-Detector with SAMX-Software at ZELMI, TU Berlin, Germany.

Surface roughness parameters, i.e., the quadratic mean (R_q , μm) of the arithmetic average surface roughness and the kurtosis (R_{ku} , dimensionless) of phytoliths were measured using a 3D confocal laser scanning microscope (Keyence VK-X100K, Keyence Company, Osaka, Japan). While R_q represents the standard deviation of the distribution of surface heights related to the mean line, i.e., the reference line about which the profile deviations are measured, R_{ku} is a measure of the peakedness of the profile about the mean line. Both parameters were used to quantify surface roughness, i.e., the microscopic asperity, as an indicator for the specific surface area of phytoliths (higher roughness parameters indicate a bigger specific surface area available for dissolution processes). Confocal laser scanning microscopy of phytoliths followed the procedure described in detail in Puppe and Leue (2018). In brief, phytoliths were transferred to clean object slides, scanned with a $1000\times$ magnification, and saved as images. Within each image various representative regions of interest (ROI) were defined (area per ROI: $10 \mu\text{m} \times 10 \mu\text{m}$) for subsequent measurements of surface roughness parameters. Per site and horizon (upper 2 horizons for arable land and grassland/meadow; upper 3 horizons for beech and pine forests) 10 ROI on each image were selected for measurements resulting in a total of 1000 measurements ($10 \text{ images} \times 10 \text{ ROI per image} \times 10 \text{ horizons}$).

2.4. Statistical analyses

Regarding surface roughness parameters R_q and R_{ku} of phytoliths outliers were defined as values that were below $Q1 - 1.5 \times \text{IQR}$ (interquartile range) or above $Q3 + 1.5 \times \text{IQR}$ and were excluded from further statistical analyses. Differences in the vertical distribution of phytolith characteristics (morphotypes, dissolution signs, and surface roughness parameters) per site, i.e., differences between the horizons at one site, were evaluated using the Mann-Whitney U test or the Kruskal-Wallis analysis of variance (ANOVA). While the Mann-Whitney U test was used to verify significances between two independent samples (two horizons: arable land), significances between more than two independent samples were tested with the Kruskal-Wallis ANOVA (more than two horizons: beech, pine, grassland/meadow). Correlations were analysed using Spearman's rank correlation. Statistical analyses were performed using the software package SPSS Statistics (version 22.0.0.0, IBM Corp.).

3. Results

3.1. Soil texture, chemistry, and mineralogy

The soils were classified as Luvisol (beech: O-Ah-E-Bt/E-Bt-Bw/C-C, pine: O-Ah-E/A-E-Bt-Bw/C-C) and eroded Luvisol (grassland/meadow:

Ah-Ap-E-E/Bt-Bt-Bw/C-C, arable land: Ap-Bt-Bw/C-C-C). The soil profiles selected for studies were characterized by a very similar grain size composition (Table A1, Fig. A1). The silt fraction dominated, with its contribution exceeding 65%; the clay fraction contributed to 2–25%; the lowest quantities of the clay fraction (2.2%) occurred in the eluvial horizon (E) of the soil developed under the pine forest and the content

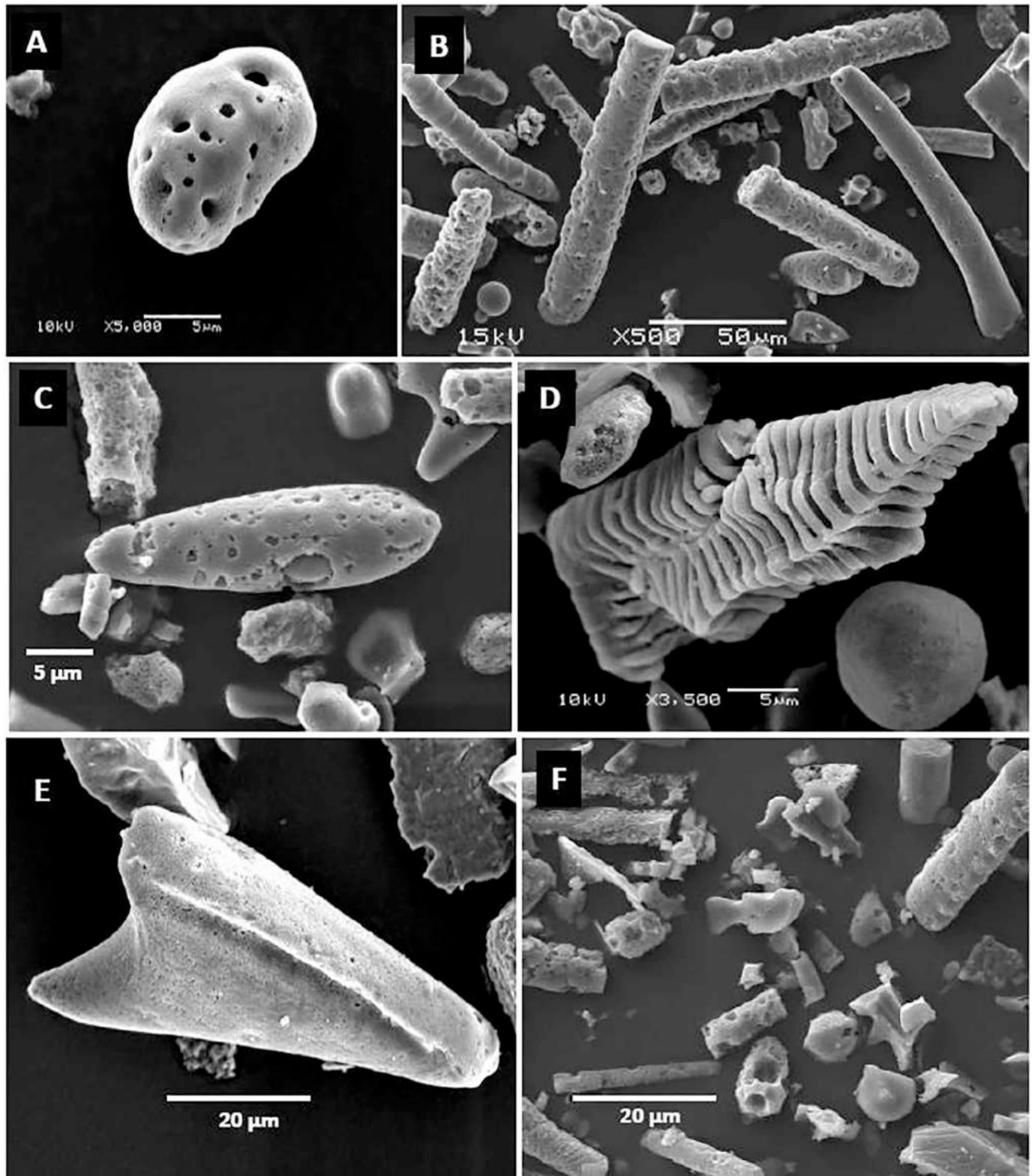


Fig. 1. SEM-micrographs of the main phytolith morphotypes recorded in this study. (A) globular phytolith, (B) elongate phytolith, (C) fusiform phytolith, (D) vascular phytolith, (E) lanceolate phytolith, (F) short cell.

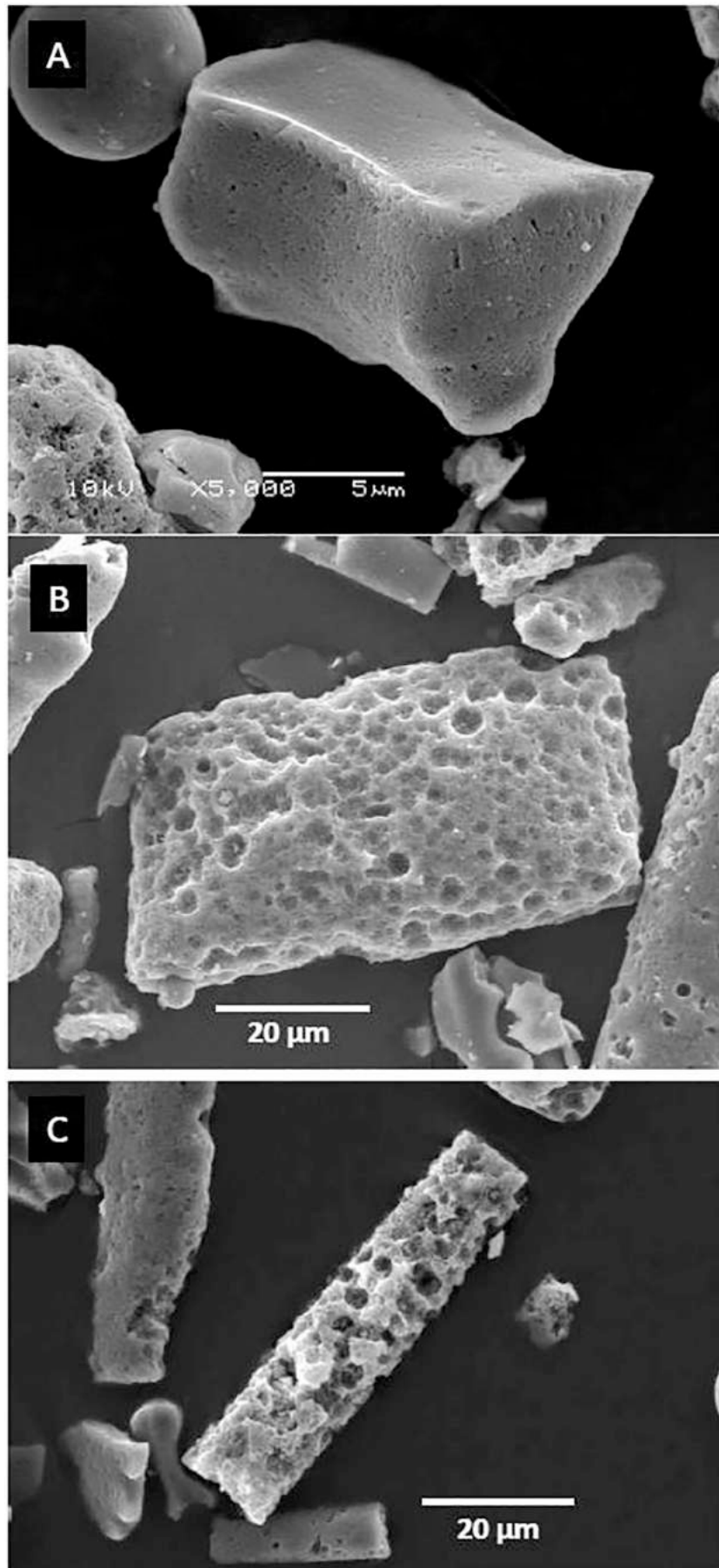


Fig. 2. SEM-micrographs of the different classes of phytolith dissolution recorded in this study. (A) plain phytolith, (B) rough-porous phytolith, (C) cratered/spongy phytolith.

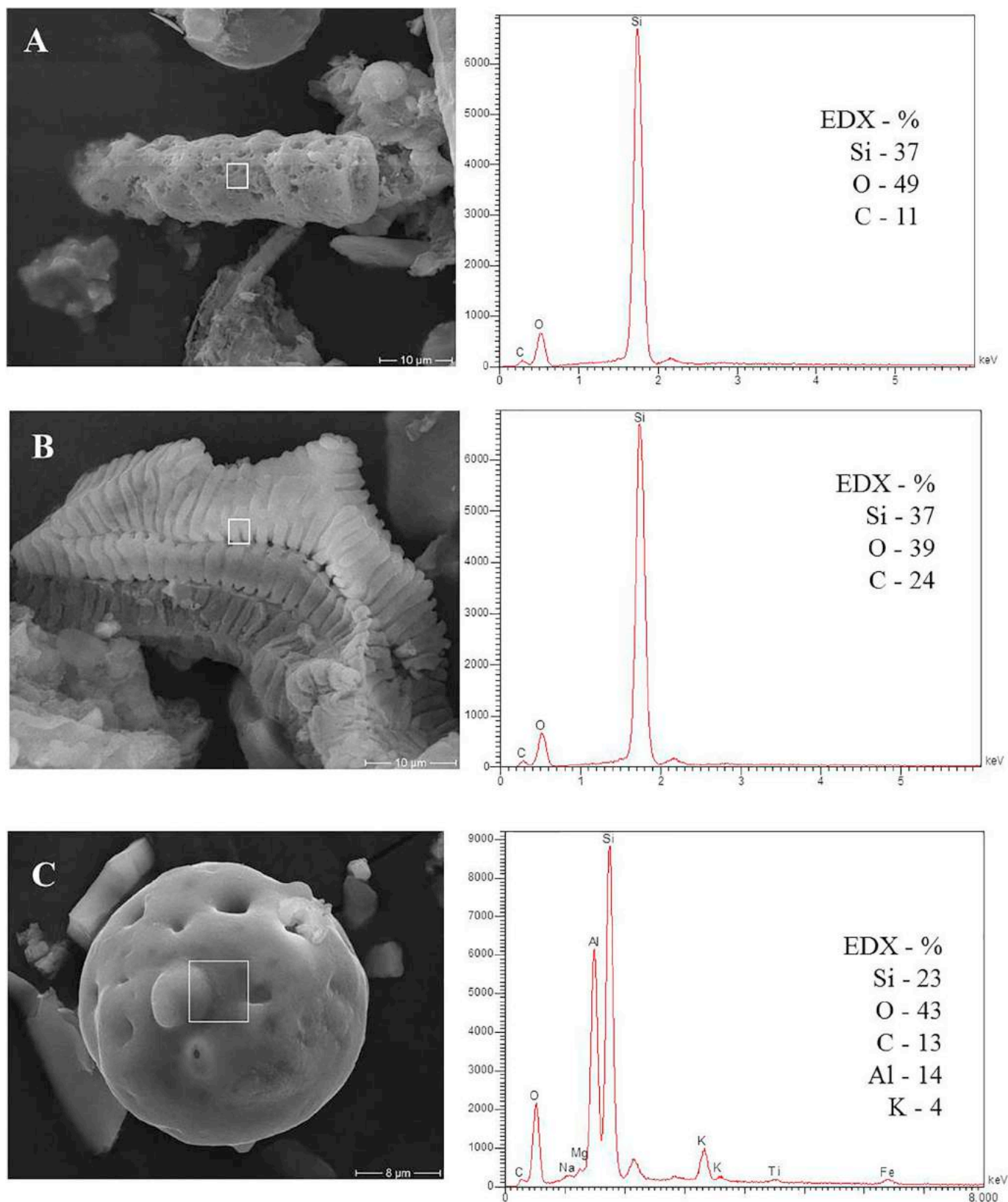


Fig. 3. SEM-micrographs of different phytolith morphotypes (A) elongate, (B) vascular, and (C) globular phytoliths and results of corresponding element mapping (EDX).

of the sand fraction in all soils was below 10%. The organic carbon content was highest in the organic soil horizons (O): 24.9% - beech forest, 26% - pine forest, 7.8% - grassland/meadow. Humus horizons (A, carbonate-free) contained much lower values of C_{org} (0.8–5.0%).

Soils developed under beech and pine trees generally were more

acid compared to soils developed under 10-year-old grassland/meadow (previously used as arable land) and arable land (Table A1, Fig. A1). Soil pH at the last-mentioned sites was largely influenced by the application of calcium/magnesium fertilizers. Secondary carbonates in deeper horizons were noted in only two profiles, i.e., in soils developed

under beech and arable land.

Depth profiles of Fe, Al, and Mn in the soils studied were mainly related to eluvial (E) and illuvial (Bt) soil horizons (Table A1, Fig. A1). The most intense vertical translocation of Fe, Al, and clay minerals took place under pine forest (Fig. A1). In soils under beech forest and grassland/meadow Fe and Al accumulation in the Bt horizons prevailed, whereas their content in the parent material horizons was much lower. Past erosion in arable soils removed eluviation horizons. Therefore significant differences in the distribution of Fe, Al, and Mn in the soil profile were not observable.

The soils studied showed a similar chemical composition (Table A2). In all profiles the content of SiO₂ was similar (70–80%) with the exception of organic layers (O), where the SiO₂ content was much lower (ca. 40%). Parent material under beech and arable land contained increased values of CaO (3.5 and 2.5%, respectively) and MgO (0.9 and 0.7%, respectively). In the Luvisol under pine the eluvial horizons (E) contained the lowest contents of Fe₂O₃ (10–13 g kg⁻¹) and Al₂O₃ (44–48 g kg⁻¹) compared to the remaining soil horizons. Quartz was the main mineral of the soils studied; ancillary minerals and minerals as admixtures included potassium feldspars, plagioclases, amphiboles, and pyroxenes (Table A3).

3.2. Si pools in soils

The distribution of plant available Si (Si_{CaCl2}) in mineral horizons in soils under beech and pine forests showed some similarity, with the lowest content in the eluvial horizons (E) (5.0 mg kg⁻¹ for pine and 7.9 mg kg⁻¹ for beech) (Table 1, Fig. A2). Notable was the high contribution of Si_{CaCl2} (79 mg kg⁻¹) in the organic layer (O) of soil developed under the beech forest. In the illuvial horizons (Bt) and parent material (C) the content of Si_{CaCl2} ranged between 13 and 48 mg kg⁻¹. Such large differences in the content of plant available Si were not observed in the soil profiles of grassland/meadow (19–35 mg kg⁻¹) and arable land (22–29 mg kg⁻¹).

The quantity of Si extracted by Tiron was the highest in relation to the quantity of Si obtained by using ammonium oxalate and calcium chloride extractions (Table 1, Fig. A2). The highest concentrations of

Si_{Tiron} occurred in the organic horizons (O: 12 g kg⁻¹) and in the Bt horizon under beech (11 g kg⁻¹), as well as in the organic horizons of pine (8 g kg⁻¹) and grassland/meadow (8 g kg⁻¹).

Si extracted by ammonium oxalate (Si_{ox}) reached highest values in the Bt horizons (209 mg kg⁻¹ for grassland/meadow, 87 mg kg⁻¹ for beech and 57 mg kg⁻¹ for pine) and parent material horizons (125 mg kg⁻¹ for grassland/meadow, 92 mg kg⁻¹ for beech and 84 mg kg⁻¹ for pine) (Table 1, Fig. A2). In soils under arable land the content of Si_{ox} increased with depth of the soil profile (Ap 19, Bt 45–55, C 72–130 mg kg⁻¹).

3.3. Phytoliths

3.3.1. Phytolith contents

The highest values of phytoliths were noted in soil under pine forest (5.5–16.0 g kg⁻¹) (Table 1, Fig. A2). Their quantity was very variable in the soil profile and reached the highest value in the eluvial horizon (35–44 cm) with 16.0 g kg⁻¹. In the remaining soils the content of phytoliths was much lower ranging between 0.01 and 2.5 g kg⁻¹ (beech forest: 1.5–2.5 g kg⁻¹, grassland/meadow: 0.01–2.4 g kg⁻¹, arable land: 0.15–0.52 g kg⁻¹). The presence of phytoliths generally was observable in each soil horizon down to a depth of up to 85 cm. Total masses of soil phytoliths resulted in 7.7 kg m⁻² for pine (0–75 cm depth), 1 kg m⁻² for beech (0–80 cm depth), 1 kg m⁻² for grassland/meadow (0–85 cm depth), and 0.3 kg m⁻² for arable land (0–70 cm depth) (data not shown). Only few single phytoliths were found in the parent material horizons, and thus a quantification of corresponding phytogetic Si pools was not possible (cf. Table 1). Phytolith contents were not correlated to soil pH, Si_{ox}, Si_{CaCl2}, or Si_{Tiron} (Fig. 4).

3.3.2. Phytolith morphotypes

Out of 15 analysed soil horizons 11 were dominated (excluding phytoliths recorded as ‘other forms’) by elongate phytoliths (23–31% beech; 24–40% pine; 22–44% grassland/meadow; 21–29% arable land) and the remaining 3 were dominated by globular phytoliths, which were most common in the organic horizons (29% for beech, 58% for pine) and in the humus horizon (Ah) under pine (34%) (Table 2). Short

Table 1

Means and standard deviations (SD) of phytogetic Si pools ($n = 3$) and extracted Si fractions ($n \geq 2$) in the horizons of the studied sites.

Study site	Depth (cm)	Phytoliths in soil (mg kg ⁻¹)		Si _{CaCl2} (mg kg ⁻¹)		Si _{Tiron} (mg kg ⁻¹)		Si _{ox} (mg kg ⁻¹)	
		Mean	SD	Mean	SD	Mean	SD	Mean	SD
Beech	0–2	2500	715	79.4	1.5	12,043	989	117.5	4.6
	2–7	1040	201	5.3	0.2	5263	402	85.3	1.5
	7–30	1800	141	3.8	0.4	3760	245	46.4	2.1
	30–45	1540	93	42.2	3.5	10,688	552	87.5	1.9
	45–80	< 10	1	48.1	0.6	4849	125	58.1	3.4
	80–105	0	0	42.7	4.0	4193	235	60.2	3.0
	105–140	0	0	48.5	2.1	3111	230	92.6	1.8
Pine	0–4	5550	721	7.7	0.7	7691	25	43.3	2.8
	4–9	8600	513	5.4	0.0	5398	511	63.6	3.1
	9–35	6060	732	5.6	0.0	4529	421	22.0	2.8
	35–55	15,920	210	6.1	0.4	2049	208	27.9	1.5
	55–75	< 10	1	32.7	2.1	4381	310	57.6	3.1
	75–125	0	0	41.1	2.4	4512	190	84.9	4.0
	125–185	0	0	17.6	1.0	3535	235	64.3	3.2
Grassland/Meadow	0–3	1900	205	7.5	0.5	7510	219	86.2	5.1
	3–23	2410	505	4.4	1.0	4405	300	77.3	3.3
	23–40	680	74	27.2	1.8	5027	125	209.8	12.1
	40–55	10	10	22.1	1.9	4797	315	198.5	8.9
	55–85	< 10	1	19.3	0.9	7002	412	72.0	1.5
	85–120	0	0	21.0	0.7	3576	189	125.5	10.8
	120–185	0	0	21.2	1.3	2951	135	72.3	2.8
Arable land	0–30	520	301	4.7	0.1	4709	3	19.7	0.9
	30–70	150	52	4.4	1.4	4426	110	45.5	2.7
	70–100	0	0	25.5	0.0	3510	155	55.9	4.1
	100–150	0	0	29.2	0.3	3249	34	72.1	3.5
	150–160	0	0	30.0	1.0	2722	144	130.1	9.1

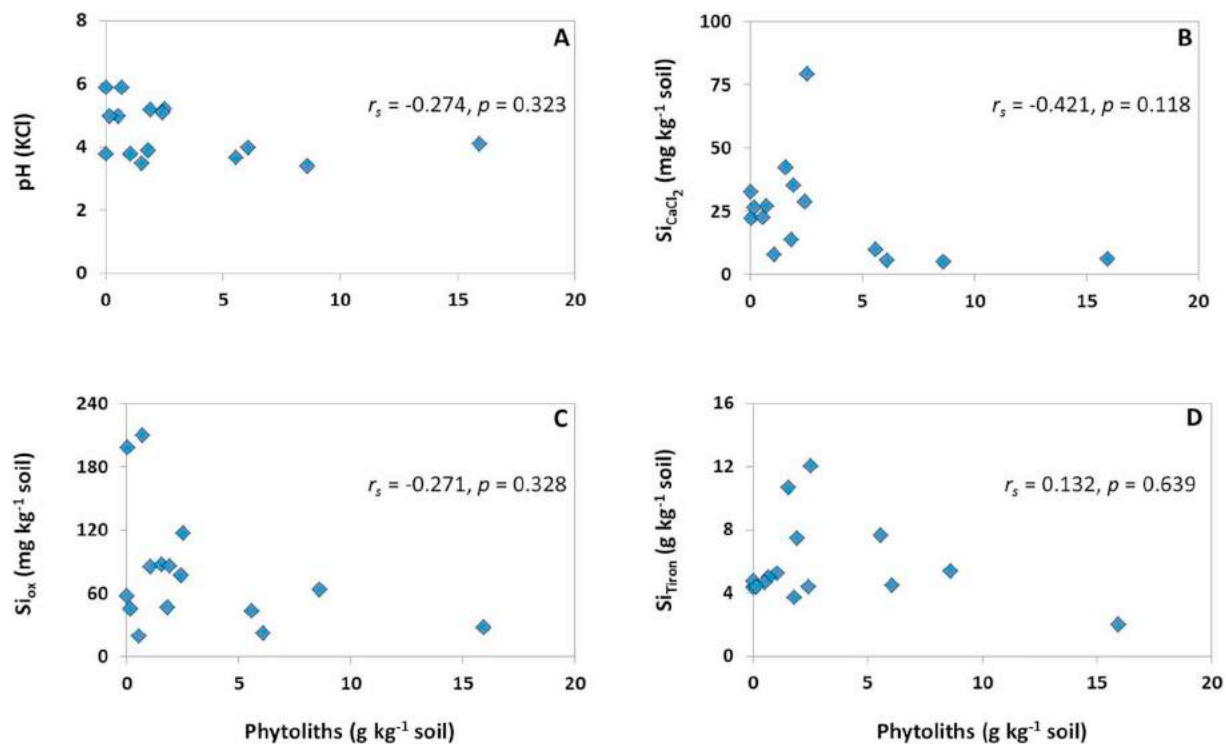


Fig. 4. Correlations between phytolith contents in soil (g kg^{-1}), soil pH, and extractable Si fractions (Si_{ox} , $\text{Si}_{\text{CaCl}_2}$, Si_{Tiron}).

cells prevailed in two horizons: under beech (26%, depth 30–45 cm) and pine (32%, depth 35–55 cm).

Phytoliths characteristic for beech (i.e., vascular phytoliths) were observed in the organic horizons (O) under beech (14%) and pine (2%), and in the humus horizon (Ah, 1%) under pine (Table 2). Moreover, the presence of fusiform (1–5%) and lanceolate phytoliths (2–18%) was observed. A relatively large part of phytoliths was recorded as ‘other forms’, because an unambiguous identification was not possible. Interestingly, only globular phytoliths were found to contain Al (and potassium (K) to a minor extent, Fig. 3).

3.3.3. Phytolith dissolution characteristics

For all phytoliths obtained, the degree of weathering or dissolution was evaluated. Plain forms were most common in the organic horizons under beech (83%) and pine (65%), whereas rough-porous forms dominated in the remaining horizons of all study sites (49–65%). The content of plain forms generally decreased with depth in the soil profiles, a fact that was not observed for rough-porous and cratered/spongy forms (Table 2).

Surface roughness parameters R_q and R_{ku} of phytoliths from the upper 3 horizons under pine showed ranges of 1.4–1.6 μm and 50–54, respectively, thus negligible differences between the horizons. Surface roughness measurements of phytoliths from the upper 3 horizons under beech revealed similar results (R_q : 1.4–1.6 μm , R_{ku} : 64–64). Phytoliths from the upper 2 horizons under grassland/meadow showed slight differences in R_q (1.2 μm vs. 1.5 μm) with the lowest measured value (1.2 μm) for phytoliths from the uppermost horizons; for R_{ku} values of 62 and 46 were measured. Phytoliths from the upper 2 horizons under arable land indicated the highest values regarding R_{ku} (74 vs. 114) and values of 1.4 μm and 1.5 μm for R_q (Table 2).

4. Discussion

4.1. Phytolith distribution and characteristics

In general, phytolith masses at our sites were in the same order of magnitude compared to other sites with similar vegetation (e.g.,

Blinnikov et al., 2013; Keller et al., 2012; Sommer et al., 2013). The phytolith mass in a soil mainly depends on the amount of plant materials (litter fall, other plant residues) supplied to a soil (i.e., the phytolith input) and the abundance of phytoliths, i.e., the Si concentration, in these materials on the one hand, and the loss of phytoliths (i.e., the phytolith output) via harvesting (crops, trees), erosion (wind, water), translocation, and dissolution on the other hand (e.g., Cornelis and Delvaux, 2016; Sommer et al., 2006; Song et al., 2016; Street-Perrott and Barker, 2008; Struyf et al., 2009; Vandevenne et al., 2015, and references therein).

Our analysed soils under beech and pine forests contained similar proportions of organic C in the organic horizons (i.e., 25–26%), whereby the process of organic matter decomposition in the humus layer under pine generally is slower compared to beech as evidenced by C_{org} contents (pine 5% vs. beech 2.4%), and thus release of phytoliths from beech litter can be assumed to be faster as well (cf. Bartoli, 1983). Despite the fact that beech nowadays represents a monoculture in the studied area, the content of recorded beech phytoliths (vascular phytoliths, see Figs. 1D and 3B; cf. Cornelis et al., 2010; Sommer et al., 2013) was only 14%, and thus about 86% of phytoliths were not distinctly assignable to beech. A high accumulation of phytoliths was observed (5.5–15.9 g kg^{-1}) in soil developed under pine; the highest amount (15.9 g kg^{-1}) was noted at the depth of 35–55 cm in the E horizon, which is characterized by a low content of clay (about 2%). The higher clay content in the horizon below, i.e., in the Bt horizon (55–75 cm) may act as a barrier for further translocation of phytoliths downwards (vertical translocation of phytoliths, cf. Alexandre et al. (1997) and Fishkis et al. (2009, 2010)), and thus might lead to an accumulation of phytoliths above this barrier. Another source of phytoliths in E horizons might be the roots of plants (Maguire et al., 2017; Turpault et al., 2018).

The organic (O) and humus (Ah) horizons generally were dominated (based on recognizable phytoliths only) by globular Al-containing phytoliths (see Fig. 3C; cf. Bartoli and Wilding, 1980), which most likely can be assigned to mosses (Golyeva, 2001; Peto, 2013). However, it has to be considered that a relatively large amount of phytolith assemblages was represented by phytoliths that were not unambiguously

Table 2
Means and standard deviations (SD; n = 10) of phytolith characteristics in the horizons of the studied sites.

Study site	Depth (cm)	Phytolith morphotypes in soil (in %)													
		Vascular		Short cells		Fusifforme		Lanceolate		Elongate		Globulare			
		Mean	SD	Mean	SD	Mean	SD	Mean	SD	Mean	SD	Mean	SD		
Beech	0-2	14	1.9	8	0.7	1	0.3	3	0.5	16	2.2	10	1.2	11	1.5
	2-7	0	0	9	1.1	1	0.7	4	1.3	22	4.4	6	1.3	4	1.5
	7-30	0	0	6	2.3	2	1.5	2	1.0	19	3.6	4	2.5	0	0.3
	30-45	0	0	26	4.6	3	1.0	5	1.6	19	2.8	12	2.3	2	0.9
	45-80 ^a	-	-	< 0.001	-	-	-	0.029	-	-	< 0.001	-	-	-	-
Pine	0-4	2	1.0	1	0.5	1	0.3	1	0.6	16	3.9	3	0.8	39	5.6
	4-9	1	0.5	7	1.5	0	0	1	0.5	9	0.8	2	0.4	26	3.0
	9-35	0	0	5	1.0	0	0.3	3	0.5	21	5.9	3	1.0	6	1.9
	35-55	0	0	32	12.0	2	0.4	4	1.1	17	6.5	12	3.4	3	1.4
	55-75	0	0	9	1.4	5	0.7	9	0.9	9	0.7	31	2.0	0	0
Grassland/ Meadow	0-3	0	0	8	1.8	2	0.6	6	1.6	19	2.1	12	2.9	0	0
	3-23	0	0	3	1.1	1	0.5	3	1.5	19	5.7	3	0.3	11	5.3
	23-40	0	0	0	0	5	0.4	18	0.9	14	1.2	23	1.2	16	0.9
	40-55	0	0	4	0.3	0	0	15	0.6	9	0.9	35	0.9	4	0.3
	55-85 ^a	-	-	< 0.001	-	-	-	< 0.001	-	-	< 0.001	-	-	< 0.001	-
Arable land	0-30	0	0	5	0.6	2	0.9	5	1.1	16	3.5	13	1.8	1	1.4
	30-70	0	0	12	0.9	2	0.4	4	0.3	11	0.8	10	0.7	0	0
		1.000		< 0.001		0.382		0.001		< 0.001		< 0.001		0.001	

Study site	Phytolith morphotypes in soil (in %)	Categories of phytolith dissolution (in %)												Surface roughness parameters			
		'Other forms'			Plain			Rough-porous			Cratered/spongy			R _a (µm)		R _{ku}	
		Mean	SD		Mean	SD		Mean	SD		Mean	SD		Mean	SD	Mean	SD
Beech	> 10 µm, mean	18	1.1	1.8	83	15	1.5	2	0.4	1.4	0.4	1.4	0.4	64	18		
	18	0.9	9.5	37	6.0	49	9.3	14	2.4	1.6	2.4	1.6	65	18			
	2	1.5	19.5	31	7.3	56	21.7	13	3.5	1.6	3.5	1.6	64	21			
	4	1.3	3.6	21	3.4	65	7.9	14	1.9	n/a	1.9	n/a	n/a	-			
Pine	0.069	< 0.001	< 0.001	< 0.001	< 0.001	< 0.001	< 0.001	< 0.001	< 0.001	0.421	-	-	-	-			
	19	3.4	4.5	65	15.5	24	5.8	11	5.5	1.6	0.421	0.5	0.946	20			
	8	1.5	7.8	30	5.6	61	8.3	9	1.9	1.5	1.6	0.3	52	17			
	6	2.9	56	21	6.9	52	9.3	27	6.5	1.4	1.4	0.3	54	12			
	4	1.3	3.2	15	2.4	62	15.0	23	3.3	n/a	n/a	0.3	n/a	-			
0	0	1.3	7	0.9	60	2.8	33	2.1	n/a	n/a	-	n/a	-				
< 0.001	< 0.001	< 0.001	< 0.001	< 0.001	< 0.001	< 0.001	< 0.001	< 0.001	< 0.001	0.586	-	-	0.798	-			

(continued on next page)

Table 2 (continued)

Study site	Phytolith morphotypes in soil (in %)				Categories of phytolith dissolution (in %)				Surface roughness parameters					
	Globulare		'Other forms'		Plain		Rough-porous		Cratered/spongy		R_q (µm)		R_{ku}	
	> 10 µm, mean	SD	Mean	SD	Mean	SD	Mean	SD	Mean	SD	Mean	SD	Mean	SD
Grassland/ Meadow	2	0.8	51	6.9	19	3.3	51	6.6	30	5.0	1.2	0.2	62	11
	6	3.3	54	15.4	26	9.6	59	14.6	15	5.2	1.5	0.3	46	16
	7	0.4	17	0.7	14	1.8	52	1.1	34	1.1	n/a	-	n/a	-
	8	0.4	25	0.6	9	0.4	58	1.1	23	0.8	n/a	-	n/a	-
Arable land	< 0.001	-	< 0.001	-	< 0.001	-	< 0.001	-	< 0.001	< 0.001	< 0.029	-	-	-
	5	0.5	53	10.0	38	6.0	49	9.2	13	1.9	1.4	0.4	74	18
	0	0	61	2.3	18	1.4	56	3.2	26	1.5	1.5	0.5	114	40
	0.058	-	< 0.001	-	< 0.001	-	< 0.001	-	< 0.001	< 0.001	0.897	-	0.016	-

Significances between the horizons at one site (i.e., differences in the vertical distribution of phytolith characteristics per site) were verified with the Mann-Whitney U test (arable land) or the Kruskal-Wallis analysis of variance (ANOVA; Beech, pine, grassland/meadow). Significant *p* values (*p* < 0.05) are stated in bold.

^a Only trace amounts of phytoliths found (not included for statistical tests); 'Other forms' = rarely occurring or ambiguous phytolith morphotypes; n/a = not analysed.

assignable to specific morphotypes, and thus were recorded as 'other forms'. In this context, it has to be considered that phytolith assemblages in soils are affected by different taphonomic processes such as fragmentation, dissolution, translocation, etc. – factors that make it generally difficult to derive an accurate reflection of the (current) local vegetation characterized by specific phytolith morphotypes (De Rito et al., 2018). Regarding our study sites 'other forms' of phytoliths were quite dominant in specific soil horizons, but absolutely dominated phytolith assemblages in soil samples of the arable land and 10-year-old grassland/meadow, which previously was used also as arable land. In this connection, mechanical tillage (including ploughing) might have caused mechanical destruction of phytoliths and thus hinder their unambiguous identification and classification.

Our study shows that differences in surface roughness parameters of phytoliths (indicating differences in the specific surface area of phytoliths) in soil horizons under different vegetation are detectable in general. This is corroborated by the results of Puppe and Leue (2018) who found differences in surface roughness parameters between fresh (extracted directly from plant materials) and aged (extracted from soils) phytoliths, which were about 10 years old. In our study, surface roughness parameters of phytoliths from different horizons in forest soils showed no significant differences indicating a comparable susceptibility to dissolution in general. In contrast, surface roughness parameters of phytoliths in the horizons under grassland/meadow and arable land were significantly different indicating differences in the susceptibility to dissolution. These differences might be assigned to differences in land use. While forest soils are characterized by an (undisturbed) annual input of large amounts of fresh phytoliths via litter fall, agricultural soils are part of a highly disturbed plant-soil-system, where large amounts of biomass, and thus (fresh) phytoliths, are removed every year (cf. Meunier et al., 2008; Struyf et al., 2010; Vandevenne et al., 2012). Our interpretation is underlined by the results of SEM analyses regarding dissolution status of phytoliths in general. Again, the analysed forest soils were characterized by a higher proportion of plain (fresh) phytoliths compared to agricultural soils indicating the above-mentioned differences in vegetation. However, it has to be stated that the course and direction of dissolution and weathering of phytoliths in a specific soil remain mainly unknown, although it is known that these processes depend mainly on factors like phytolith size, porosity, chemical composition, etc. (e.g., Bartoli and Wilding, 1980; Cabanes and Shahack-Gross, 2015; Fraysse et al., 2006, 2009; Li et al., 2014, 2019; Nguyen et al., 2018; Puppe and Leue, 2018).

Furthermore, it has to be considered that fresh phytoliths entering the soil may not be synthesized flawlessly and thus look like aged (weathered) phytoliths under the microscope. Dissolution processes of different phytolith morphotypes may attain different pathways; while larger morphotypes like elongate phytoliths frequently show characteristic signs of dissolution at their surfaces, smaller morphotypes like globular phytoliths often appear smooth, i.e., without clear signs of dissolution or weathering. In fact, the dominance (excluding phytoliths recorded as 'other forms') of elongate phytoliths might be a hint for their comparatively low susceptibility to dissolution (cf. Wilding and Drees 1974, De Rito et al., 2018). In this context, Cabanes and Shahack-Gross (2015) hypothesized phytolith morphotypes (i.e., phytolith geometry) to be more important for phytolith dissolution and corresponding preservation in soils compared to nanoscopic surface areas of phytoliths.

4.2. Interactions between phytolith pools and chemically extractable Si fractions

Our results on hand indicate changes in phytolith contents in general (see 4.1), which might be caused by differences in vegetation driven by land use. This generally is in line with the results of various authors who showed the effects of human influence on Si cycling (e.g., Barão et al., 2014; Vandevenne et al., 2015). However, these changes are not reflected one-to-one in the extracted Si fractions at our sites as

Table 3
Current knowledge of phytogenic silica in soils as described in the present article.

	Phytogenic silica in soils		
	'Classic' phytoliths (> 5 µm)	Phytoliths (< 5 µm)	Fragile Si structures
Origin in plants	Cell wall and cell lumen	Cell wall and cell lumen	Intercellular space and extracellular (cuticular) layer
Limitations of physical extraction	Extraction of non-phytogenic Si cannot be excluded	Extraction of non-phytogenic Si cannot be excluded	Extraction of non-phytogenic Si cannot be excluded; Fragmentation/destruction of fragile Si structures while extraction
Proportion of phytogenic Si	+ (?)	+++ (?)	++ (?)
Solubility	++ (several orders of magnitude more soluble than silicate minerals)	+ (?)	+++ (?)
Preservation in soils	Durable up to centuries	Durable up to centuries (?)	Non-durable (?)
Importance for Si cycling	Known since decades	Potential recognized	Potential recognized

+ = high, ++ = higher, +++ = highest; (?) indicates that there is no information on this aspect available in literature yet.

the content of physically extracted phytoliths does not correlate with the concentrations of chemically extractable Si fractions at all. It is believed that concentrations of plant available Si and amorphous Si are considerably affected by (i) phytolith contents (e.g., Street-Perrott and Barker, 2008; Struyf et al., 2009) and (ii) specific differences in phytolith solubility attributed to differences in, e.g., specific surface areas and/or water content of phytoliths (e.g., Bartoli and Wilding, 1980; Frayse et al., 2009). Self-evidently this effect should be especially prominent in the organic horizons where phytoliths dominate the amorphous silica pool in soils.

However, our results showed that the concentrations of $\text{Si}_{\text{CaCl}_2}$ and Si_{Tiron} extracted from the organic horizon (O) under beech were not correlated to the amount of phytoliths in this horizon. The same is true for the soil horizons under pine: Despite relatively high phytolith contents under pine the values of plant available Si were the lowest at this site with regard to all soil horizons studied. Moreover, the concentration of Si_{Tiron} was comparable in soils of pine forest, grassland/meadow, and arable land. In fact, the arable land showed the lowest content of phytoliths in our study ($0.15\text{--}0.52\text{ g kg}^{-1}$), mainly driven by removal of plants and corresponding phytoliths via harvesting and increased erosional processes (Guntzer et al., 2012; Keller et al., 2012; Vandevenne et al., 2012). Altogether, our results corroborate the conclusions of Meunier et al. (2014) and Li et al. (2019), who question the suitability of the so-called DeMaster technique (which represents the de facto standard method) for quantification of amorphous biogenic Si, especially phytoliths, in soils.

Alkaline extraction methods (e.g., Tiron extraction) are known to extract not only biogenic silica, i.e., mainly phytoliths, but also non-biogenic or pedogenic (minerogenic or poorly/micro-crystalline) amorphous Si forms (e.g., Saccone et al., 2007; Georgiadis et al., 2013, 2014; Li et al., 2019). Thus, Si_{Tiron} can include (i) amorphous biogenic and pedogenic silica, (ii) Si adsorbed to/occluded in pedogenic oxides/hydroxides (Si_{ox}), and (iii) mobile or plant available Si ($\text{Si}_{\text{CaCl}_2}$) (cf. Cornelis et al., 2011). In general, Si_{ox} and $\text{Si}_{\text{CaCl}_2}$ fractions in our soils were relatively small, and thus Si_{Tiron} mainly consisted of extracted amorphous biogenic and pedogenic silica. However, due to the short extraction time of one hour we exclude extensive extraction of pedogenic Si forms and assume a more or less exclusively extraction of biogenic Si (cf. Barão et al., 2014), i.e., mainly phytoliths (next to, e.g., testate amoeba or diatom shells, see, e.g., Creevy et al., 2016; Puppe et al., 2015, 2016, Wanner et al., 2019), at least in the uppermost (organic) horizons. We further assume phytoliths < 5 µm, which were filtered out from phytolith extracts and thus not included in gravimetric quantification of phytolith contents (cf. subSection 2.3), to be the main driver of extractable Si fractions in soils.

This is corroborated by some earlier studies: Puppe et al. (2017) found phytoliths larger than 5 µm to represent only about 16% of total

Si contents of plant materials of *Calamagrostis epigejos* and *Phragmites australis* (Poaceae); Wilding and Drees (1971) showed that about 72% of leaf phytoliths of American beech (*Fagus grandifolia*) are smaller than 5 µm. These findings clearly point to the potential significance of phytoliths < 5 µm for Si cycling in general. In addition, Meunier et al. (2017) and Puppe et al. (2017) highlighted the importance of fragile phytogenic Si structures for Si cycling as they seem to represent another huge and most reactive Si pool in soils. However, as long as we do not exactly know how big the different phytogenic Si pools (represented by phytoliths > 5 µm, phytoliths < 5 µm, and fragile phytogenic Si structures) in soils are, how soluble the different phytogenic Si forms are, and how long they are preserved in soils, any interpretation of phytogenic Si pools in soils and their role in Si cycling (and their potential in carbon sequestration, see Hodson 2019) remains more or less vague (an overview of the current knowledge of phytogenic Si in soils as described in our article can be found in Table 3).

4.3. Conclusions

In conclusion, for examinations of Si cycling in biogeosystems a combination of microscopic analyses and Si extraction techniques should be applied whenever possible, because extractions of Si fractions alone (i) do not necessarily reflect the quantities of phytogenic Si pools in a specific soil and (ii) do not deliver any information on phytolith characteristics in this soil or on interactions between phytolith pools and chemically extractable Si fractions. Furthermore, we urgently need detailed analyses of phytogenic Si < 5 µm and fragile phytogenic Si structures, corresponding phytogenic Si pools, and their correlations with extractable Si fractions in the future, because only a minor part of phytogenic Si seems to be reflected by 'classic' phytoliths > 5 µm. Only the knowledge of the entire phytogenic Si pool (fragile phytogenic Si structures plus phytogenic Si < 5 µm plus phytoliths > 5 µm), the dissolution kinetics of these phytoliths/phytogenic Si structures, and corresponding impacts on different extractable Si fractions in soils will allow us to fully understand Si cycling in different biogeosystems.

Acknowledgements

This study was funded by the Polish Scientific Research Committee (KBN) – Project No. 2 P06S 032 30 (*Characteristics of amorphous bio-/pedogenic forms of silicon in Polish soils*). DP was funded by the Deutsche Forschungsgemeinschaft (DFG) under grant PU 626/2-1 (*Biogenic Silicon in Agricultural Landscapes (BiSiAL) – Quantification, Qualitative Characterization, and Importance for Si Balances of Agricultural Biogeosystems*). Last but not least we would like to thank two anonymous reviewers for their comments on our manuscript.

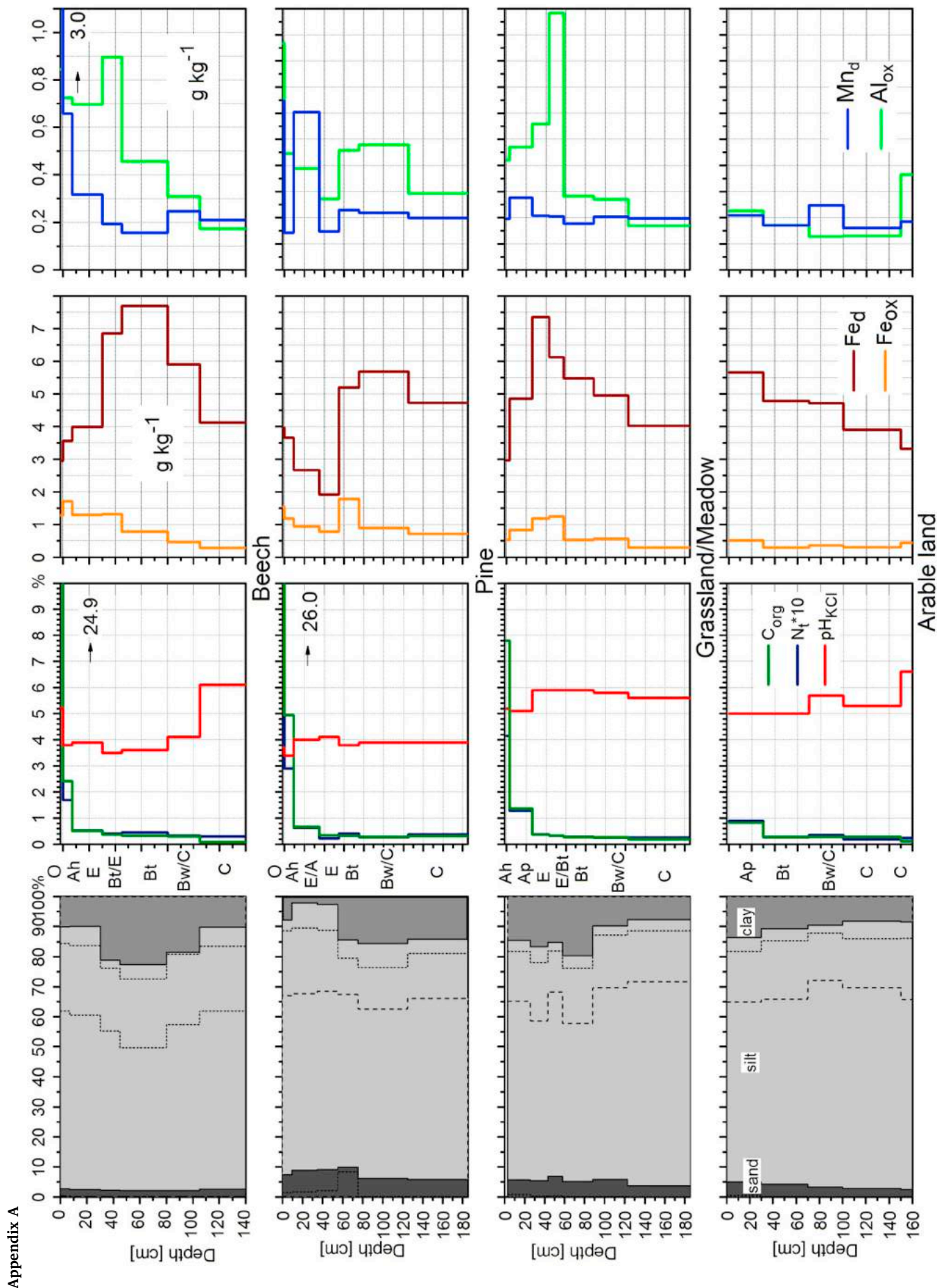


Fig. A1. Vertical distribution of physicochemical soil properties at the studied sites.

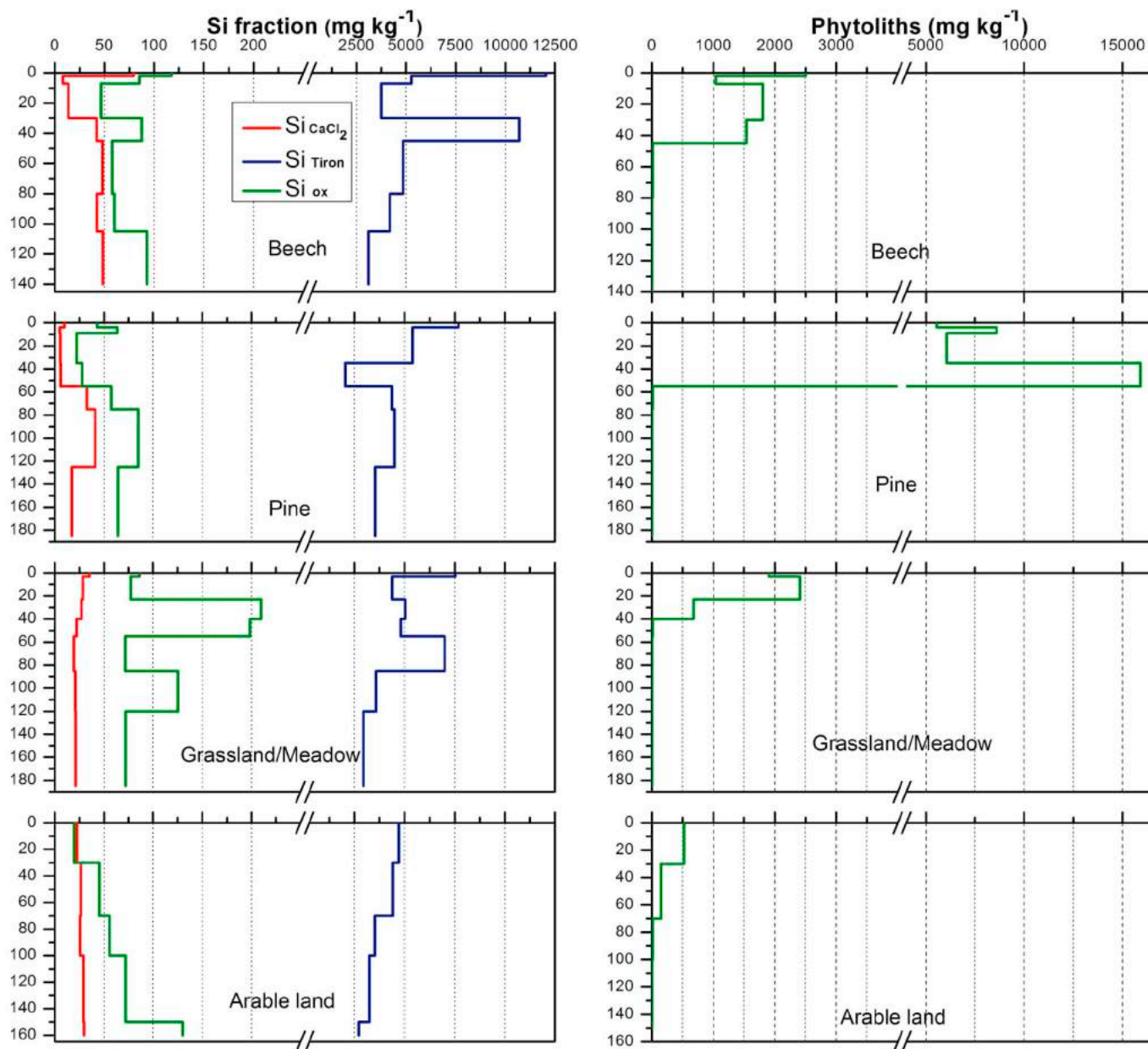


Fig. A2. Vertical distribution of phytogenic Si pools and extracted Si fractions in soils of the studied sites.

Table A1
Physicochemical soil properties of the studied sites.

Study site	Depth	pH	C _{org}	N _t	Fe _{ox}	Fe _d	Al _{ox}	Mn _d	Sand	Silt	Clay
	cm	KCl	%	%	mg kg ⁻¹	mg kg ⁻¹	mg kg ⁻¹	mg kg ⁻¹	%	%	%
Beech	0–2	5.2	24.87	1.27	1281	2945	843	3082	-	-	-
	2–7	3.8	2.42	0.17	1723	3561	724	658	2.7	87.2	10.1
	7–30	3.9	0.52	0.05	1287	3991	696	316	2.5	87.6	9.9
	30–45	3.5	0.37	0.04	1322	6855	896	193	2.2	76.6	21.2
	45–80	3.6	0.33	0.05	775	7693	455	156	2.1	75.3	22.6
	80–105	4.1	0.30	0.03	474	5895	308	247	2.1	79.4	18.5
Pine	105–140	6.1	0.09	0.03	278	4132	172	209	2.6	87.2	10.2
	0–4	3.7	26.01	1.23	1539	3960	867	646	-	-	-
	4–9	3.4	4.94	0.29	1185	3653	446	142	7.4	84.8	7.8
	9–35	4.0	0.67	0.06	943	2673	387	603	8.8	89.0	2.2
	35–55	4.1	0.34	0.02	793	1922	272	146	9.1	88.3	2.6
	55–75	3.8	0.32	0.04	1780	5198	457	229	9.9	75.7	14.4
	75–125	3.9	0.29	0.03	885	5679	479	219	6.2	78.2	15.6
125–185	3.9	0.31	0.04	717	4730	292	199	5.8	80.1	14.1	

Grassland/Meadow	0–3	5.2	4.15	0.78	532	2957	421	196	-	-	-
	3–23	5.1	1.29	0.14	826	4859	470	276	5.7	79.8	14.5
	23–40	5.9	0.38	0.04	1177	7352	558	207	5.4	77.9	16.7
	40–55	5.9	0.32	0.03	1238	6125	983	204	6.9	77.9	15.2
	55–85	5.9	0.29	0.03	531	5484	282	177	5.2	75.1	19.7
	85–120	5.8	0.26	0.03	564	4947	270	202	5.8	84.4	9.8
	120–185	5.6	0.26	0.02	290	4015	169	196	3.8	88.5	7.7
Arable land	0–30	5.0	0.83	0.09	509	5647	226	208	5.0	81.3	13.7
	30–70	5.0	0.28	0.03	292	4789	172	171	4.2	85.1	10.7
	70–100	5.7	0.28	0.04	362	4722	128	247	3.4	87.1	9.5
	100–150	5.3	0.28	0.02	296	3898	130	160	2.8	89.0	8.2
	150–160	6.6	0.12	0.02	441	3323	365	184	2.5	89.1	8.4

Table A2

Chemical composition of the different horizons in the studied soils.

Horizon	Depth cm	SiO ₂	Al ₂ O ₃	CaO	Fe ₂ O ₃	K ₂ O	MgO	MnO	Na ₂ O	P ₂ O ₅	TiO ₂
		g kg ⁻¹	g kg ⁻¹	g kg ⁻¹	g kg ⁻¹	g kg ⁻¹	mg kg ⁻¹	mg kg ⁻¹	mg kg ⁻¹	mg kg ⁻¹	mg kg ⁻¹
Beech											
O	2	390	54.4	12.5	10.2	10.7	2860	3814	4165	2294	3276
Ah	7	761	57.9	2.0	14.3	19.0	2471	1053	8121	735	6266
E	30	793	59.6	1.9	15.5	20.1	3173	495	8510	475	6488
Bt/E	45	724	88.1	2.7	29.8	21.5	6047	362	7659	603	6400
Bt	80	738	91.0	3.5	32.2	21.4	6616	315	7586	850	6338
Bw/C	105	765	82.1	4.1	26.7	21.7	5714	475	8909	853	6295
C	140	720	74.7	35.2	21.0	21.1	9928	452	8937	858	5625
Pine											
O	4	406	55.8	4.9	16.0	10.1	1585	998	3671	2278	3373
Ah	9	754	48.9	1.8	13.6	16.9	1795	261	6385	1614	5611
E/A	35	781	45.8	1.6	11.1	16.9	1827	1026	6496	796	5989
E	55	810	44.8	1.7	9.7	17.5	1784	341	6840	716	5927
Bt	75	767	64.3	2.5	22.5	18.1	4344	489	6315	960	5883
Bw/C	125	748	66.1	3.1	25.0	18.0	5122	382	6480	636	5829
C	185	777	57.0	3.0	20.2	18.3	4199	377	7365	690	5932
Grassland/Meadow											
Ah	3	719	62.7	6.4	23.1	2.4	8865	503	7502	1077	5788
Ap	23	742	59.8	5.0	20.7	17.6	4052	460	6247	951	6050
E	40	731	72.2	5.0	28.2	18.3	5535	370	6114	948	6079
E/Bt	55	739	63.4	4.4	24.4	18.1	4862	400	6587	933	6060
Bt	85	758	65.6	4.4	23.0	19.5	4585	351	7283	882	6093
Bw/C	120	780	61.7	3.6	20.3	18.5	3947	350	7670	679	5826
C	185	774	59.0	3.6	19.0	19.0	3980	383	8338	665	5928
Arable land											
Ap	30	766	63.6	3.9	22.6	18.3	4609	381	7017	1002	6102
Bt	70	782	62.4	3.6	19.6	19.0	4189	339	8233	555	5963
Bw/C	100	766	61.6	3.7	20.0	19.1	4001	412	8446	642	5873
C	150	787	66.5	4.0	20.1	20.1	4338	330	8950	734	6246
C	160	758	70.1	25.0	20.0	20.1	7587	371	8805	827	6102

Table A3

Mineralogical composition of the different horizons in the studied soils.

Study site	Mineral composition						
	Horizon	Depth (cm)	Quartz	K-feldspar	Plagioclase	Pyroxene	Amphiboles
Beech	O	2	-	-	-		
	Ah	7	+++	+	+		
	E	30	+++	+	+		
	Bt/E	45	+++	+	+		+
	Bt	80	+++	++	+		
	Bw/C	105	+++	+	++		
Pine	O	4	-	-	-		
	Ah	9	+++	+	+	+	+
	E/A	35	+++	++	+	+	
	E	55	+++	++	+	+	
	Bt	75	+++	++	+		+
	Bw/C	125	+++	+	+		
Grassland/Meadow	C	185	+++	+	++		
	Ah	3	-	-	-		
	Ap	23	+++	+	+		

	E	40	+++	++	+
	E/Bt	55	+++	+	++
	Bt	85	+++	++	+
	Bw/C	120	+++	+	+
	C	185	+++	+	+
Arable land	Ap	30	+++	++	+
	Bt	70	+++	++	+
	Bw/C	100	+++	+	++
	C	150	+++	+	+
	C	160	+++	+	+

+++ main mineral, ++ ancillary mineral, + mineral as an admixture.

References

- Alexandre, A., Meunier, J.D., Colin, F., Koud, J.M., 1997. Plant impact on the biogeochemical cycle of silicon and related weathering processes. *Geochim. Cosmochim. Acta* 61, 677–682.
- Alexandre, A., Bouvet, M., Abbadié, L., 2011. The role of savannas in the terrestrial Si cycle: a case study from Lamto, Ivory Coast. *Glob. Planet. Chang.* 78, 162–169.
- Barão, L., Clymans, W., Vandevenne, F., Meire, P., Conley, D.J., Struyf, E., 2014. Pedogenic and biogenic alkaline-extracted silicon distributions along a temperate land-use gradient. *Eur. J. Soil Sci.* 65, 693–705.
- Bartoli, F., 1983. The biogeochemical cycle of silicon in two temperate forest ecosystems. *Environ. Biogeochem. Ecol. Bull.* 35, 469–476.
- Bartoli, F., Wilding, L.P., 1980. Dissolution of biogenic opal as a function of its physical and chemical properties. *Soil Sci. Soc. Am. J.* 44, 873–878.
- Biermans, V., Baert, L., 1977. Selective extraction of the amorphous Al, Fe and Si oxides using an alkaline Tiron solution. *Clay Miner.* 12, 127–135.
- Blinnikov, M.S., Bagent, M.C., Reyerson, E.P., 2013. Phytolith assemblages and opal concentrations from modern soils differentiate temperate grasslands of controlled composition on experimental plots at Cedar Creek, Minnesota. *Quat. Int.* 287, 101–113.
- Borrelli, N., Alvarez, M.F., Osterrieth, M.L., Marcovecchio, J.E., 2010. Silica content in soil solution and its relation with phytolith weathering and silica biogeochemical cycle in Typical Argiudolls of the Pampean Plain, Argentina – a preliminary study. *J. Soils Sediments* 10, 983–994.
- Cabanes, D., Shahack-Gross, R., 2015. Understanding fossil phytolith preservation: the role of partial dissolution in paleoecology and Archaeology. *J. Archaeol.* 10 (5), 1–16.
- Carey, J.C., Fulweiler, R.W., 2012. Human activities directly alter watershed dissolved silica fluxes. *Biogeochemistry* 111, 125–138.
- Carey, J.C., Fulweiler, R.W., 2016. Human appropriation of biogenic silicon – the increasing role of agriculture. *Funct. Ecol.* 30 (8).
- Clymans, W., Struyf, E., Govers, G., Vandevenne, F., Conley, D.J., 2011. Anthropogenic impact on amorphous silica pools in temperate soils. *Biogeosciences* 8, 2281–2293. <https://doi.org/10.5194/bg-8-22812011>.
- Cornelis, J.-T., Delvaux, B., 2016. Soil processes drive the biological silicon feedback loop. *Funct. Ecol.* 30, 1298–1310.
- Cornelis, J.T., Ranger, J., Iserebant, A., Delvaux, B., 2010. Tree species impact the terrestrial cycle of silicon through various uptakes. *Biogeochem* 97, 231–245.
- Cornelis, J.T., Titeux, H., Ranger, J., Delvaux, B., 2011. Identification and distribution of the readily soluble silicon pool in a temperate forest below three distinct tree species. *Plant Soil* 342, 369–378.
- Creevy, A.L., Fisher, J., Puppe, D., Wilkinson, D.M., 2016. Protist diversity on a nature reserve in NW England—with particular reference to their role in soil biogenic silicon pools. *Pedobiologia* 59 (1–2), 51–59.
- de Lima Rodrigues, L., Daroub, S.H., Rice, R.W., Snyder, G.H., 2003. Comparison of three soil test methods for estimating plant-available silicon. *Commun. Soil Sci. Plant Anal.* 34, 2059–2071.
- De Rito, M., Honaine, M.F., Osterrieth, M., Morel, E., 2018. Silicophytoliths from a Pampean native tree community (*Celtis ehrenbergiana* community) and their representation in the soil assemblage. *Rev. Palaeobot. Palynol.* 257, 19–34.
- DIN ISO 11277, 1998. Bodenbeschaffenheit: Bestimmung der Partikelgrößenverteilung in Mineralböden – Verfahren mittels Siebung und Sedimentation. Deutsches Institut für Normung, Beuth, Berlin.
- Fishkis, O., Ingwersen, J., Streck, T., 2009. Phytolith transport in sandy sediment: experiments and modeling. *Geoderma* 151 (3–4), 168–178.
- Fishkis, O., Ingwersen, J., Lamers, M., Denysenko, D., Streck, T., 2010. Phytolith transport in soil: a field study using fluorescent labelling. *Geoderma* 157 (1–2), 27–36.
- Frayse, F., Pokrovsky, O.S., Schott, J., Meunier, J.D., 2006. Surface properties, solubility and dissolution kinetics of bamboo phytoliths. *Geochim. Cosmochim. Acta* 70, 1939–1951.
- Frayse, F., Pokrovsky, O.S., Schott, J., Meunier, J.D., 2009. Surface chemistry and reactivity of plant phytoliths in aqueous solutions. *Chem. Geol.* 258, 197–206.
- Georgiadis, A., Sauer, D., Herrmann, L., Breuer, J., Zarei, M., Stahr, K., 2013. Development of a method for sequential Si extraction from soils. *Geoderma* 209, 251–261.
- Georgiadis, A., Sauer, D., Herrmann, L., Breuer, J., Zarei, M., Stahr, K., 2014. Testing a new method for sequential silicon extraction on soils of a temperate-humid climate. *Soil Research* 52 (7), 645–657.
- Golyeva, A., 2001. Phytoliths and Their Information Role in Natural and Archaeological Objects, Moscow, Syktyvkar Elista.
- Guntzer, F., Keller, C., Poulton, P.R., McGrath, S.P., Meunier, J.D., 2012. Long-term removal of wheat straw decreases soil amorphous silica at Broadbalk, Rothamsted. *Plant Soil* 352, 173–184.
- Haysom, M.B.C., Chapman, L.S., 1975. Some aspects of the calcium silicate trials at Mackay. *Proc. Aust. Sugar Cane Technol.* 42, 117–122.
- Hodson, M.J., 2016. The development of phytoliths in plants and its influence on their chemistry and isotopic composition. Implications for palaeoecology and archaeology. *J. Archaeol. Sci.* 68, 62–69.
- Hodson, M.J., 2019. The Relative Importance of Cell Wall and Lumen Phytoliths in Carbon Sequestration in Soil: A Hypothesis. *Front. Earth Sci.* 7, 167. <https://doi.org/10.3389/feart.2019.00167>.
- Keller, C., Guntzer, F., Barboni, D., Labreuche, J., Meunier, J.D., 2012. Impact of agriculture on the Si biogeochemical cycle: input from phytolith studies. *Compt. Rendus Geosci.* 344, 739–746.
- Kendrick, K.J., Graham, R.C., 2004. Pedogenic silica accumulation in chronosequence soils, Southern California. *Soil Sci. Soc. Am. J.* 68, 1295–1303.
- Kodama, H., Ross, G.J., 1991. Tiron dissolution method used to remove and characterize inorganic components in soils. *Soil Sci. Soc. Am. J.* 55, 1180–1187.
- Li, Z., Song, Z., Cornelis, J.T., 2014. Impact of rice cultivar and organ on elemental composition of phytoliths and the release of bio-available silicon. *Front. Plant Sci.* 5 (529).
- Li, Z., Unzué-Belmonte, D., Cornelis, J.T., Vander Linden, C., Struyf, E., Ronsse, F., Delvaux, B., 2019. Effects of phytolithic rice-straw biochar, soil buffering capacity and pH on silicon bioavailability. *Plant Soil* 438, 187–203.
- Madella, M., Alexandre, A., Ball, T., 2005. International code for phytolith nomenclature 1.0. *Ann. Bot.* 96, 253–260.
- Maguire, T.J., Templer, P.H., Battles, J.J., Fulweiler, R.W., 2017. Winter climate change and fine root biogenic silica in sugar maple trees (*Acer saccharum*): implications for silica in the Anthropocene. *J. Geophys. Res. Biogeosci.* 122, 708–715. <https://doi.org/10.1002/2016JG003755>.
- Markewitz, D., Richter, D.D., 1998. The bio in aluminium and silicon biogeochemistry. *Biogeochemistry* 42, 235–252.
- Mehra, O.P., Jackson, M.L., 1960. Iron oxide removal from soils and clays by a dithionite-citrate system buffered with sodium bicarbonate. In: Swineford, A. (Ed.), *Clays and Clay Minerals. Proc. 7th Natl. Conf.*, Washington DC, 1958 Pergamon Press, New York, pp. 317–327.
- Meunier, J.D., Guntzer, F., Kirman, S., Keller, C., 2008. Terrestrial plant-Si and environmental changes. *Mineral. Mag.* 72, 263–267.
- Meunier, J.D., Keller, C., Guntzer, F., Riotte, J., Braun, J.J., Anupama, K., 2014. Assessment of the 1% Na₂CO₃ technique to quantify the phytolith pool. *Geoderma* 216, 30–35.
- Meunier, J.D., Barboni, D., Anwar-ul-Haq, M., Levard, C., Chaurand, P., Vidal, V., Grauby, O., Huc, R., Laffont-Schwob, I., Rabier, J., Keller, C., 2017. Effect of phytoliths for mitigating water stress in durum wheat. *New Phytol.* 215, 229–239. <https://doi.org/10.1111/nph.14554>.
- Nguyen, M.N., Meharg, A.A., Carey, M., Dultz, S., Marone, F., Cichy, S.B., Tran Ch, T., Le, G.H., Mai, N.T., Nguyen, T.T.H., 2018. Fern, *Dicranopteris linearis*, derived phytoliths in soil: morphotypes, solubility and content in relation to soil properties. *Eur. J. Soil Sci.* 1–11.
- Osterrieth, M., Borrelli, N., Alvarez, M.F., Honaine, M.F., 2015. Silica biogeochemical cycle in temperate ecosystems of the Pampean Plain, Argentina. *J. S. Am. Earth Sci.* 63, 172–179.
- Peto, A., 2013. Studying modern soil profiles of different landscape zones in Hungary: an attempt to establish a soil-phytolith identification key. *Quat. Int.* 287, 149–161.
- Piperno, D., 2006. R.: Phytoliths: A Comprehensive Guide for Archaeologists and Paleoecologists. Alta Mira Press, Lanham, MD.
- Puppe, D., Leue, M., 2018. Physicochemical surface properties of different biogenic silicon structures: results from spectroscopic and microscopic analyses of protistic and phytogenic silica. *Geoderma* 330, 212–220.
- Puppe, D., Ehrmann, O., Kaczorek, D., Wanner, M., Sommer, M., 2015. The protozoic Si pool in temperate forest ecosystems – quantification, abiotic controls and interactions with earthworms. *Geoderma* 243–244, 196–204.
- Puppe, D., Höhn, A., Kaczorek, D., Wanner, M., Sommer, M., 2016. As time goes by – spatiotemporal changes of biogenic Si pools in initial soils of an artificial catchment in NE Germany. *Appl. Soil Ecol.* 105, 9–16.
- Puppe, D., Höhn, A., Kaczorek, D., Wanner, M., Wehrhan, M., Sommer, M., 2017. How big is the influence of biogenic silicon pools on short-term changes in water-soluble silicon in soils? Implications from a study of a 10-year-old soil-plant system. *Biogeosciences* 14, 5239–5252.
- Saccone, L., Conley, D.J., Koning, E., Sauer, D., Sommer, M., Kaczorek, D., Blecker, S.W.,

- Kelly, E.F., 2007. Assessing the extraction and quantification of amorphous silica in soils of forest and grassland ecosystems. *Eur. J. Soil Sci.* 58, 1446–1459.
- Sangster, A.G., Hodson, M.J., Tubb, H.J., 2001. Silicon deposition in higher plants. In: Datnoff, L.E., Snyder, G.H., Korndörfer, G.H. (Eds.), *Silicon in Agriculture*. 8. Elsevier, Amsterdam, The Netherlands, pp. 85–113.
- Schlichting, E., Blume, H.P., Stahr, K., 1995. *Soils Practical*. Blackwell, Berlin, Wien, Germany, Austria 295 pp.
- Schwertmann, U., 1964. Differenzierung der Eisenoxide des Bodens durch Extraktion mit Ammoniumoxalat Lösung. *Z. Pflanzenernähr. Bodenkd.* 105, 194–202.
- Sommer, M., Kaczorek, D., Kuzyakov, Y., Breuer, J., 2006. Silicon pools and fluxes in soils and landscapes – a review. *J. Plant Nutr. Soil Sci.* 169, 310–329.
- Sommer, M., Jochheim, H., Höhn, A., Breuer, J., Zagorski, Z., Busse, J., Barkusky, D., Meier, K., Puppe, D., Wanner, M., Kaczorek, D., 2013. Si cycling in a forest biogeo-system – the importance of transient state biogenic Si pools. *Biogeosciences* 10, 4991–5007. <https://doi.org/10.5194/bg-10-4991-2013>.
- Song, Z., McGrouther, K., Wang, H., 2016. Occurrence, turnover and carbon sequestration potential of phytoliths in terrestrial ecosystems. *Earth Sci. Rev.* 158, 19–30.
- Street-Perrott, F.A., Barker, P.A., 2008. Biogenic silica: a neglected component of the coupled global continental biogeochemical cycles of carbon and silicon. *Earth Surf. Process. Landf.* 33, 1436–1457.
- Struyf, E., Smis, A., Van Damme, S., Meire, P., Conley, D.J., 2009. The global biogeochemical silicon cycle. *SILICON* 1 (4), 207–213.
- Struyf, E., Smis, A., Van Damme, S., Garnier, J., Govers, G., Van Wesemael, B., Conley, D.J., Batelaan, O., Frot, E., Clymans, W., Vandevenne, F., Lancelot, C., Goos, P., Meire, P., 2010. Historical land use change has lowered terrestrial silica mobilization. *Nat. Commun.* 1, 129. <https://doi.org/10.1038/ncomms1128>.
- Turpault, M.P., Calvaruso, C., Kirchen, G., Redon, P.O., Cochet, C., 2018. Contribution of fine tree roots to the silicon cycle in a temperate forest ecosystem developed on three soil types. *Biogeosciences* 15 (7), 2231–2249.
- Vandevenne, F., Struyf, E., Clymans, W., Meire, P., 2012. Agricultural silica harvest: have humans created a new loop in the global silica cycle? *Front. Ecol. Environ.* 10, 243–248.
- Vandevenne, F.I., Barão, L., Ronchi, B., Govers, G., Meire, P., Kelly, E.F., Struyf, E., 2015. Silicon pools in human impacted soils of temperate zones. *Glob. Biogeochem. Cycles* 29, 1439–1450.
- Wanner, M., Birkhofer, K., Fischer, T., Shimizu, M., Shimano, S., Puppe, D., 2019. Soil testate amoebae and diatoms as bioindicators of an old heavy metal contaminated floodplain in Japan. *Microb. Ecol.* 1–11.
- Wilding, L.P., Drees, L.R., 1971. Biogenic opal in Ohio soils. *Soil Sci. Soc. Am. Proc.* 35, 1004–1010.
- Wilding, L.P., Drees, L.R., 1974. Contributions of forest opal and associated crystalline phases to fine silt and clay fractions of soils. *Clays and Clay Minerals* 22 (3), 295–306.



Si cycling in a forest biogeosystem – the importance of transient state biogenic Si pools

M. Sommer^{1,2}, H. Jochheim³, A. Höhn¹, J. Breuer⁴, Z. Zagorski⁵, J. Busse⁶, D. Barkusky⁷, K. Meier⁸, D. Puppe^{1,9}, M. Wanner⁹, and D. Kaczorek^{1,5}

¹Leibniz Centre for Agricultural Landscape Research (ZALF), Institute of Soil Landscape Research, Eberswalder Str. 84, 15374 Müncheberg, Germany

²University of Potsdam, Institute of Earth and Environmental Sciences, Karl-Liebknecht-Str. 24–25, 14476 Potsdam, Germany

³Leibniz Centre for Agricultural Landscape Research (ZALF), Institute of Landscape Systems Analysis, Eberswalder Str. 84, 15374 Müncheberg, Germany

⁴Landwirtschaftliches Technologiezentrum Augustenberg (LTZ), Referat 12, Neßlerstr. 23–32, 76227 Karlsruhe, Germany

⁵Department of Soil Environment Sciences, Warsaw University of Life Science (SGGW), Nowoursynowska 159, 02-776 Warsaw, Poland

⁶Leibniz Centre for Agricultural Landscape Research (ZALF), Institute for Landscape Biogeochemistry, Eberswalder Str. 84, 15374 Müncheberg, Germany

⁷Leibniz Centre for Agricultural Landscape Research (ZALF), Research Station Müncheberg, Eberswalder Str. 84, 15374 Müncheberg, Germany

⁸Leibniz Centre for Agricultural Landscape Research (ZALF), Institute of Land Use Systems, Eberswalder Str. 84, 15374 Müncheberg, Germany

⁹Brandenburg University of Technology Cottbus-Senftenberg, Chair General Ecology, 03013 Cottbus, Germany

Correspondence to: M. Sommer (sommer@zalf.de)

Received: 30 September 2012 – Published in Biogeosciences Discuss.: 19 December 2012

Revised: 11 June 2013 – Accepted: 18 June 2013 – Published: 24 July 2013

Abstract. The relevance of biological Si cycling for dissolved silica (DSi) export from terrestrial biogeosystems is still in debate. Even in systems showing a high content of weatherable minerals, like Cambisols on volcanic tuff, biogenic Si (BSi) might contribute > 50 % to DSi (Gerard et al., 2008). However, the number of biogeosystem studies is rather limited for generalized conclusions. To cover one end of controlling factors on DSi, i.e., weatherable minerals content, we studied a forested site with absolute quartz dominance (> 95 %). Here we hypothesise minimal effects of chemical weathering of silicates on DSi. During a four year observation period (05/2007–04/2011), we quantified (i) internal and external Si fluxes of a temperate-humid biogeosystem (beech, 120 yr) by BIOME-BGC (version ZALF), (ii) related Si budgets, and (iii) Si pools in soil and beech, chemically as well as by SEM-EDX. For the first time two compartments of biogenic Si in soils were analysed, i.e., phyto-

genic and zoogenic Si pool (testate amoebae). We quantified an average Si plant uptake of 35 kg Si ha⁻¹ yr⁻¹ – most of which is recycled to the soil by litterfall – and calculated an annual biosilicification from idiosomic testate amoebae of 17 kg Si ha⁻¹. The comparatively high DSi concentrations (6 mg L⁻¹) and DSi exports (12 kg Si ha⁻¹ yr⁻¹) could not be explained by chemical weathering of feldspars or quartz dissolution. Instead, dissolution of a relictic, phytogenic Si pool seems to be the main process for the DSi observed. We identified canopy closure accompanied by a disappearance of grasses as well as the selective extraction of pine trees 30 yr ago as the most probable control for the phenomena observed. From our results we concluded the biogeosystem to be in a transient state in terms of Si cycling.

1 Introduction

In recent years our understanding of Si cycling in different terrestrial biogeosystems has been improved substantially. Research on steppe (Blecker et al., 2006; Borrelli et al., 2010, White et al., 2012), savannah (Melzer et al., 2010, 2012; Alexandre et al., 2011), forest (Gerard et al., 2008; Cornelis et al., 2010a, 2011a) and wetland biogeosystems (Struyf and Conley, 2009; Struyf et al., 2009) enhanced our understanding of the “plant factor”, i.e., the importance of the biological Si cycling in terrestrial biogeosystems which had been studied in tropical and temperate climates so far (Sommer et al., 2006).

Recently, the complex effects of natural disturbances and anthropogenic perturbations on Si cycling came into focus in Si research. Deforestation (Conley et al., 2008), invading insects (Grady et al., 2007), or fire (Engle et al., 2008) clearly modifies annual DSi exports from catchments. Land use change (LUC) was added as another control on DSi exports at regional scale and conceptual models including those for human activities were developed (Struyf et al. 2010; Carey and Fulweiler, 2012). The results of these studies challenge the steady state assumption implied in most studies on Si budgets.

Although a spatial hierarchy of driving factors for DSi exports is well known (Sommer et al., 2006; Cornelis et al., 2011b), the origin of DSi is still under debate. The major research questions are the following: How large is the contribution of BSi pool to DSi compared to litho-/pedogenic sources? What are the main drivers of the relative importance of biogenic and mineral sources – climate, lithology, state of soil development, soil pattern, land use? To answer these questions Cornelis et al. (2011b) developed a conceptual framework. They defined four different scenarios (“end members”) based on climate, soil, and vegetation: scenario 1 (weathering unlimited) represents optimal climate and soil conditions. Here the DSi exports from soil-plant systems are controlled by climate, i.e., temperature and runoff. In scenario 2 (soil weathering limited) climate is optimal, but soils are poor in weatherable minerals. Consequently, DSi export is controlled by a near-surface biogeochemical cycling in the plant-soil system rather than by geochemical processes in deeper soil layer. In scenario 3 (climate weathering limited) soils contain weatherable minerals. Therefore, DSi might be controlled by either biogenic or pedo-/lithogenic sources. Their relative proportions depend on local conditions (lithology, geomorphology, land use). By scenario 4 (weathering limited) deserts are covered where eolian fluxes are the only relevant Si export from the system. According to Cornelis et al. (2011b) each scenario should be characterized by distinct DSi geochemical signatures ($\delta^{30}\text{Si}$, Ge/Si) which can be used in tracing Si pathways in soil-plant systems.

However these signatures have to be combined with Si flux analysis (incl. mass balances) and Si pool quantifications in order to understand the fate of Si in terrestrial bio-

geosystems. Unfortunately, the number of studies in which Si fluxes in/from the soil-plant system are directly linked to a detailed analysis of Si pools is still limited (e.g., Alexandre et al., 1997; Lucas, 2003; Blecker et al. 2006; Gerard et al., 2008; White et al. 2012). Furthermore, no study included a zoogenic Si pool, although first results on testate amoebae dynamics already showed its relevance in terms of biosilicification (comparable to plants, Aoki et al., 2007).

Here we present results on Si cycling in a forest biogeosystem which experienced vegetation shifts due to forest management. We hypothesised that the effects of Si biocycling on DSi must be most pronounced in cases of very low silicate weathering. Therefore, we selected a biogeosystem showing a quartz dominance in soils and parent material (> 95 %). Based on a system approach, we quantified Si fluxes (internal, external) for a 4 yr period and interpreted DSi exports in terms of litho-/pedogenic and biogenic sources as well as vegetation shifts. For the first time the quantification of the biogenic Si pool comprises two compartments, the phytogenic and zoogenic pool.

2 Materials and methods

2.1 Environmental setting

Our study site “Beerenbusch” is located in northern Brandenburg close to the village Rheinsberg (53°09' N, 12°59' E; 78 m a.s.l.; Fig. S1 in Supplement). The climate is characterised by mean annual air temperature of 8.7 °C and average precipitation of 600 mm y⁻¹ according to long-term measurements (1981–2010) of the meteorological station Neuglobsow/Menz of the German Weather Service (DWD) which is located 4 km E of the forest stand. The mean precipitation during the study period (05/2007–04/2011) was 15 % higher (689 mm) compared to the 30 yr average.

The study site is located at a Weichselian outwash plain (sandur) of the Rheinsberg Basin in the foreland of Late Pleistocene terminal moraines (“Fürstenberger Staffel”, Ginzler and Ertl, 2004). The soil is classified as *Brunic Arenosol (Dystric)* according to WRB (2006) and *Lamellic Udipsamment* according to Soil Taxonomy (Soil Survey Staff, 1999). Humus enriched topsoils extend down to a depth of 35 cm (Fig. S2 in Supplement). Bleached quartz grains indicate a slight podzolization for the first mineral horizon (AE). Brunification leads to a bright brownish color in the subsoil (Bw horizons) down to a depth of 80 cm. Single thin clay lamellae in subsoil and parent material indicate clay translocation macroscopically (down to 120 cm).

2.2 Land use and forest management history

The study site is embedded into a large forested area, called “Naturpark Stechlin-Ruppiner Land”. Reconstruction of land use history revealed Beerenbusch to be covered by forests for at least 230 yr (Fig. S3 in Supplement). Before 1888 the site

was used as pine forest (*Pinus sylvestris* L., planted in 1826) (Figs. S4, S5 in Supplement). In 1888 European beech (*Fagus sylvatica* L.) was planted into the pine stand as an understorey. A mixed forest of beech and pine developed since. As canopy closure continued, grasses of the understorey successively disappeared due to light limitation. Already in 1954 only few local spots with grasses in the ground vegetation existed (Table S6 in Supplement). Canopy closure was accomplished in the early 1980s. From 1985 to 1988, the upper pine layer of the mixed forest stand was cut stepwise. The recent plant community classifies as a *Majanthemo-Fagetum* with coverages of 85 % beech in the upper storey, 5 % in the intermediate layer and 20 % in the understorey. The recent ground vegetation shows herbs (1 % coverage), mosses (5 %), and lichens (< 1 %) (F. Becker, personal communication, 2004), but no grasses (Fig. S3 in Supplement). In 2008 the mature beech stand is characterised by a mean tree height of 28 m and a timber volume of 369 m³ ha⁻¹. An ICP Forests site (DE1207) was established and instrumented at a 0.5 ha fenced area in 2001 (Fig. S2 in Supplement).

2.3 Sampling and analysis of soils, plants, phytoliths, and testate amoebae

A representative soil and a sediment core had been analysed for basic textural and chemical properties prior to this study (Lachmann, 2002; Jochheim et al., 2007a; Fig. S2 in Supplement). Spatial soil heterogeneity was characterized in a 25 × 25 m raster by Lachmann (2002). From his results a quite similar soil horizonation and sediment layering can be concluded for the 0.5 ha study site. Therefore, we merged results of both samplings (soil pit, core) into one depth function (down to 2.8 m). For Si analysis a resampling from the original soil pit occurred end of September 2009.

Litter and soil material was taken by horizons down to a depth of 1.25 m and stored in plastic bags. Undisturbed soil cores (100 cm³) were taken in the middle of soil horizons and dried at 105 °C for determination of bulk density (BD) (Lachmann, 2002). Bulk densities for sediments of the core were calculated by bulk density = (1 – total porosity) × density. Assuming a total porosity of 0.36 (36 Vol. %), which is reasonable for near-surface glaciofluvial sands, and a quartz density of 2.65 g cm⁻³ we calculated a bulk density of 1.7 g cm⁻³. Bulk soil samples were air dried, gently crushed and sieved at 2 mm to separate the fine earth fraction (< 2 mm) from gravel (> 2 mm). The particle size distribution of the fine earth was determined by a combined wet sieving (> 63 μm) and pipette (< 20 μm) method (DIN ISO 11277, 1998). Pretreatment for particle size analysis was done by wet oxidation of organic matter using H₂O₂ (10 Vol. %) at 80 °C and dispersion by shaking the sample end over end for 16 h with a 0.01 M Na₄P₂O₇-solution (Schlichting et al., 1995). Soil pH was measured using a glass electrode in 0.01 M CaCl₂ suspensions at a soil to solution ratio of 1 : 5 (*w/v*) (DIN ISO 10390, 1997) af-

ter a 60 minute equilibration period. The total carbon content was determined by dry combustion using an elemental analyser (Vario EL, Elementar Analysensysteme, Hanau, Germany). CaCO₃ was determined conductometrically following Scheibler (Schlichting et al., 1995). Organic carbon (C_{org}) was calculated as the difference between total carbon and carbonate carbon. In soil horizons and sediments without carbonates total carbon equals soil organic carbon. Pedogenic oxides were characterised by dithionite-soluble (DCB) Fe (Fe_d) and dark acid-oxalate soluble Fe, Al, and Si (Al_o, Fe_o, Si_o) following the procedures of Mehra and Jackson (1960) and Schwertmann (1964), respectively (Schlichting et al., 1995). The element concentrations in solutions were determined by ICP-OES. All basic soil analyses were performed in two lab replicates.

2.3.1 Water extractable Si (Si_{H₂O})

Water extractable Si was determined by the method of Schachtschabel and Heinemann (1967). Ten grams of dry soil (< 2 mm) were weighted into 80 mL plastic centrifuge tubes and 50 mL distilled water added together with three drops of a 0.1 % NaN₃-solution to prevent microbial activity. The total extraction lasted seven days in which tubes were shaken by hand twice a day. Tubes were not shaken mechanically to avoid abrasion of coarse mineral particles colliding during shaking (Mc Keague and Cline, 1963). Finally the extraction solution was centrifuged (4000 rpm, 20 min), filtrated (0.45 μm polyamide membrane filters) and Si was measured by ICP-OES. Analyses were performed in three lab replicates.

2.3.2 Tiron extractable Si (Si_{Tiron})

The Tiron (C₆H₄Na₂O₈S_{2x}H₂O) extraction procedure was developed by Biermans and Baert (1977) and modified by Kodama and Ross (1991). It has been used to quantify amorphous biogenic and pedogenic Si, so-called “pedogenic silica” (Kendrick and Graham, 2004), although a partial dissolution of primary minerals is well known (Kodama and Ross, 1991; Sauer et al., 2006). The extraction procedure is as follows: dilution of 31.42 g Tiron (ACROS Organics, Geel, Belgium) with 800 mL of distilled water, followed by addition of 100 ml sodium carbonate solution (5.3 g Na₂CO₃ in 100 mL distilled water) under constant stirring. After that the pH of the solution increases from 3.3 to 7.5. Finally, the pH is brought to 10.5 by adding small volumes of a 4 M NaOH-solution. The Tiron solution is transferred into a 1 L volumetric flask and has a final concentration of 0.1 M. For the extraction 30 mg of dry soil is weighted into 80 mL centrifuge tubes and a 30 mL aliquot of the Tiron solution added. The tubes are then heated at 80 °C in a water bath for 1 h. After cooling adhering water on the surface of the tubes is removed, the tubes are weighted and water lost by evaporation is replaced. The extracted solutions were centrifuged at

4000 rpm for 30 min, filtrated (0.45 μm polyamide membrane filters, Whatman NL 17) and elements were measured by ICP-OES. Analyses were performed in three lab replicates.

2.3.3 Mineralogy, micromorphology and SEM-EDX analysis

Powder samples of each soil horizon (< 2 mm fraction) were analysed for basic mineral composition using a BRUCKER AXS D5000 Diffractometer (Cu-K α radiation). The relative intensities of the diffraction maxima were used for a semiquantitative estimation of the concentration of mineral species present. The counts from the main reflection peak of all minerals were summed up and the relative proportion of each mineral was calculated as percent of the total. A subsample of the < 2 mm fraction was placed on an Al-stub, fixed by adhesive tape, coated with minimal amount of gold-palladium and analysed on element composition by microprobe analysis (Hitachi S-2700 device, EDX-X-Flash-Detector with SAMX-Software at ZELMI, TU-Berlin).

Four undisturbed soil samples (Kubiena boxes of 8 cm height) were taken from 0–8 cm (AE, Ah), 10–18 cm (AB), 44–52 cm (Bw₁) and 104–112 cm (2Cwt) (Fig. S2 in Supplement). Air-dried samples were impregnated with Leguval resin under vacuum. After hardening 24 μm thick thin sections were prepared. The micromorphological features were described according to the concepts and terminology proposed by Stoops (2003). For thin section descriptions a SM-LUX-POL (Leitz) microscope with polarisation filter was used. After description thin sections were coated with carbon in a vacuum evaporator, and then examined with electron microprobe analyses (Cameca Camebax Microbeam, ZELMI at TU Berlin), using an accelerating potential of 20 kV. Element distribution maps (Si, Al, Fe, K, Mg, Ca, Na, Ti) were obtained with the same instrument. Feldspar grains and cutans (Fig. 5) were identified by microscopic examination on all thin sections (between 10 and 20 replicates, depending on the number of feldspar grains in each thin section). To obtain information about the weathering state of potassium feldspars, strewn slides of soil material from three different depths (10–20, 40–60, and 100–130 cm) were prepared and analysed using SEM (Fig. 6). For identification of feldspars, samples were analysed with REM-EDX and the potassium distribution in the slides was recorded. Each strewn slide was divided into four subsections and a minimum of ten replicates per subsection were analysed.

2.3.4 Phytolith separation from plants and soils, SEM-EDX analysis

Phytoliths were extracted from litterfall, the organic surface layer (L) as well as from the first three mineral horizons (AE, Ah, AB). Litterfall from one sampling date (May to August 2008) was separated into four groups: leaves, bud scales, fruit capsules and wood from twigs and branches. The ex-

traction procedure for litterfall was similar to soil horizons except steps 3 and 4 (see below). From each horizon 10 g of dry soil material (< 2 mm) were processed in four steps (adapted from Alexandre et al., 1997). First organic matter is oxidized using H₂O₂ (35 Vol. %), HNO₃ (65 Vol. %), HClO₄ (70 Vol. %) at 80 °C until reaction subsides. Secondly, carbonates and Fe oxides are dissolved by boiling the sample in HCl (10 Vol. %) for 30 min. Thirdly, the < 2 μm granulometric fraction is removed by dispersion of remaining solid phase of step 2 with 2 Vol. % sodium hexametaphosphate solution (6–12 h), centrifugation at 1000 rpm for 2–3 min, and subsequent decantation. Finally, the phytoliths are separated by shaking the remaining solid phase of step 3 with 30 mL of sodium polytungstate Na₆(H₂W₁₂O₄₀) · H₂O (density of 2.3 g cm⁻³), centrifugation at 3000 rpm for 10 min, carefully pipetting the supernatant, and filtering by 5 μm teflon filter. This step was repeated three times. The filter residue was washed with water, bulked, dried at 105 °C, and weighted.

A subsample was placed on an Al-stub, fixed by adhesive tape, and coated with minimal amount of gold-palladium. Ten micrographs per stub were made using a JEOL JSM6060 LV SEM microscope (500 \times magnification). Phytoliths of each micrograph (coverage approx. 200 \times 200 μm^2) were counted. The database comprises a total number of 462 (L), 459 (AE), 422 (Ah), and 238 phytoliths (AB). They were described by shape according to ICPN (Madelá et al., 2005) and assigned to vegetation (Golyeva, 2001) wherever applicable. Further, all counted phytoliths were assigned to one of three classes of phytolith dissolution: (i) plain phytoliths, (ii) phytoliths showing some surface etching, and (iii) phytoliths with strong dissolution features. Phytoliths at stubs were analysed on element composition by microprobe analysis (Hitachi S-2700 device, EDX-X-Flash-Detector with SAMX-Software at ZELMI, TU Berlin).

The Si pool of phytoliths was calculated assuming phytoliths to consist of pure SiO₂. This results in a slight overestimation of the real Si pools, because biogenic opal contains ca. 10 % H₂O and some accessory elements (< 1 %) (Bartoli and Wilding, 1980).

2.3.5 Plant analysis

The collected plant litter (see Sect. 2.4) was oven dried at 105 °C and milled in a planet type ball mill using milling vessels and balls made from ZrO₂. Sample aliquots of approximately 200 mg were digested under pressure in PFA digestion vessels using a mixture of 2.5 mL HNO₃ and 1 mL HF at 220 °C and approximately 100 bar (Ultra Clave II, MLS GmbH, Leutkirch, Germany). Silicon was measured by ICP-OES (Vista Pro, Varian Inc., Australia) using a HF-resistant sample introduction system, radial viewing of the plasma, and matrix matched external calibration.

2.3.6 Quantification of testate amoebae and related Si pool

For testate amoebae analysis 5 field replicates (20 cm × 20 cm) were placed randomly at Beerenbusch site avoiding areas close to stems (April 2011; Fig. S2 in Supplement). The litter layer (beech leaves) was removed and volumetric soil samples were taken in two segments: 0–2.5 cm and 2.5–5 cm (= sample volume of 1000 cm³). Aliquots of 2 g were taken for amoebae analysis in the field and stored in 8 mL formalin (4% aqueous formaldehyde solution). Total soil material of each depth increment and 20 cm × 20 cm area was oven dried at 105 °C and weighted. Bulk densities were calculated by dividing total soil mass by sample volume (1000 cm³). Testate amoebae were determined at species level and enumerated directly with an inverted microscope using stained (aniline blue) soil suspensions received from serial dilution (30–500 mg soil in 8 mL water per sample) as reported by Wanner (1999). Thereby living individuals and empty tests were distinguished. All species were assigned either to idiosomic or xenosomic amoebae taxa building up their tests from idiosomes (siliceous platelets synthesised by amoebae from H₄SiO₄ in soil solution) or xenosomes (extraneous materials such as mineral particles), respectively (e.g., Meisterfeld 2002a, b). Idiosomic Si pools (g m⁻²) of the upper 5 cm were calculated by (1) multiplying Si content of tests (Table 1 in Aoki et al., 2007) with counted individuals of each species, (2) multiplying these data with bulk densities and thickness (2.5 cm), and (3) finally summing up both depth increments.

2.4 Site instrumentation for flux determinations

The investigations of the study site water budget started in May 2001. The instrumentation as well as results of the first 4 yr are described in Jochheim et al. (2007a). Precipitation was measured continuously at an open field located 500 m south of the study site using a heated rain gauge (F&C GmbH Gülzow). Gaps in the precipitation data were filled by using open land precipitation data of either (i) the ICP Forests level II plot DE1202, or (ii) the weather station in Neuglobsow/Menz of the German Weather Service (DWD). For silicon analysis (started in May 2007) precipitation water of two rain samplers (RS200, UMS GmbH, Munich; 314 cm² each) were collected weekly. Throughfall was measured continuously using a gutter of 0.8 m² area with a tipping bucket rain gauge. Additionally, weekly measurements were carried out using 15 rain samplers (see above). Stemflow was measured continuously at one stem with a tipping bucket rain gauge, and additional weekly on 4 stems by sampling the water in barrels. For silicon analysis the weekly samples of open land precipitation, throughfall, and stemflow were bulked to monthly samples. Si concentrations in all waters were determined by ICP-OES.

Table 1. Mineralogical composition (wt.-%) of soil horizons and sediment layers by semiquantitative X-ray diffraction.

Depth (cm)	Quartz	Feldspar	Pyroxene
0–10	97.1	2.5	0.4
10–20	96.0	3.6	0.4
30–60	97.7	1.8	0.5
60–80	96.5	3.0	0.5
80–100	93.0	6.6	0.4
100–130	97.4	2.1	0.5
240–260	97.4	2.6	nd
480–500	98.0	2.0	nd

nd = not detected.

Litterfall was collected in 8 inverted pyramidal litter traps (0.25 m² each) bi-weekly during four years (05/2006–04/2010) and separated into leaves, flowers, bud scales, beechnuts, fruit capsules, and wood from twigs and branches. Each fraction was bulked into three periods per year (Jan–Apr, May–Aug, Sep–Dec). For silicon analysis see Sect. 2.3.5.

Soil solution was sampled using borosilicate suction probes (EcoTech Bonn GmbH) from 20, 70, and 250 cm soil depths (mean of 150 cm and 250 cm distance to stem; 4 replicates per depth and distance). The samples were collected by applying a suction of –30 kPa in 20 and 70 cm, and –35 kPa in 250 cm. Water was stored within the shafts of the suction probes and sampled bi-weekly. For silicon analysis the 4 field replicates per depth and distance were bulked. Si in soil water was measured by ICP-OES.

Analysis of water content was conducted hourly at different distances to stem (50, 150, 250 cm) of one stem in soil depths 20, 70, and 250 using Theta-probes ML2 (Delta-T Devices Ltd Cambridge, UK). Additionally, close to two further trees using identical distances to stem soil moisture were measured bi-weekly using TDR-probes (FOM/m-TDR, EasyTest Lublin, Poland) at identical soil depths.

Xylem sap flux was measured continuously during the vegetation periods of 2002–2005 on ten selected trees in 1.3 m tree height using the method after Granier (1985) and calculated to representative stand canopy transpiration following Lüttschwager and Remus (2007).

Aboveground woody tree biomass and forest growth were calculated by measuring stem diameter at breast height and tree height of all 108 trees of the plot in spring of 2006, 2008, and 2010 using form factors derived from the beech yield table (Dittmar et al., 1986), wood density (Trendelenburg and Mayer-Wegelin, 1955), bark density (Dietz, 1975), and bark fractions (Altherr et al., 1974).

2.5 Calculation and modeling of Si fluxes

Deposition of Si was calculated from the open land precipitation. Si fluxes were calculated by multiplying water fluxes

with Si concentrations. Stand precipitation equals the sum of Si fluxes in throughfall and stemflow, whereas leaching from canopy is the difference of Si fluxes in stand precipitation and open land precipitation. Silicon uptake equals the sum of Si fluxes in litter fall, leaching from canopy, and wood increment. Si export through harvest was calculated as a sum of current accumulation of Si in stem wood including bark.

The simulation of water budget was carried out with the dynamic model Biome-BGC (version ZALF; Jochheim et al., 2007b; Puhlmann and Jochheim, 2007) which is based on Biome-BGC (Thornton et al., 2002). The model runs in daily time steps. It was re-calibrated and validated on the basis of data from intensive forest monitoring sites (Jochheim et al., 2009) as well as on forest yield tables. For this application the model was calibrated based on the measurements of the stand started in 2001. Silicon fluxes with drainage water were calculated for four years (05/2007–04/2011) by multiplying the Si concentrations in soil water from suction probes with simulated soil water fluxes. Vertical distribution of passive Si uptake in soil was estimated from vertical distributed soil water uptake rates multiplied by Si concentrations in soil water. As the Si concentrations in soil water were analyzed in 3 soil depths only (20, 70, 250 cm), they were extrapolated to all other soil depths using the vertical distribution of water extractable Si.

3 Results

3.1 Basic soil properties and soil mineralogy

The studied soil is very sandy showing a sand content > 85 % and a dominance of medium sand fraction (0.2–0.63 mm, Fig. 1). In the upper 50 cm a slight increase in silt can be observed. Clay content is always below 3 % with slightly higher values in the upper 1.5 m. The soil is decalcified down to a depth of 1.8 m (Fig. 1). Acidification leads to pH values between 4.3 and 4.5 in the upper 1.6 m. Below that depth pH increases to > 7.0 due to carbonatic sediments (2–4 % CaCO₃). Quartz is the dominant mineral throughout the soil horizons and sediment layers (Table 1). Only minor additions of feldspars (orthoclase > plagioclase), pyroxene and calcite occurred. Organically complexed Fe, Al and pedogenic oxides (Fe, Al) decreased from C-enriched surface horizons (upper 20 cm) to subsoil horizons as crystallinity of iron oxides increased (Fe_o : Fe_d 0.6 → 0.2). The molar Si / Al ratios in oxalate extracts (Si_o : Al_o) remained below 0.3 in all soil horizons rendering neof ormation of short-range order minerals, like allophane or imogolite (Si / Al ≈ 0.5), hardly probable.

3.2 Si pools in soils

Water soluble Si shows a decrease from 16 mg kg⁻¹ in the upper 2 cm to 4 mg kg⁻¹ in subsoil horizons and a recurring increase in sediments containing carbonates (Fig. 1).

The water-soluble Si pool down to 2.8 m equals 21 g Si m⁻² (= 210 kg Si ha⁻¹). The uppermost meter contains 6 g Si m⁻² (= 60 kg Si ha⁻¹).

Tiron extractable Si is three orders of magnitude higher compared to water soluble Si. The depth function of Tiron extractable Si shows a continuous decrease from 3 g kg⁻¹ in topsoil horizons to < 2 g kg⁻¹ in deepest sediments. The highest Si content can be observed in the uppermost horizon (AE). The Tiron extractable Si pool down to 2.8 m equals 10 kg Si m⁻² (= 100 Mg Si ha⁻¹). The uppermost meter contains 4 kg Si m⁻² (= 40 Mg Si ha⁻¹).

3.2.1 Phytogenic Si pool in soil

Phytolith contents decrease from litter to mineral soil horizons by one order of magnitude (Table 2a). The upper 20 cm of the soil contain 140 g phytoliths m⁻² (= 1400 kg ha⁻¹). Assuming all phytoliths to consist of pure SiO₂ (EDX spectra in Fig. 2c) we calculated 66 g Si m⁻² for the phytolith Si pool in the upper 20 cm (= 660 kg Si ha⁻¹). This simplification results in a slight overestimation of the true phytogenic Si pool as biogenic opal contains approx. 10 % H₂O and some accessory elements (< 1 %) (Bartoli and Wilding, 1980).

The phytolith assemblage of soil horizons – as assignable by shape (ICPN, Madella et al., 2005) – is dominated by elongate (polylobate, fusiform) and short-cell phytoliths (bilobate, trapeziform) with minor contribution of globular and vascular phytoliths. In terms of vegetation a dominance of grass phytoliths were found in mineral soil horizons below 2 cm (Table 2b, Fig. 2b). This fits very well to the vegetation survey from 1954 which showed plants high in Si, such as *Calamagrostis epigejos* (2.2 % Si), *Brachypodium sylvaticum* (3.1 % Si), and *Agrostis capillaris* (1.4 % Si), dominating the ground vegetation (Table S6 in Supplement, Si data from Hodson et al., 2005). Pine and moss phytoliths (rounded particles, Al-rich) can be identified as well (Table 2b, Fig. 2b). However, as there are no more pine and grasses growing at the study site (at least for the last 30 yr) pine and grass phytoliths extracted from the soil represent a relictic biogenic Si pool. Surprisingly, clearly identifiable beech phytoliths only account for a minor portion in the upper centimeters. Further, those forms isolated from litterfall (Fig. 2a) are hardly detectable in their original shape in the soil, even not in the upper 2 cm (Fig. 2b). From these findings either a rapid mechanical destruction or a preferential dissolution of beech phytoliths can be concluded. Nevertheless, one has to recognize that 50–75 % of all phytoliths counted cannot be assigned to any vegetation throughout the uppermost 20 cm of the soil (Table 2b).

3.2.2 Zoogenic Si pool in soil

A total number of 6.1 × 10⁸ m⁻² testate amoebae (60 % living individuals) was determined in the upper 5 cm of the soil. This number lies in the range of published data (e.g.,

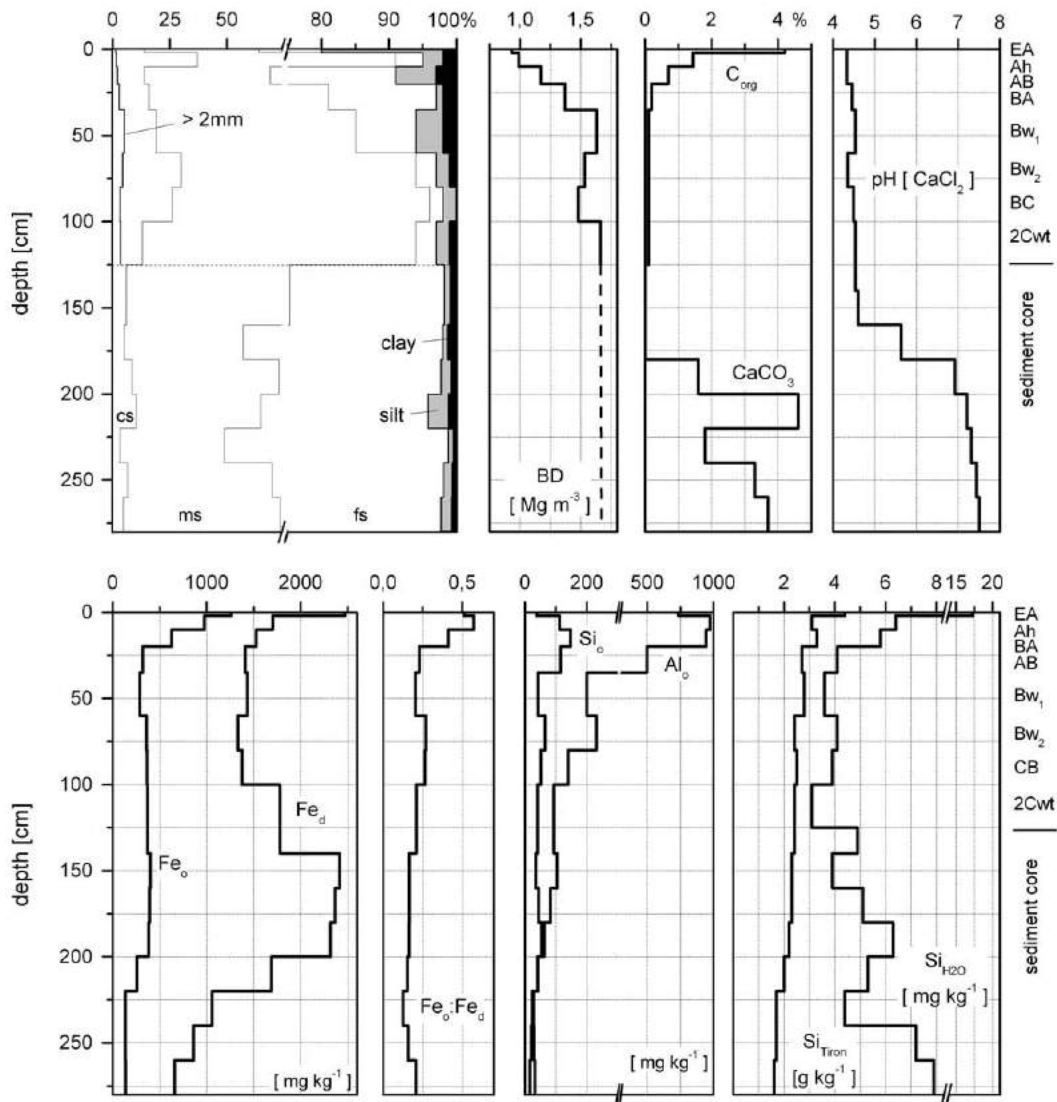


Fig. 1. Depth functions of basic soil properties from the *Brunic Arenosol* (Dystric).

Aoki et al., 2007; Ehrmann et al., 2012; Wanner and Dunger, 2001). Approximately 50 % of all individuals (living and empty tests) belong to either idiosomic or xenosomic taxa of testate amoebae. Xenosomic taxa build up their tests from extraneous materials such as mineral soil particles. Dominant xenosomic taxa at our site are *Phryganella acropodia*, *Plagiopyxis declivis*, and *Centropyxis sphagnicola* (Fig. 3d). Dominant idiosomic taxa embrace *Trinema complanatum*, *Euglypha rotunda*, and *Trinema lineare* (Fig. 3a–c). Only idiosomic taxa can be regarded as a biogenic Si pool influencing dissolved Si (DSi), because they synthesise siliceous platelets for their tests from silica of the soil solution (Anderson, 1994). Therefore, we calculated the zoogenic Si pool only on basis of idiosome-producing amoebae and came up with 0.19 g Si m^{-2} in the upper 5 cm of the soil ($= 1.9 \text{ kg Si ha}^{-1}$, Table 3). Compared to soil's phytolith Si

pool as derived from density separation, these numbers are two orders of magnitude lower.

3.3 Si in aboveground plant biomass

Beech leaves showed the highest Si concentrations followed by bark of branch and stem wood, bud scales, and fruit capsules (Table 4). Beechnuts and woody biomass without bark contain the lowest Si concentrations. Interannual variations in Si concentrations are largest in leaves, bud scales, and fruit capsules. In 2006 lowest Si concentrations in leaves were measured (7 g kg^{-1}). In litterfall of 2007 Si concentrations nearly doubled (13.6 g kg^{-1}) which might be an effect of the length of growing period (dry summer in 2006). In terms of intra-annual variations a seasonal trend of Si concentrations can be observed: Si concentrations of leaves from early

Table 2a. Phytoliths and related Si pools.

		Depth (cm)	Bulk density (Mg m ⁻³)	Phytolith (g kg ⁻¹)	Phytolith (g m ⁻²)	Si content (g kg ⁻¹)	Phytolith Si, calculated (g kg ⁻¹)	Phytolith Si, calculated (g m ⁻²)
Litterfall (5–8/08)	leaves	–		5.1	–	4.4	2.4	–
	bud scales	–		7.0	–	3.6	3.3	–
	fruit capsules	–		1.1	–	1.1	0.5	–
	branches	–		1.0	–	1.4	0.5	–
Soil	litter layer (L)			8.7			4.1	
	AE	0–2	0.92	0.9	17		0.4	8
	Ah	2–10	0.99	1.2	92		0.5	43
	AB	10–20	1.17	0.3	32		0.1	15
	<i>sum</i>	0–20				140		66

Table 2b. Morphological description and identification of phytoliths; n.a. = not assignable.

Soil Horizon	Depth (cm)	Count-% of total phytolith number (10 SEM micrographs)									
		Globular	Elongate	Short cell	Vascular	n.a.	Grasses	Beech	Mosses	Pine	n.a.
Litter layer (L)		7	25	18	1	49	7	12	4	1	75
AE	0–2	7	25	20	2	45	16	5	5	3	72
Ah	2–10	0	38	15	0	47	44	0	1	2	53
AB	10–20	0	27	8	0	64	45	0	0	1	54

Table 3. Si pools of idiosomic testate amoebae; mean values and standard deviation (in brackets), $n = 5$ field replicates.

Depth (cm)	Bulk density (Mg m ⁻³)	Living mg Si m ⁻²	Empty shells mg Si m ⁻²	Total mg Si m ⁻²
0–2.5	0.10 (0.04)	81(110)	54 (48)	135 (158)
2.5–5	0.36 (0.11)	34 (25)	22 (11)	57 (23)
<i>sum</i> 0–5		116 (106)	76 (43)	192 (148)

stages of vegetation development (May–Aug) were lowest (4.4–6.8 g kg⁻¹), whereas during autumn/winter (Sep–Dec) or winter/spring (Jan–Apr) Si concentrations range from 6 to 14 g kg⁻¹ (depending on single year).

Taking into account the biomass of each plant compartment the total Si pool in aboveground biomass summarises up to 83 kg Si ha⁻¹ (Table 4). The stem bark contributes the largest fraction (50 %) followed by leaves (36 %), branch bark (6 %), and stem wood (3 %).

3.4 Internal and external Si fluxes

Si uptake by plants contributes the largest internal Si flux in the biogeosystem (35 kg Si ha⁻¹ yr⁻¹, Fig. 4). The major part is transported into the leaves (30 kg Si ha⁻¹ yr⁻¹) rendering autumn litter fall the most important annual flux component to the soil. Minor fluxes are related to annual litterfall of twigs, bud scales, fruits, and flowers (4 kg Si ha⁻¹ yr⁻¹) or

dendromass increments (0.7 kg Si ha⁻¹ yr⁻¹). Although the Si pool size of testate amoebae is very small their relevance for internal Si cycling cannot be neglected. Due to relatively short generation times of idiosome-producing amoebae, e.g., Euglyphida with 2–16 days resulting in 12–130 generations per year (Schönborn, 1975, 1982; Lousier, 1984; Aoki et al., 2007), the annual biosilicification by idiosomes are in the order of the cumulative annual Si uptake by plants: using a conservative estimate of 15 generations per year we calculated an annual biosilicification of 17 kg Si ha⁻¹ yr⁻¹ (Si pool of living idiosomic taxa). The turnover rates of idiosomic Si pool must be much higher compared to phytolithic Si pool as can be deduced from (only) 47 % empty tests of total idiosomic Si pool. Consequently, testate amoebae can be regarded as a temporal Si pool on a very short, monthly timescale.

The total Si input with open land precipitation is rather low (< 1 kg Si ha⁻¹ yr⁻¹) which fits to the data from literature (Sommer et al., 2006; Cornelis et al., 2011b). The Si export by seepage equals 12 kg Si ha⁻¹ yr⁻¹ showing average silica concentrations of approx. 6 mg Si L⁻¹ (Table 5). The high temporal variability between years (CV = 50–64 %) can be related to varying seepage (Table 5), while temporal variability in silica concentrations were rather small (CV increase with depth: 4 → 11 %). Mean silica concentration increases only slightly from acid soil horizons (0.2 m, 0.7 m) to the calcareous parent material in 2.5 m (4.9 → 5.7 mg Si L⁻¹,

Table 4. Pools and increments of plant biomass, Si concentrations (mass weighted mean values), Si pools in aboveground biomass, Si fluxes with increment of tree biomass; *: calculated from litter fall of 05/2006–04/2010; **: calculated from stem volume of 2010 or stem growth of 2006–2009; no. in brackets = std.dev. ($n = 4$ yr).

	Biomass pools (t DM ha ⁻¹)	Litterfall/ increment (t DM ha ⁻¹ yr ⁻¹)	Si content (mg kg ⁻¹)	Si pools (kg ha ⁻¹)	Si fluxes (kg ha ⁻¹ yr ⁻¹)
Leaves*	3.4	3.4 (0.30)	8952 (3101)	29.7	29.7 (7.5)
Bud scales*	0.5	0.5 (0.04)	2395 (431)	1.2	1.2 (0.3)
Beechnuts*	0.7	0.7 (0.80)	280 (252)	0.2	0.2 (0.3)
Fruit capsules*	1.6	1.6 (1.20)	913 (275)	1.4	1.4 (1.1)
Other*		0.1 (0.03)	10229 (2979)		0.6 (0.4)
Branches/twigs including bark*		0.4 (0.30)	1649 (183)		0.7 (0.5)
<i>Total litterfall</i>		<i>6.7</i>			<i>33.7</i>
Branch wood without bark**	24.4	0.4	17	0.4	0.01
Stem wood without bark**	196.1	3.1	17	3.4	0.05
Bark of branch wood**	2.0	0.0	2565	5.2	0.08
Bark of stem wood**	16.3	0.2	2565	41.9	0.59
<i>Dendromass increment</i>		<i>3.7</i>			<i>0.70</i>
<i>Aboveground biomass</i>	<i>245.0</i>			<i>83.4</i>	

Table 5). This increase goes along with an increase in the water-soluble Si fraction (Fig. 1).

We set the annual accumulation rate of Si in stem wood and bark (0.6 kg Si ha⁻¹ yr⁻¹) as the (annual) harvest export. Although not realized yet, at the end of a rotation period stem harvest leads to a complete Si export of this compartment. By adding this Si export to seepage losses we come up with a gross Si loss of 13 kg Si ha⁻¹ yr⁻¹. Taking into account the inputs by deposition our biogeosystem reveals a net loss of 12 kg Si ha⁻¹ yr⁻¹.

4 Discussion

The low atmospheric Si input is in accordance with reported values from other forested biogeosystems (< 2 kg ha⁻¹ yr⁻¹, Sommer et al., 2006; Cornelis et al., 2011b). Throughfall and stemflow can also be neglected in terms of Si fluxes. The small annual increase in Si stored in the vegetation (biomass increment = 0.7 kg Si ha⁻¹ yr⁻¹) is lower compared to reported data (European beech = 3.5 kg Si ha⁻¹ yr⁻¹, Cornelis et al., 2010a) which might be explained by the lower forest growth of our mature beech stand (120 yr). The Si uptake by beech (35 kg Si ha⁻¹ yr⁻¹) and return flux by litterfall (34 kg Si ha⁻¹ yr⁻¹) lies in the range of other European beech stands in temperate climates (19–47 kg Si ha⁻¹ yr⁻¹; Pavlov, 1972; Bartoli and Souchier, 1978; Ellenberg et al., 1986; Cornelis et al., 2010a). We calculated an averaged passive Si-uptake of 17 kg Si ha⁻¹ yr⁻¹ as the product of vertically distributed mean Si concentrations and modeled transpiration flux (239 mm yr⁻¹). When compared to the measured

Table 5. Water fluxes, Si concentrations, and Si fluxes in water (m = measurements, s = simulation); all fluxes are expressed as mean annual values for a four year period (5/2007–4/2011), number in brackets = std.dev ($n = 4$ yr).

	Water flux (L m ⁻² yr ⁻¹)	Si concentr. (mg L ⁻¹)	Si flux (kg ha ⁻¹ yr ⁻¹)
Precipitation (m)	689 (195)	0.1 (0.03)	0.6 (0.2)
Leaching from canopy (m)			0.3 (0.1)
Canopy evaporation (s)	168 (28)		
Transpiration (s)	239 (24)		
Evapotranspiration (s)	476 (62)		
Throughfall (m)	491 (189)	0.1 (0.04)	0.8 (0.3)
Stemflow (m)	32 (13)	0.3 (0.03)	0.1 (0.0)
Stand precipitation (m)	523 (203)		0.9 (0.3)
Drainage from 20 cm (s)	316 (152)	4.9 (0.20)	15.4 (7.6)
Drainage from 70 cm (s)	262 (139)	5.3 (0.30)	13.9 (8.0)
Drainage from 250 cm (s)	214 (133)	5.7 (0.60)	12.3 (7.9)

Si-uptake of 34 kg Si ha⁻¹ yr⁻¹ an active uptake of 50 % of total uptake can be inferred.

Generally, the magnitude of Si uptake at Beerenbusch surprises, when considering the very low content of weatherable minerals in the rooting zone (soils, sediments). In principal three processes might cause the silica concentrations observed: (i) quartz dissolution, (ii) weathering of silicates, and (iii) dissolution of the biogenic Si pool (non-steady state).

4.1 Quartz dissolution and silicate weathering

Quartz has a water solubility of 1–7 mg L⁻¹ (36–250 μmol L⁻¹) depending on particle size and temperature (Iler, 1979; Bartoli and Wilding, 1980; Dove, 1995). The

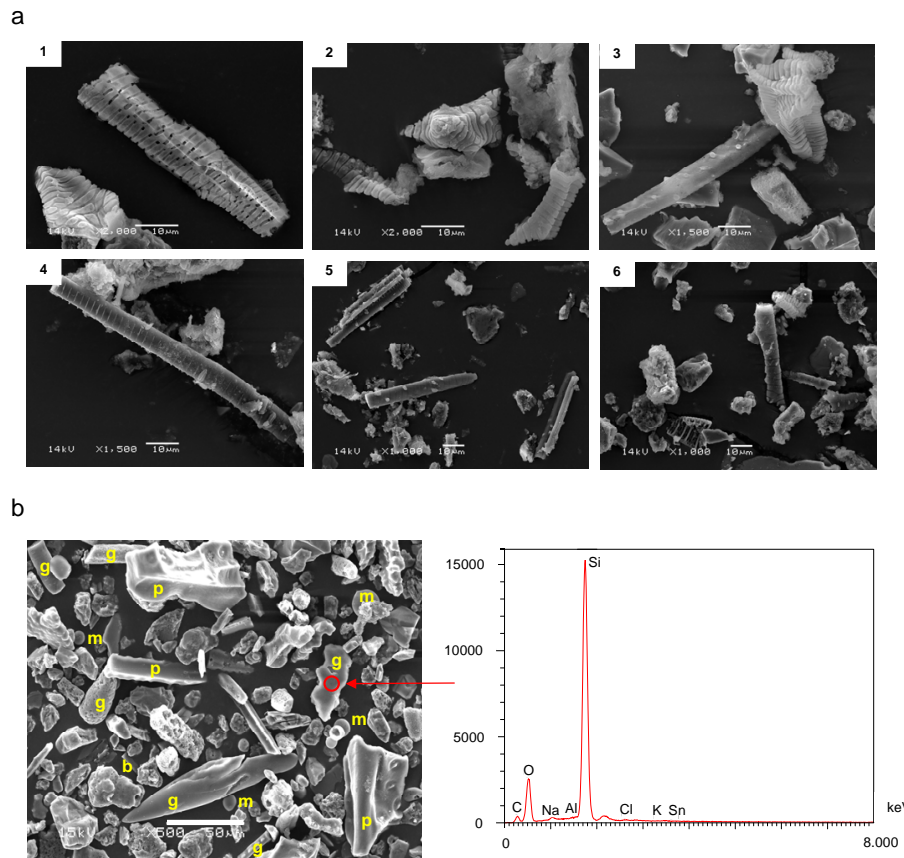


Fig. 2. (a) SEM micrographs of opal phytoliths in *Fagus sylvatica* litterfall (1, 2, 3 leaves, 4, 5 bud scales, 6 fruit capsules), scale bars at all micrographs = 10 µm; (b) SEM micrographs of opal phytoliths in AE horizon, 0–2 cm, scale bar = 50 µm (b = beech, p = pine, g = grass, m = moss); (c) element distribution of a grass opal phytolith (SEM-EDX).

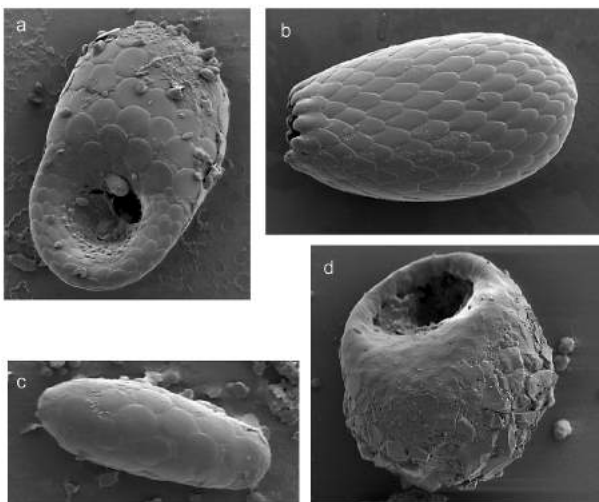


Fig. 3. SEM micrographs of dominant testate amoebae; idiosomic taxa: (a) *Trinema complanatum* (length = 46 µm), (b) *Euglypha rotunda* (length = 49 µm), (c) *Trinema lineare* (length = 23 µm); xenosomic taxa: (d) *Centropyxis sphagnicola* (length = 65 µm).

lower value is more realistic for soils. This is supported by soil water data from quartz-rich, non-redoximorphic soils developed on quartzitic or granitic lithologies in the Black Forest (Podzols, Cambisols) showing silica concentrations always $< 2.5 \text{ mg L}^{-1}$ (Sommer et al., 2006). Studies from tropical soils with absolute quartz dominance also confirm low silica concentrations in soil waters ($< 1.2 \text{ mg Si L}^{-1}$; Cornu et al., 1998; Lucas, 2001; Patel-Sorentino et al., 2007; do Nascimento et al., 2008).

There are two reasons for observed lower in situ silica concentrations compared to lab experiments on pure phases: (i) lab studies on quartz dissolution kinetics mostly use samples ground to silt size which leads to fresh mineral surfaces and high surface: volume ratios compared to our site showing sand as the dominating particle size class. (ii) Surface coatings (Fe oxides, organic matter) protect quartz grains from intense dissolution, because of the reduced access of soil solution to quartz surfaces. Chemical interactions between soil solution and solid phase mainly take place at the surface of coatings. The latter occur at all soil depths as depicted from thin sections (Fig. 5, upper). Coatings show dark to light brown colors and an average thickness

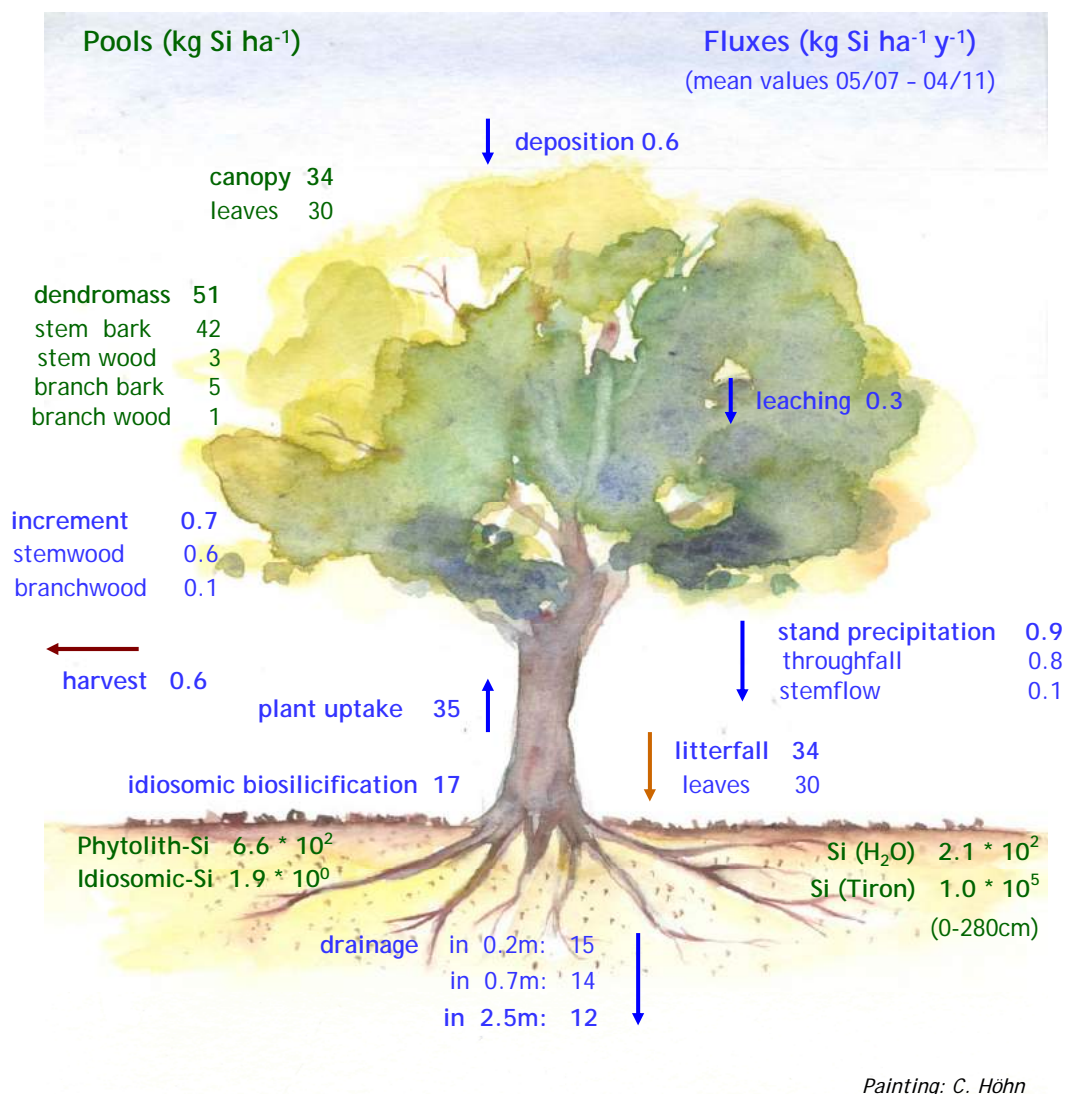


Fig. 4. Si pools and fluxes at Beerenbusch (mean values 05/2007–04/2011) (painting: Cornelia Höhn, Müncheberg).

of 10–20 μm . From element distribution (EDX analysis on several coatings, Fig. 5 lower) two different mineral phases can be inferred – an iron bearing oxyhydroxide, most probably goethite, and kaolinite. Subsoil horizons show a higher percentage of Fe in the coatings (“ferri-argillans”, compare Chartres, 1987; Stoops, 2003; Li et al., 2008). Because feldspar and quartz coatings showed a similar chemical composition they cannot be interpreted as weathering rinds. Instead, a vertical redistribution of fine material by clay translocation (see macroscopic lamellae in 2Cwt) and podzolization (precipitation of organic Fe-Al-complexes), combined with a μm -scale horizontal redistribution of fines during desiccation (water films around grains) are the most probable explanations. From these findings we conclude that quartz dissolution will contribute only a minor fraction to the silica concentrations observed.

Weatherable silicates (mainly K-feldspars, few plagioclase) contribute 3 % (average) to the mineral assemblage of our soil and sediments. Due to the low content and a higher stability of orthoclase, we expected a comparative low contribution of feldspar weathering to DSi. Nevertheless, we checked feldspar weathering intensity by thin sections and SEM. In thin sections some feldspars have been found as part of compact multiminerall sand grains (Fig. S2 in Supplement), probably derived from glacier grinding of granites and subsequent glaciofluvial sorting processes. Here the accessible surface area for chemical weathering is very limited. Further, single feldspar grains appear only slightly weathered in SEM micrographs compared, e.g., to feldspars in White et al. (2008). Furthermore there is no trend with depth (Fig. 6). These findings are surprising, because the high input of organic acids by podzolization should enhance acid hydrolysis.

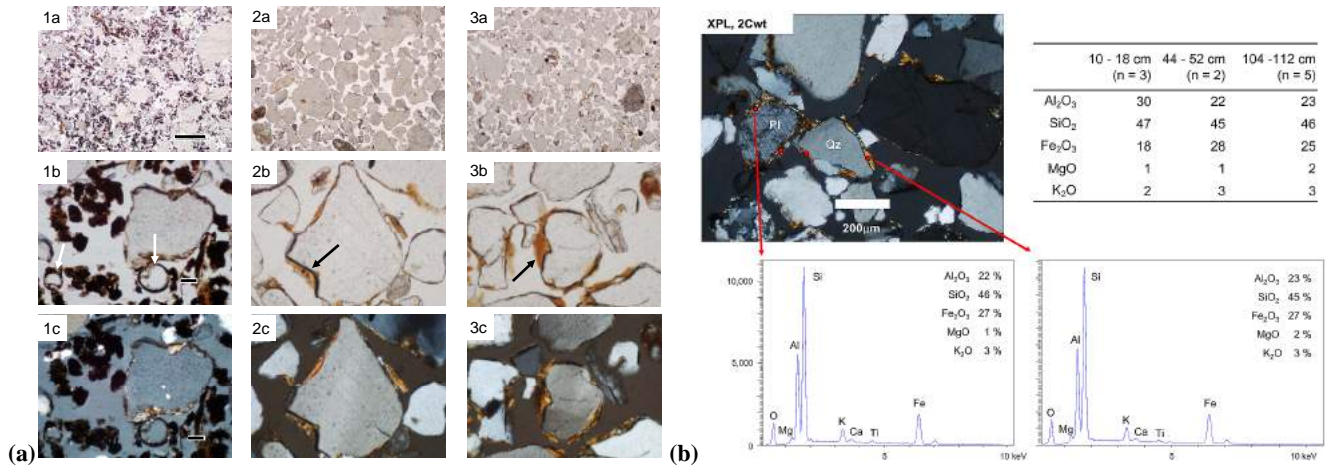


Fig. 5. (a) Micromorphological properties of soil horizons; microstructure (a, b = PPL, c = XPL) of selected soil horizons: (1) AE (0–2 cm), arrows point to testate amoebae; (2) Bw₁ (44–51 cm), arrow points to Fe-oxides/clay coating; (3) 2 Cwt (104–112 cm), arrow points to Fe-oxides/clay coating; widths of photo: 1a, 2a, 3a = 6 mm; other = 0.6 mm. (b) SEM-EDX micrographs of cutans in 2 Cwt (104–112 cm); average chemical composition (wt.-%) of coatings of different depths analysed by electron microprobe; number in brackets = no. of cutans analysed by EDX in each thin section.

Coatings on feldspar grains (Fig. 5) most probably explain this apparent contradiction as coatings reduce accessibility of soil water to feldspar surfaces, hence chemical reactions. Soil solution chemistry measured from 2001 to 2012 supports our SEM findings (mean concentrations at 20, 70, 250 cm in mg L⁻¹): Neither Na (5.8, 5.5, 5.9) nor Cl (7.9, 7.4, 8.7) give evidence for a silicate weathering front. Instead, the depth trends of DOC (23.6, 15.1, 6.7 mg L⁻¹), Al (1.5, 0.5, 0.03 mg L⁻¹), and Fe (41, 12, 5 μg L⁻¹) confirms podzolization to be the main pedogenic process. In summary, we conclude feldspar weathering to be of very low influence on DSi concentrations.

4.2 Dissolution of biogenic Si pool

The biogenic Si pool contains the phytogenic and the zoogenic Si pool, both of which differ remarkably in dynamics and turnover rates. The annual biosilicification of idiosomic amoebae by binary fission adds up to 17 kg Si ha⁻¹ which is in the order of magnitude of the Si flux by litterfall, hence phytogenic silicification. On the other hand, the idiosomic Si pool of 2 kg Si ha⁻¹ is comparatively small. Empty tests comprise only 40 % (0.8 kg Si ha⁻¹) of total idiosomic Si pool, while living amoebae make up 60 % (1.2 kg Si ha⁻¹). This leads to our conclusion of a very high solubility of the idiosomic Si pool. Consequently, turnover rates are too high for interannual pool changes to become relevant for DSi exports.

Annual biosilicification by plants sums up to 35 kg Si ha⁻¹, most of which is returned to the soil by litterfall. Compared to the phytolith Si pool of 660 kg Si ha⁻¹ this flux is relatively large, hence residence time is rather short (pool/flux = 19 yr). Therefore decadal changes of phytogenic

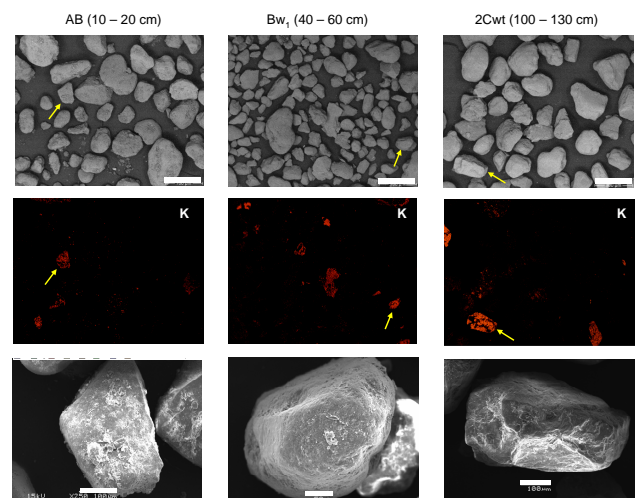


Fig. 6. SEM-micrographs and EDX element mapping (K) of soil material (< 2 mm) from three different depths; scale bars: upper row = 700 μm; lower row, left and right = 100 μm, middle = 50 μm; yellow arrows point to orthoclase mineral grains shown in lower row.

Si pools are relevant for DSi exports in principal. Early experiments on phytolith dissolution in distilled water showed silicic acid equilibrium concentrations of 2–10 mg Si L⁻¹ (Bartoli and Wilding, 1980) depending on plant species as well as surface area. These concentrations were higher than those determined for quartz (1 mg Si L⁻¹), but lower than synthesised pure silica gels (56 mg Si L⁻¹). The latter might be closer to solubilities of nm-sized phytogenic Si. Recent experiments on the reactivity of plant phytoliths in soil solutions have shown the solubility product to be close

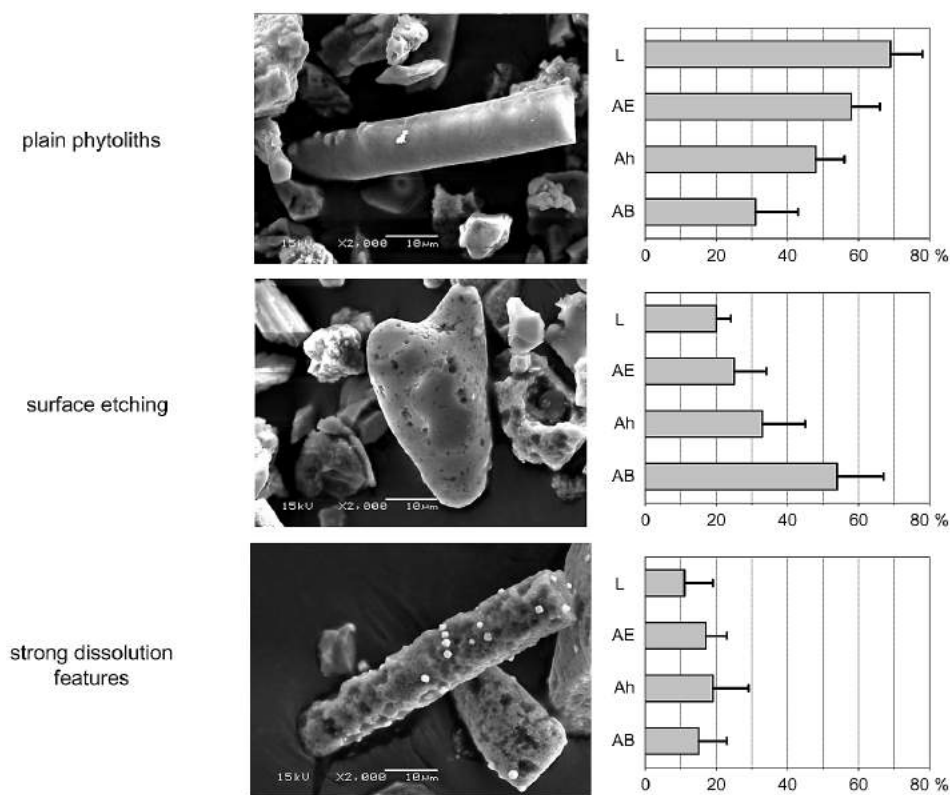


Fig. 7. Categories and depth functions of phytolith dissolution (based on counting in SEM micrographs): fresh, plain phytoliths (upper), phytoliths showing clear signs of surface etching (middle), and phytoliths showing strong dissolution features (lower); horizontal bars = mean \pm SD ($n = 10$ micrographs), total number of phytoliths counted: L = 462, AE = 459, Ah = 422, AB = 238.

to that of amorphous silica and up to one order of magnitude higher than those of clay minerals (Frayse et al., 2009, 2010). Half-life times of the studied phytoliths range from 10–12 yr ($\text{pH} < 3$) to < 1 yr ($\text{pH} > 6$). From these studies it is concluded that phytoliths represent a very reactive Si pool in soil solutions which contributes substantially to DSi.

To check the status of phytolith dissolution in our soil we defined three classes of increasing dissolution and counted assigned phytoliths in SEM micrographs (Fig. 7). The percentage of plain phytoliths showing no signs of dissolution or surface etching significantly decreased from 69 % at the soil surface to 31 % in the AB horizon (10–20 cm). Simultaneously phytoliths showing slight surface etching increased to 54 %. Strongly dissolved phytoliths revealed a maximum of 19 % in Ah (2–10 cm), but no clear trend with depth. Combining these findings with (i) the observation of missing fresh beech phytoliths in soil horizons (see Sect. 3.2), and (ii) the parallel increase of water-soluble Si with phytolith Si pool (upper 25 cm), we regard dissolution of phytogenic Si as the most important driver of DSi concentrations, hence DSi exports.

The influence of phytogenic Si on DSi must be regarded even stronger as the total phytogenic Si pool in soils is definitely higher than the phytolith Si pool. Only the $> 5 \mu\text{m}$ frac-

tions of soil horizons are quantified by phytolith separation procedure (see Sect. 2.3). Comparing the Si content of leaves calculated on basis of the phytolith content with measured Si content supports this consideration: the calculated Si content of 2.4 g kg^{-1} (Table 2a) only comprises 55 % of the measured Si content of 4.4 g kg^{-1} (Table 2a). BSi in the $< 2 \mu\text{m}$ fraction probably explains this difference, because this fraction is lost during phytolith extraction procedure. In their early work Wilding and Drees (1971) quantified 50 % of total leaf opal (*Fagus grandifolia*) in the $< 2 \mu\text{m}$ fraction, another 22 % in the 2–5 μm fraction. Watteau and Villemin (2001) provided evidence for nm-size phytogenic Si granules in leaves and soils. This fraction has a higher reactivity in soil solutions compared to phytoliths due to its higher surface : volume ratio.

Our conclusion about BSi as the main driver for the DSi observed is indirectly supported by process-based modeling of the Si cycle in a forest biogeosystem (Gerard et al., 2008). In a Cambisol from volcanic tuff – containing less quartz (30 %) and higher percentages of clays and weatherable minerals (K-feldspars) compared to our site – the BSi still account for 60 % of DSi after all. Finally, as grasses – which are now absent at the beech stand – contribute a major part to recent phytolith pool, we concluded the phytogenic Si pool

not to be at steady state, but transient state: the continuous decomposition of the relictic phytogenic Si pool is actually not compensated by an equivalent upbuilding.

5 Conclusions

Our studied forest biogeosystem exhibits surprisingly high DSi concentrations and exports compared to the very low content of weatherable minerals in soil and sediments. From our findings we excluded geochemical weathering processes as a major control on DSi, but concluded a strong biogenic footprint on DSi. The disappearance of Si-rich grasses during canopy closure as well as pine logging 30 yr ago seems to be the ultimate reason for the phenomena observed. The related phytogenic Si pool is in disequilibrium with recent vegetation and is dissolving successively. This has to be confirmed by Si isotope analysis of the different phases like it has been done in Cornelis et al. (2010b), Engström et al., (2010), Opfergelt et al. (2010), or Steinhöfel et al. (2011). Furthermore, phytolith dissolution experiments on grasses are needed in future research to understand the dissolution kinetics of Si-rich species, like *Calamagrostis epigejos*.

We regard our study as another example highlighting the importance of disturbances and perturbations in Si cycling (Ittekkot et al., 2006; Laruelle et al., 2009; Struyf et al., 2010; Clymans et al., 2011; Struyf and Conley, 2012). Our study complements the conceptual model of Struyf et al. (2010). It adds vegetation changes by forest management, i.e., without dramatic LUC, as another driver for transient state Si cycling. Future research on Si cycling should explicitly consider decadal transient states and their main drivers.

Supplementary material related to this article is available online at: <http://www.biogeosciences.net/10/4991/2013/bg-10-4991-2013-supplement.pdf>.

Acknowledgements. First of all the authors would like to thank three anonymous reviewers for very helpful comments as well as Jürgen Kesselmeier for editing. Further we would like to thank Angela Müsebeck, Matthias Lemme, Regina Richter, Jürgen Beutler, and Michael Bähr for technical assistance and collecting samples at Beerenbusch, Dagmar Schulz for chemical analysis of samples, Dietmar Lüttschwager for providing data on sap flow analyses. Martin Kaupenjohann (TU Berlin), Francois Galbert and Jörg Nissen supported and performed EDX analysis at ZELMI (TU Berlin). Alexander Konopatzky (LFE Brandenburg, Eberswalde) provided historical data of soil and vegetation surveys. We are deeply grateful about his support. Alexandra Golyeva and Chad Yost from the *Phy-Talk* forum provided help in identifying vegetation from phytoliths. This study was funded by the German Research Foundation (DFG) – PAK 179 “Multiscale analysis of Si cycling in terrestrial biogeosystems”.

Edited by: J. Kesselmeier

References

- Alexandre, A., Meunier, J. D., Colin, F., and Koud, J. M.: Plant impact on the biogeochemical cycle of silicon and related weathering processes, *Geochim. Cosmochim. Ac.*, 61, 677–682, 1997.
- Alexandre, A., Bouvet, M., and Abbadie, L.: The role of savannas in the terrestrial Si cycle: A case study from Lamto, Ivory Coast, *Global Planet. Change*, 78, 162–169, 2011.
- Altherr, E., Unfried, P., Hradetzky, J., and Hradetzky, V.: Statistische Rindenbeziehungen als Hilfsmittel zur Ausformung und Aufmessung unentrindeten Stammholzes, *Mitteilungen der Forstlichen Versuch- und Forschungsanstalt Baden-Württemberg*, 61, 1–137, 1974.
- Anderson, O. A.: Cytoplasmic origin and surface deposition of siliceous structures in Sarcodina, *Protoplasma*, 181, 61–77, 1994.
- Aoki, Y., Hoshino, M., and Matsubara, T.: Silica and testate amoebae in a soil under pine-oak forest, *Geoderma*, 141, 29–35, 2007.
- Bartoli, F. and Souchier, B.: Cycle et rôle du silicium d'origine végétale dans les écosystèmes forestiers tempérés, *Ann. Sci. For.*, 35, 187–202, 1978.
- Bartoli, F. and Wilding, L. P.: Dissolution of biogenic opal as a function of its physical and chemical properties, *Soil Sci. Soc. Am. J.*, 44, 873–878, 1980.
- Biermans, V. and Baert, L.: Selective extraction of the amorphous Al, Fe and Si oxides using an alkaline Tiron solution, *Clay Miner.*, 12, 127–135, 1977.
- Blecker, S. W., McCulley, R. L., Chadwick, O. A., and Kelly, E. F.: Biologic cycling of silica across a grassland bioclimosequence, *Global Biogeochem. Cy.*, 20, GB3023, doi:10.1029/2006GB002690, 2006.
- Borrelli, N., Alvarez, M. F., Osterrieth, M. L., and Marcovecchio, J. E.: Silica content in soil solution and its relation with phytolith weathering and silica biogeochemical cycle in Typical Argiudolls of the Pampean Plain, Argentina – a preliminary study, *J. Soils Sediments*, 10, 983–994, 2010.
- Carey, J. C. and Fulweiler, R. W.: Human activities directly alter watershed dissolved silica fluxes, *Biogeochemistry*, 111, 125–138, 2012.
- Chartres, C. J.: The composition and formation of grainy void cutans in some soils with textural contrast in Southeastern Australia, *Geoderma*, 39, 209–233, 1987.
- Clymans, W., Struyf, E., Govers, G., Vandevenne, F., and Conley, D. J.: Anthropogenic impact on amorphous silica pools in temperate soils, *Biogeosciences*, 8, 2281–2293, doi:10.5194/bg-8-2281-2011, 2011.
- Conley, D. J., Likens, G. E., Buso, D. C., Saccone, L., Bailey, S. W., and Johnson, C. E.: Deforestation causes increased dissolved silicate losses in the Hubbard Brook Experimental Forest, *Glob. Change Biol.*, 14, 2548–2554, 2008.
- Cornelis, J. T., Ranger, J., Iserentant, A., and Delvaux, B.: Tree species impact the terrestrial cycle of silicon through various uptakes, *Biogeochem.*, 97, 231–245, 2010a.
- Cornelis, J. T., Delvaux, B., Cardinal, D., Andre, L., Ranger, J., and Opfergelt, S.: Tracing mechanisms controlling the release of dissolved silicon in forest soil solutions using Si isotopes and Ge/Si ratios, *Geochim. Cosmochim. Ac.*, 74, 3913–3924, 2010b.
- Cornelis, J. T., Titeux, H., Ranger, J., and Delvaux, B.: Identification and distribution of the readily soluble silicon pool in a temperate forest below three distinct tree species, *Plant Soil*, 342, 369–378, 2011a.

- Cornelis, J.-T., Delvaux, B., Georg, R. B., Lucas, Y., Ranger, J., and Opfergelt, S.: Tracing the origin of dissolved silicon transferred from various soil-plant systems towards rivers: a review, *Biogeosciences*, 8, 89–112, doi:10.5194/bg-8-89-2011, 2011b.
- Cornu, S., Lucas, Y., Ambrosi, J. P., and Desjardins, T.: Transfer of dissolved Al, Fe and Si in two Amazonian forest environments in Brazil, *Eur. J. Soil Sci.*, 49, 377–384, 1998.
- Dietz, P.: Dichte und Rindengehalt von Industrieholz, *Holz Roh. Werkst.*, 33, 135–141, 1975.
- DIN ISO 1039.: Bodenbeschaffenheit: Bestimmung des pH-Wertes, Deutsches Institut für Normung, Beuth, Berlin, 1997.
- DIN ISO 11277: Bodenbeschaffenheit: Bestimmung der Partikelgrößenverteilung in Mineralböden – Verfahren mittels Siebung und Sedimentation, Deutsches Institut für Normung, Beuth, Berlin, 1998.
- Dittmar, O., Knapp, E., and Lembcke, G.: DDR-Buchenertragstafel 1983, Institut für Forstwissenschaften Eberswalde, Eberswalde, 1986.
- do Nascimento, N. R., Fritsch, E., Bueno, G. T., Bardy, M., Grimaldi, C., and Melfi, A. J.: Podzolization as a deferralization process: dynamics and chemistry of ground and surface waters in an Acrisol – Podzol sequence of the upper Amazon Basin, *Eur. J. Soil Sci.*, 59, 911–924, 2008.
- Dove, P. M.: Kinetic and thermodynamic controls on silica reactivity in weathering environments, in: *Chemical weathering rates of silicate minerals*, Mineralogical Society of America and the Geochemical Society, *Rev. Mineral. Geochem.*, 31, 235–290, 1995.
- Ehrmann, O., Puppe, D., Wanner, M., Kaczorek, D., and Sommer, M.: Testate amoebae in 31 mature forest ecosystems – densities and micro-distribution in soils, *Eur. J. Protistol.*, 48, 161–168, doi:10.1016/j.ejop.2012.01.003, 2012.
- Ellenberg, H., Mayer, R., and Schauer, J.: *Ökosystemforschung – Ergebnisse des Sollingprojekts 1966–1986*, Verlag Eugen Ulmer, Stuttgart, 1986.
- Engle, D. L., Sickman, J. O., Moore, C. M., Esperanza, A. M., Melack, J. M., and Keeley, J. E.: Biogeochemical legacy of prescribed fire in a giant sequoia-mixed conifer forest: A 16-year record of watershed balances, *J. Geophys. Res.*, 113, G01014, doi:10.1029/2006JG000391, 2008.
- Engström, E., Rodushkin, I., Ingri, J., Baxter, D. C., Ecke, F., Österlund, H., and Öhlander, B.: Temporal isotopic variations of dissolved silicon in a pristine boreal river, *Chem. Geol.*, 271, 142–152, 2010.
- Frayse, F., Pokrovsky, O. S., Schott, J., and Meunier, J.-D.: Surface chemistry and reactivity of plant phytoliths in aqueous solutions, *Chem. Geol.*, 258, 197–206, 2009.
- Frayse, F., Pokrovsky, O. S., and Meunier, J.-D.: Experimental study of terrestrial plant litter interaction with aqueous solutions, *Geochim. Cosmochim. Ac.*, 74, 70–84, 2010.
- Gerard, F., Francois, M., and Ranger, J.: Processes controlling silica concentration in leaching and capillary soil solutions of an acidic brown forest soil (Rhône, France), *Geoderma*, 107, 197–226, 2002.
- Gerard, F., Mayer, K. U., Hodson, M. J., and Ranger, J.: Modelling the biogeochemical cycle of silicon in soils: Application to a temperate forest ecosystem, *Geochim. Cosmochim. Ac.*, 72, 741–758, 2008.
- Ginzel, G., and Ertl, C.: *Geologie, Hydrologie und Klima*, in: *Das Naturschutzgebiet Stechlin*, edited by: Lütkepohl, M. and Flade, M., Natur & Text in Brandenburg, Rangsdorf, 15–23, 2004.
- Golyeva, A.: *Phytoliths and their information role in natural and archaeological objects*, Moscow, Syktyvkar Elista, 2001.
- Grady, A. E., Scanlon, T. M., and Galloway, J. N.: Declines in dissolved silica concentrations in western Virginia streams (1988–2003): Gypsy moth defoliation stimulates diatoms?, *J. Geophys. Res.*, 112, G01009, doi:10.1029/2006JG000251, 2007.
- Granier, A.: Une nouvelle methode pour la mesure du flux de serve brute dans le tronc des arbres, *Ann. Sci. Forest.*, 42, 193–200, 1985.
- Guntzer, F., Keller, C., and Meunier, J.-D.: Determination of the silicon concentration in plant material using Tiron extraction, *New Phytol.*, 188, 902–906, 2010.
- Hodson, M. J., White, P. J., Mead, A., and Broadley, M. R.: Phylogenetic variation in the silicon composition of plants, *Ann. Bot.*, 96, 1027–1046, 2005.
- Iler, R. K.: *The chemistry of silica*, Wiley-Interscience, New York, 1979.
- Ittekkot, V., Unger, D., Humborg, C., and Tac An, N. (Eds.): *The silicon cycle – Human perturbations and impacts on aquatic systems*, SCOPE 66, Island Press, Washington, 2006.
- Jochheim, H., Einert, P., Ende, H.-P., Kallweit, R., Lüttschwager, D., and Schindler, U.: Wasser- und Stoffhaushalt eines Buchen-Albestandes im Nordostdeutschen Tiefland – Ergebnisse einer 4jährigen Messperiode, *Archiv für Forstwesen und Landschaftsökologie*, 41, 1–14, 2007a.
- Jochheim, H., Puhlmann, M., and Pohle, D.: Implementation of a forest management module into BIOME-BGC and its application, *EOS Transactions Supplement*, 88, B24A-04, 2007b.
- Jochheim, H., Puhlmann, M., Beese, F., Berthold, D., Einert, P., Kallweit, R., Konopatzky, A., Meesenburg, H., Meiwes, K. J., Raspe, S., Schulte-Bisping, H., and Schulz, C.: Modelling the carbon budget of intensive forest monitoring sites in Germany using the simulation model BIOME-BGC, *iForest*, 2, 7–10, 2009.
- Kendrick, K. J. and Graham, R. C.: Pedogenic silica accumulation in chronosequence soils, Southern California, *Soil Sci. Soc. Am. J.*, 68, 1295–1303, 2004.
- Kodama, H. and Ross, G. J.: Tiron dissolution method used to remove and characterize inorganic components in soils, *Soil Sci. Soc. Am. J.*, 55, 1180–1187, 1991.
- Lachmann, M.: *Intensität und räumliche Verteilung der Durchwurzelung im Buchenbestand in Abhängigkeit von den Bodenbedingungen auf einer Dauerbeobachtungsfläche*, BSc. Thesis, International Forest Ecosystem Management, FH Eberswalde, 2002.
- Laruelle, G. G., Roubex, V., Sferratore, A., Brodherr, B., Ciuffa, D., Conley, D. J., Dürr, H. H., Garnier, J., Lancelot, C., Le Thi Thuong, Q., Meunier, J.-D., Meybeck, M., Michalopoulos, P., Moriceau, B., Ní Longphuirt, S., Loucaides, S., Papush, L., Presti, M., Ragueneau, O., Regnier, P., Saccone, L., Slomp, C. P., Spiteri, C., and Van Cappellen, P.: Anthropogenic perturbations of the silicon cycle at the global scale: Key role of the land-ocean transition, *Global Biogeochem. Cy.*, 23, GB4031, doi:10.1029/2008GB003267, 2009.
- Li, H., Jun, H., Wenfeng, T., Hongqing, H., Fan, L., and Mingkuang, W.: Characteristics of micromorphology and element distribution of iron-manganese cutans in typical soils of subtropical China, *Geoderma*, 146, 40–47, 2008.

- Lucas, Y.: The role of plants in controlling rates and products of weathering: Importance of biological pumping, *Annu. Rev. Earth Planet. Sci.*, 29, 135–163, 2001.
- Lüttschwager, D. and Remus, R.: Radial distribution of sap flux density in trunks of a mature beech stand, *Ann. Sci. Forest.*, 64, 431–438, 2007.
- Madella, M., Alexandre, A., and Ball, T.: International code for phytolith nomenclature 1.0, *Ann. Bot.*, 96, 253–260, 2005.
- McKeague, J. A. and Cline, M. G.: Silica in soil solutions I. The form and concentration of dissolved silica in aqueous extracts of some soils, *Can. J. Soil Sci.*, 43, 70–82, 1963.
- Mehra, O. P. and Jackson, M. L.: Iron oxide removal from soils and clays by a dithionite-citrate system buffered with sodium bicarbonate, in: *Clays and Clay Minerals*, edited by: Swineford, A., Proc. 7th Natl. Conf., Washington DC, 1958, Pergamon Press, New York, 317–327, 1960.
- Meisterfeld, R.: Order Arcellinida Kent, 1880, in: *An Illustrated Guide to the Protozoa*, 2nd Edition, edited by: Lee J. J., Leedale, G. F., and Bradbury, P., Society of Protozoologists, Lawrence, 827–860, 2002a.
- Meisterfeld, R.: Testate amoebae with filopodia, in: *An Illustrated Guide to the Protozoa*, 2nd Edition, edited by: Lee J. J., Leedale, G. F., and Bradbury, P., Society of Protozoologists, Lawrence, 1054–1084, 2002b.
- Melzer, S. E., Knapp, A. K., Kirkman, K. P., Smith, M. D., Blair, J. M., and Kelly, E. F.: Fire and grazing impacts on silica production and storage in grass dominated ecosystems, *Biogeochem.*, 97, 263–278, 2010.
- Melzer, S. E., Chadwick, O. A., Hartshorn, A. S., Khomo, L. M., Knapp, A. K., and Kelly, E. F.: Lithological controls on biogenic silica cycling in South African savanna ecosystems, *Biogeochem.*, 108, 317–334, doi:10.1007/s10533-011-9602-2, 2012.
- Opfergelt, S., Cardinal, D., Andre, L., Delvigne, C., Bremond, L., and Delvaux, B.: Variations of $\delta^{30}\text{Si}$ and Ge/Si with weathering and biogenic input in tropical basalt ash soils under monoculture, *Geochim. Cosmochim. Ac.*, 74, 225–240, 2010.
- Patel-Sorrentino, N., Lucas, Y., Eyrolle, F., and Melfi, A. J.: Fe, Al and Si species and organic matter leached off a ferrallitic and podzolic soil system from Central Amazonia, *Geoderma*, 137, 444–454, 2007.
- Pavlov, M. B.: Bioelement-Inventur von Buchen- und Fichtenbeständen im Solling, *Göttinger Bodenkundliche Berichte*, 25, 1–174, 1972.
- Puhlmann, M. and Jochheim, H.: Implementation of a multi-layer soil model into Biome-BGC- calibration and application, *EOS Transactions Supplement*, 88, B24A-05, 2007.
- Saccone, L., Conley, D. J., Koning, E., Sauer, D., Sommer, M., Kaczorek, D., Blecker, S. W., and Kelly, E. F.: Assessing the extraction and quantification of amorphous silica in soils of forest and grassland ecosystems, *Eur. J. Soil Sci.*, 58, 1446–1459, 2007.
- Sauer, D., Saccone, L., Conley, D. J., Herrmann, L., and Sommer, M.: Review of methodologies for extracting plant-available and amorphous Si from soils and aquatic sediments, *Biogeochem.*, 80, 89–108, 2006.
- Schachtschabel, P. and Heinemann, C. G.: Wasserlösliche Kieselsäure in Lössböden, *Z. Pflanzenern. Bodenk.*, 118, 22–35, 1967.
- Schlichting, E., Blume, H. P., and Stahr, K.: *Soils Practical* (in German), Blackwell, Berlin, Wien, Germany, Austria, 1995.
- Schönborn, W.: Ermittlung der Jahresproduktion von Boden-Protozoen. I. Euglyphidae (Rhizopoda, Testacea), *Pedobiologia*, 15, 415–424, 1975.
- Schönborn, W.: Estimation of annual production of Testacea (Protozoa) in mull and moder (II), *Pedobiologia*, 23, 383–393, 1982.
- Schwertmann, U.: Differenzierung der Eisenoxide des Bodens durch Extraktion mit Ammoniumoxalat Lösung, *Z. Pflanzenern. Bodenk.*, 105, 194–202, 1964.
- Soil Survey Staff: *Soil Taxonomy – A basic system of soil classification for making and interpreting soil surveys*, USDA-NRCS, Agriculture Handbook 436, <http://soils.usda.gov/technical/classification/taxonomy>, 1999.
- Sommer, M., Kaczorek, D., Kuzyakov, Y., and Breuer, J.: Silicon pools and fluxes in soils and landscapes – a review, *J. Plant Nutr. Soil Sci.*, 169, 310–329, 2006.
- Steinboefel, G., Breuer, J., Blanckenburg, F., Horn, I., Kaczorek, D., and Sommer, M.: Micrometer silicon isotope diagnostics of soils by UV femtosecond laser ablation, *Chem. Geol.*, 286, 280–289, 2011.
- Stoops, G.: *Guidelines for analysis and description of soil and regolith thin sections*, Soil Sci. Soc. Am., Madison, WI, 2003.
- Struyf, E. and Conley, D. J.: Silica: an essential nutrient in wetland biogeochemistry, *Front. Ecol. Environ.*, 7, 88–94, doi:10.1890/070126, 2009.
- Struyf, E. and Conley, D. J.: Emerging understanding of the ecosystem silica filter, *Biogeochem.*, 107, 9–18, 2012.
- Struyf, E., Opdekamp, W., Backx, H., Jacobs, S., Conley, D. J., and Meire, P.: Vegetation and proximity to the river control amorphous silica storage in a riparian wetland (Biebrza National Park, Poland), *Biogeosciences*, 6, 623–631, doi:10.5194/bg-6-623-2009, 2009.
- Struyf, E., Smis, A., Van Damme, S., Garnier, J., Govers, G., Van Wesemael, B., Conley, D. J., Batelaan, O., Frot, E., Clymans, W., Vandevenne, F., Lancelot, C., Goos, P., and Meire, P.: Historical land use change has lowered terrestrial silica mobilization, *Nat. Commun.*, 1, 129, doi:10.1038/ncomms1128, 2010.
- Thornton, P. E., Law, B. E., Gholz, H. L., Clark, K. L., Falge, E., Ellsworth, D. S., Golstein, A. H., Monson, R. K., Hollinger, D., Falk, M., Chen, J., and Sparks, J. P.: Modelling and measuring the effects of disturbance history and climate on carbon and water budgets in evergreen needle leaf forests, *Agr. Forest Meteorol.*, 113, 185–222, 2002.
- Trendelenburg, R. and Mayer-Wegelin, H.: *Das Holz als Rohstoff*, Hanser, München, 1955.
- Wanner, M.: A review on the variability of testate amoebae: Methodological approaches, environmental influences and taxonomical implications, *Acta Protozool.*, 38, 15–29, 1999.
- Wanner, M. and Dunger, W.: Biological activity of soils from reclaimed open-cast coal mining areas in Upper Lusatia using testate amoebae (protists) as indicators, *Ecol. Eng.* 17, 323–330, 2001.
- Watteau, F. and Villemin, G.: Ultrastructural study of the biogeochemical cycle of silicon in the soil and litter of a temperate forest, *Eur. J. Soil Sci.*, 52, 385–396, 2001.
- White, A. F., Schulz, M. S., Vivit, D. V., Blum, A. E., Stonestrom, D. A., and Anderson, S. P.: Chemical weathering of a marine terrace chronosequence, Santa Cruz, California I: Interpreting

- rates and controls based on soil concentration-depth profiles, *Geochim. Cosmochim. Acta*, 72, 36–68, 2008.
- White, A. F., Vivit, D. V., Schulz, M. S., Bullen, T. D., Evett, R. R., and Agarwal, J. : Biogenic and pedogenic controls on Si distributions and cycling in grasslands of the Santa Cruz soil chronosequence, California, *Geochim. Cosmochim. Ac.*, 94, 72–94, 2012.
- Wilding, L. P. and Drees, L. R.: Biogenic opal in Ohio soils, *Soil Sci. Soc. Am. Proc.*, 35, 1004–1010, 1971.
- WRB-World reference base for soil resources, *World Soil Resources Reports*, 103, p. 128, Rome, FAO, 2006.

Supplementary material to:

**Si cycling in a forest biogeosystem – the importance of
transient state biogenic Si pools**

M. Sommer^{1,2*}, H. Jochheim³, A. Höhn¹, J. Breuer⁴, Z. Zagorski⁵, J. Busse⁶, D. Barkusky⁷,
K. Meier⁸, D. Puppe^{1,9}, M. Wanner⁹, D. Kaczorek^{1,5}

* Corresponding author: sommer@zalf.de

¹ Leibniz Centre for Agricultural Landscape Research (ZALF), Institute of Soil Landscape Research, Eberswalder Str. 84, D-15374 Müncheberg, Germany.

² University of Potsdam, Institute of Earth and Environmental Sciences, Karl-Liebknecht-Str. 24-25, D-14476 Potsdam, Germany.

³ Leibniz Centre for Agricultural Landscape Research (ZALF), Institute of Landscape Systems Analysis, Eberswalder Str. 84, D-15374 Müncheberg, Germany.

⁴ Landwirtschaftliches Technologiezentrum Augustenberg (LTZ), Referat 12, Neßlerstr. 23-32, D-76227 Karlsruhe, Germany.

⁵ Department of Soil Environment Sciences, Warsaw University of Life Science (SGGW), Nowoursynowska 159, 02-776 Warsaw, Poland.

⁶ Leibniz Centre for Agricultural Landscape Research (ZALF), Institute for Landscape Biogeochemistry, Eberswalder Str. 84, D-15374 Müncheberg, Germany.

⁷ Leibniz Centre for Agricultural Landscape Research (ZALF), Research Station Müncheberg, Eberswalder Str. 84, D-15374 Müncheberg, Germany.

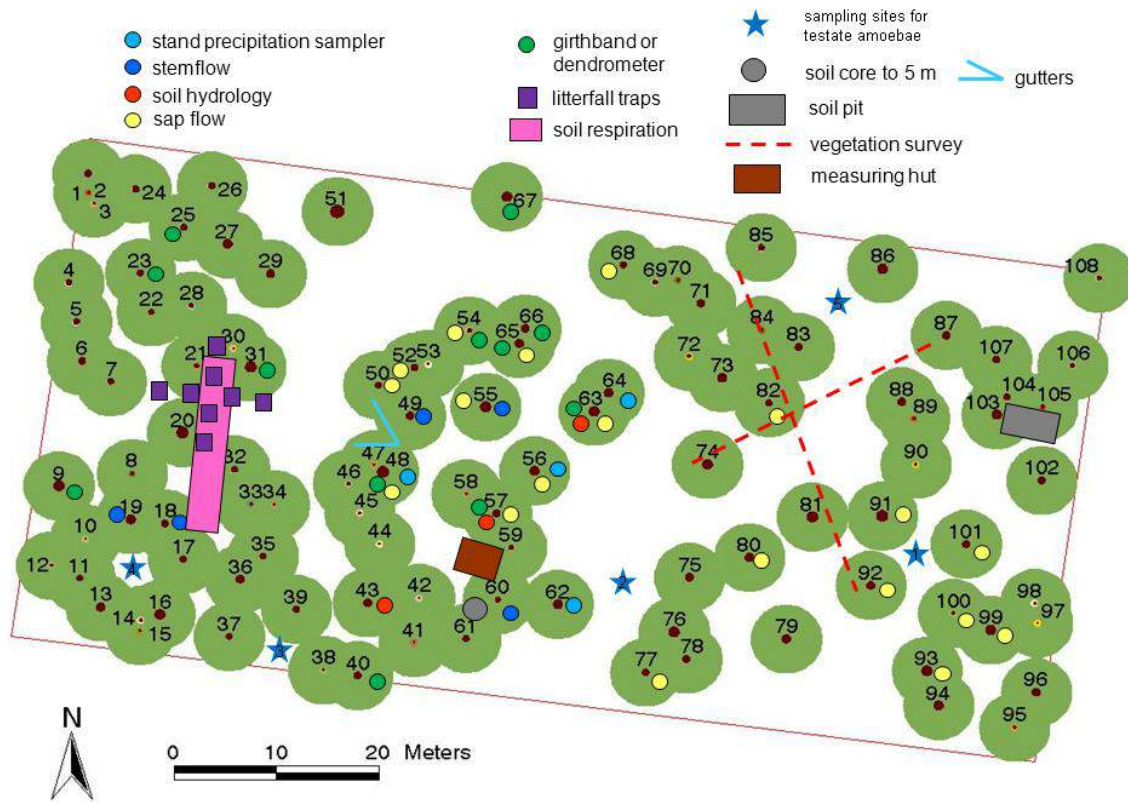
⁸ Leibniz Centre for Agricultural Landscape Research (ZALF), Institute of Land Use Systems, Eberswalder Str. 84, D-15374 Müncheberg, Germany.

⁹ Brandenburg University of Technology Cottbus-Senftenberg, Chair General Ecology, 03013 Cottbus, Germany.

Figure S1: Recent land cover of the study site Beerenbusch (53°09'10''N, 12°59'22''E); yellow dot: location of site characterization in 1954 (soil pit, vegetation survey)



Figure S2: Instrumentation, sampling sites, soil pit with position of Kubiena boxes, thin sections & SEM-EDX of feldspars at Beerenbusch (ICP Forests DE1207)

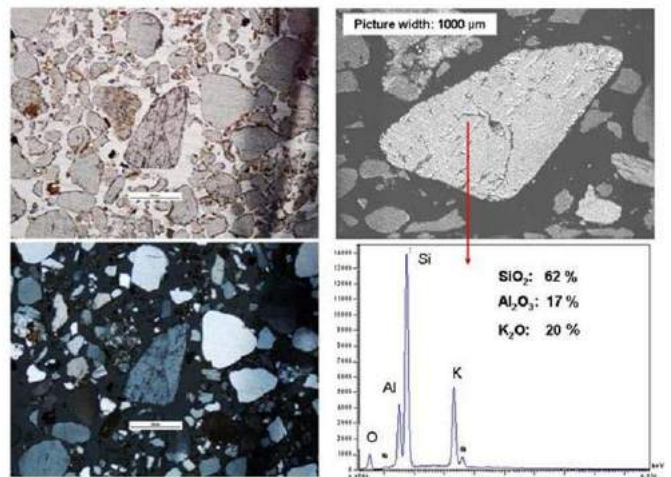


Brunic Arenosol (Dystric)



Feldspar weathering

Unweathered orthoclase, Beerenbusch 10-18 cm



Multi-mineral grain in coarse sand fraction: feldspar + quartz

Beerenbusch

Figure S3: History of land use / forest management at Beerenbusch from 1780-2010

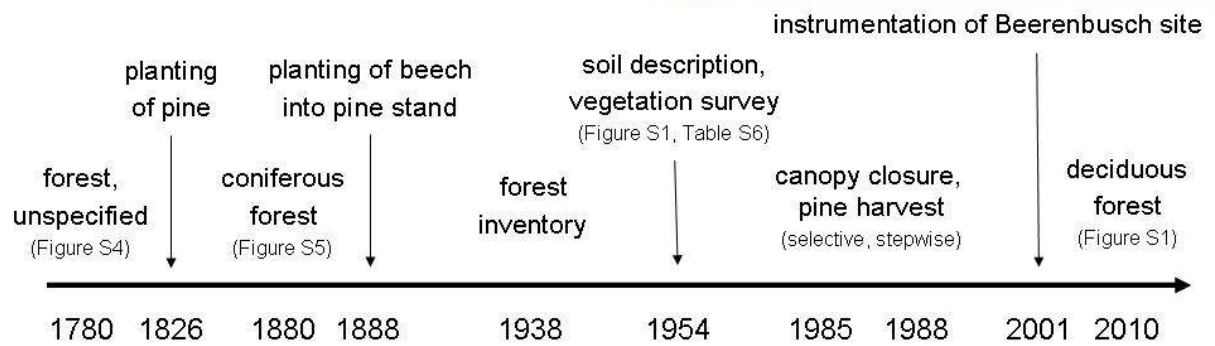


Figure S4: Land cover at Beerenbusch around 1780

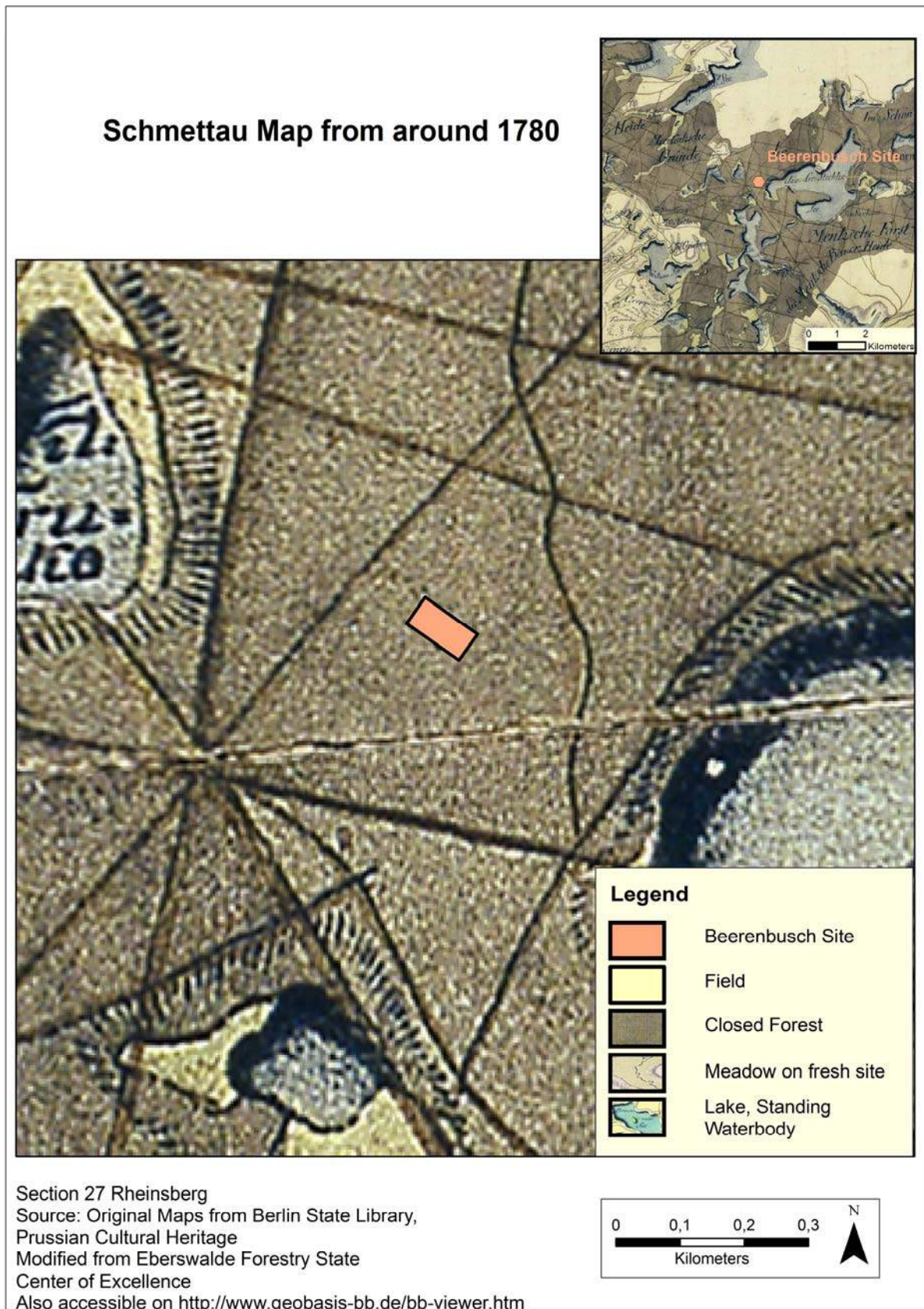


Figure S5: Land cover at Beerenbusch around 1880

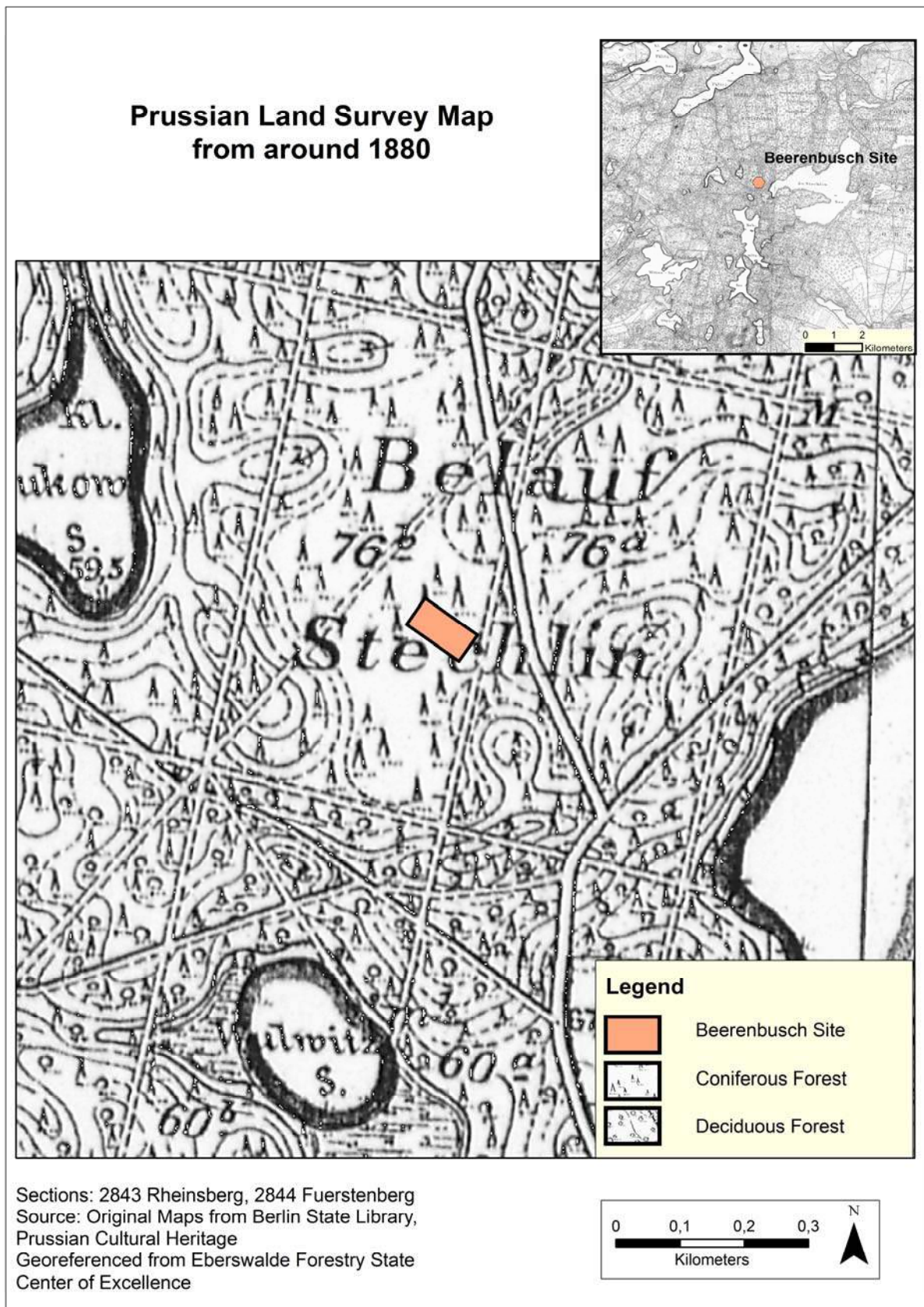


Table S6: Ground vegetation (20 x 20 m²) at site 255 (yellow dot in S1) in 1954

Species	Braun-Blanquet	coverage (%)	% Si in d.m. (mean) Hodson et al. (2005)
<i>Calamagrostis epigejos</i>	3.3	25-49	2.2
<i>Pteridium aquilinum</i>	2.3	5-24	1.5
<i>Brachypodium sylvaticum</i>	1.2	1-4	3.1
<i>Oxalis acetosella</i>	1.2	1-4	n.a.
<i>Agrostis capillaris</i>	1.1	1-4	1.4
<i>Veronica officinalis</i>	1.1	1-4	n.a.
<i>Anthoxanthum odoratum</i>	+1	<1	0.5
<i>Carex leporina</i>	+1	<1	n.a.
<i>Fragaria vesca</i>	+1	<1	n.a.
<i>Hypericum perforatum</i>	+1	<1	n.a.
<i>Melica uniflora</i>	+1	<1	1.9
<i>Poa compressa</i>	+1	<1	1.2
<i>Potentilla spec.</i>	+1	<1	n.a.
<i>Rubus idaeus</i>	+1	<1	0.1
<i>Urtica dioica</i>	+1	<1	1.3

n.a. = no data available

Sources:

Forstliche Standortkartierung des Staatlichen Forstwirtschaftsbetriebes Rheinsberg 1954:
Bohrpunktunterlagen (Kartierer: Schultz). Archiv der Standortkartierung im LFE,
Eberswalde, unpublished data;
vegetation list comes from a stand gap - “under beech and pine no ground vegetation”
(handwritten note of Schultz in German)

Si contents assigned from data in Hodson et al. (2005)



How big is the influence of biogenic silicon pools on short-term changes in water-soluble silicon in soils? Implications from a study of a 10-year-old soil–plant system

Daniel Puppe¹, Axel Höhn¹, Danuta Kaczorek^{1,2}, Manfred Wanner³, Marc Wehrhan¹, and Michael Sommer^{1,4}

¹Leibniz Centre for Agricultural Landscape Research (ZALF) e.V., Institute of Soil Landscape Research, 15374 Müncheberg, Germany

²Department of Soil Environment Sciences, Warsaw University of Life Science (SGGW), Nowoursynowska 159, 02-776 Warsaw, Poland

³Brandenburg University of Technology Cottbus-Senftenberg, Department Ecology, 03013 Cottbus, Germany

⁴Institute of Earth and Environmental Sciences, University of Potsdam, 14476 Potsdam, Germany

Correspondence to: Daniel Puppe (daniel.puppe@zalf.de)

Received: 5 May 2017 – Discussion started: 20 June 2017

Revised: 5 October 2017 – Accepted: 14 October 2017 – Published: 23 November 2017

Abstract. The significance of biogenic silicon (BSi) pools as a key factor for the control of Si fluxes from terrestrial to aquatic ecosystems has been recognized for decades. However, while most research has been focused on phytogenic Si pools, knowledge of other BSi pools is still limited. We hypothesized that different BSi pools influence short-term changes in the water-soluble Si fraction in soils to different extents. To test our hypothesis we took plant (*Calamagrostis epigejos*, *Phragmites australis*) and soil samples in an artificial catchment in a post-mining landscape in the state of Brandenburg, Germany. We quantified phytogenic (phytoliths), protistic (diatom frustules and testate amoeba shells) and zoogenic (sponge spicules) Si pools as well as Tiron-extractable and water-soluble Si fractions in soils at the beginning (t_0) and after 10 years (t_{10}) of ecosystem development. As expected the results of Tiron extraction showed that there are no consistent changes in the amorphous Si pool at Chicken Creek (*Hühnerwasser*) as early as after 10 years. In contrast to t_0 we found increased water-soluble Si and BSi pools at t_{10} ; thus we concluded that BSi pools are the main driver of short-term changes in water-soluble Si. However, because total BSi represents only small proportions of water-soluble Si at t_0 (<2 %) and t_{10} (2.8–4.3 %) we further concluded that smaller (<5 μm) and/or fragile phytogenic Si structures have the biggest impact on short-term changes in water-soluble Si. In this context, extracted phytoliths (>5 μm) only amounted to about 16 % of total Si con-

tents of plant materials of *C. epigejos* and *P. australis* at t_{10} ; thus about 84 % of small-scale and/or fragile phytogenic Si is not quantified by the used phytolith extraction method. Analyses of small-scale and fragile phytogenic Si structures are urgently needed in future work as they seem to represent the biggest and most reactive Si pool in soils. Thus they are the most important drivers of Si cycling in terrestrial biogeosystems.

1 Introduction

Various prokaryotes and eukaryotes are able to synthesize hydrated amorphous silica ($\text{SiO}_2 \cdot n\text{H}_2\text{O}$) structures from monomeric silicic acid (H_4SiO_4) in a process called biosilicification (Ehrlich et al., 2010). In terrestrial biogeosystems, biogenic silicon (BSi) synthesized by bacteria and fungi, plants, diatoms, testate amoebae and sponges can be found forming corresponding microbial, phytogenic, protophytic, protozoic and zoogenic BSi pools, respectively (Puppe et al., 2015; Sommer et al., 2006). BSi has been recognized as a key factor in the control of Si fluxes from terrestrial to aquatic ecosystems as it is in general more soluble compared to silicate minerals (e.g., Fraysse et al., 2006, 2009). These fluxes influence marine diatom production on a global scale (Dürr et al., 2011; Sommer et al., 2006; Struyf and Conley, 2012). Marine diatoms in turn can fix large quan-

ties of carbon dioxide via photosynthesis, because up to 54 % of the biomass in the oceans is represented by diatoms; thus diatoms have an important influence on climate change (Tréguer and De La Rocha, 2013; Tréguer and Pondaven, 2000).

While the importance of phytogenic Si pools for global Si fluxes has been recognized for three decades (e.g., Bartoli, 1983; Meunier et al., 1999; Street-Perrott and Barker, 2008), information on the other BSi pools is comparatively rare (Clarke, 2003). However, in recent publications the potential importance of diatoms, testate amoebae and sponge spicules in soils for Si cycling has been highlighted (Aoki et al., 2007; Creevy et al., 2016; Puppe et al., 2014, 2015, 2016). Furthermore, evidence arises that BSi pools are in disequilibrium at decadal timescales due to disturbances and perturbations by humans, e.g., by changes in forest management or farming practices (Barão et al., 2014; Keller et al., 2012; Vandevenne et al., 2015). As a consequence, BSi accumulation and BSi dissolution are not balanced, which influences Si cycling in terrestrial biogeosystems, not only on decadal but also on millennial scales (Clymans et al., 2011; Frings et al., 2014; Sommer et al., 2013; Struyf et al., 2010). Sommer et al. (2013), for example, found the successive dissolving of a relict phytogenic Si pool to be the main source of dissolved Si in soils of a forested biogeosystem. Due to the fact that the continuous decomposition of this relict phytogenic Si pool is not compensated by an equivalent buildup by recent vegetation the authors concluded that a BSi disequilibrium occurred on a decadal scale. On a millennial scale Clymans et al. (2011) estimated the total amorphous Si storage in temperate soils to be decreased by approximately 10 % since the onset of agricultural development about 5000 years ago. This decrease does not only have consequences for land–ocean Si fluxes but also influences agricultural used landscapes, because Si is a beneficial element for many crops (e.g., Epstein, 2009; Ma and Yamaji, 2008).

For a better understanding of BSi dynamics, chronosequence studies are well suited, because they allow us to analyze time-related changes in BSi pools during biogeosystem development. In the present study we analyzed various BSi pools in differently aged soils of an initial artificial catchment (Chicken Creek; *Hühnerwasser*) in a post-mining landscape in NE Germany. Chicken Creek represents a study site with defined initial conditions and offers the rare opportunity to monitor BSi dynamics from the very beginning. Former studies at this site revealed (i) a formation of protophytic (diatom frustules), protozoic (testate amoeba shells) and zoogenic (sponge spicules) Si pools within a short time (< 10 years) and (ii) a strong relation of spatiotemporal changes in protistic (diatoms and testate amoebae) BSi pools to the vegetation, because plants provide, e.g., rhizospheric micro-habitats including enhanced food supply (Puppe et al., 2014, 2016). From these results it can be concluded that vegetated spots in particular represent hotspots of BSi accumulation of various origin at initial biogeosystem sites (compare Wanner and

Elmer, 2009). Furthermore, construction work with large machines resulted in differently structured sections of Chicken Creek with slight differences in abiotic conditions (for details see Sect. 2.1.) (Gerwin et al., 2010). These differences in turn lead to section-specific vegetation dynamics at Chicken Creek (Zaplata et al., 2010).

Knowledge about BSi accumulation dynamics is crucial for the understanding of Si cycling in terrestrial biogeosystems. We regard water-extractable Si as a useful proxy for desilication and biological uptake (plants, testate amoebae etc.). In addition, we used an alkaline extractant (Tiron) to detect eventual short-term changes in the amorphous Si fraction. We hypothesized that (i) BSi pools influence short-term changes in water-soluble Si in initial soils but not short-term changes in amorphous Si fractions, (ii) the phytogenic Si pool is the most prominent one in size and thus the biggest driver of short-term changes in water-soluble Si, and (iii) BSi pool changes are section-specific, i.e., related to vegetation dynamics. The aims of the present study were (i) to quantify various BSi pools, i.e., protophytic, protozoic, zoogenic and phytogenic Si pools, during initial soil and ecosystem development; (ii) to analyze potential section-specific short-term changes in these BSi pools after a decade of ecosystem development; and (iii) to evaluate the influence of different BSi pools on water-soluble Si in these soils.

2 Material and methods

2.1 Study site

The study site Chicken Creek (51°36'18" N, 14°15'58" E) represents an artificial catchment in a post-mining landscape located in the active mining area of Welzow South (lignite open-cast mining, 150 km southeast of Berlin) in the state of Brandenburg, Germany (Kendzia et al., 2008; Russell et al., 2010). Climate at Chicken Creek is characterized by an average air temperature of 9.6 °C and an annual precipitation of 568 mm comprising data from 1981 to 2010 (Meteorological Station Cottbus, German Weather Service).

To construct the ~ 6 ha sized catchment a 1–3 m thick base layer (aquiclude) of Tertiary clay was covered by a 2–3 m thick sandy, lignite- and pyrite-free Quaternary sediment serving as a water storage layer (aquifer) (Gerwin et al., 2010; Kendzia et al., 2008). Quaternary material was taken from a depth of 20 to 30 m during lignite mining process and its texture is classified as sand to loamy sand (Table 1) with low contents of carbonate (Gerwin et al., 2009, 2010; Russell et al., 2010). Dumping of material and construction work with large machines (e.g., stackers and bulldozers) resulted in differently structured sections of Chicken Creek. Generally, the catchment area can be divided into four sections: (i) an eastern part (ca. 1.8 ha), (ii) a western part (ca. 1.6 ha), (iii) a central trench (ca. 0.9 ha) separating the eastern from the western part and (iv) a southern part (ca. 1.5 ha) with a pond

Table 1. Contents of skeleton (>2 mm), fine earth (<2 mm), sand, silt and clay fractions (upper 30 cm) at the sampling points in western, eastern and southern sections at Chicken Creek (t_0 , calculations based on data of Gerwin et al., 2010). Minimal (min.) as well as maximal (max.) values, means (\bar{x}) and standard deviations (SD) are given.

Section		>2 mm	<2 mm	Sand	Silt	Clay
		%				
West	Min.	9	80	77	7	5
	Max.	20	91	88	13	10
	\bar{x}	13	87	83	10	7
	SD	5	5	4	2	2
East	Min.	2	77	69	6	4
	Max.	23	98	91	20	11
	\bar{x}	13	87	82	11	7
	SD	7	7	9	6	3
South	Min.	0.2	84	78	7	4
	Max.	17	99.8	89	17	8
	\bar{x}	8	92	83	11	6
	SD	8	8	4	4	2

at the lowest point (Fig. 1). Construction work was completed in September 2005 (time zero, t_0). Analyses subsequent to catchment completion indicated slight differences in abiotic conditions between the eastern and the western parts (in soil pH, conductivity, skeleton content with soil particle diameter >2 mm, proportions of sand, silt and clay, concentration of organic and inorganic carbon; Gerwin et al., 2010). The primary mineral component in all particle size fractions at t_0 was quartz (only small amounts of K-feldspar, plagioclase). Calcite comprised 0.5–4.5 % of the initial sediment, dolomite was only detectable in a few samples with contents of 0.5 %, and magnesite (MgCO_3) was not detectable by mineralogical analysis (W. Schaaf, personal communication, 2011). For detailed information on the site construction and initial ecosystem development see Gerwin et al. (2010) and Schaaf et al. (2010), respectively.

2.2 Soil sampling

We used samples taken shortly after the construction of Chicken Creek (2005, t_0) and after an ecosystem development period of about 10 years (2015, t_{10}). For t_0 (no vegetation detectable) we assumed that biogenic siliceous structures were homogeneously distributed across the whole area of Chicken Creek, i.e., no section-specific distribution of BSi (BSi t_0 east \approx BSi t_0 west \approx BSi t_0 south) at the beginning of ecosystem development (Puppe et al., 2016). This is why we did not sample all different sections of the catchment but took soil samples in six field replicates to quantify BSi pools at t_0 . However, for t_{10} we hypothesized section-specific differences in BSi pool quantities related to section-specific vegetation dynamics. To evaluate these differences after a decade of ecosystem development and to cover the biggest

possible BSi accumulation in soil we focused on spots where Si-accumulating plant species, i.e., *Calamagrostis epigejos* and *Phragmites australis*, became dominant (Zaplata et al., 2010). Thus we took samples in the eastern (*C. epigejos* dominant) and western (mainly *C. epigejos* dominant, one spot with *P. australis*) and southern section (*P. australis* dominant) of Chicken Creek.

For an accurate description of changes in abiotic soil conditions and related phylogenetic Si in every section, we took soil and plant samples in eastern, western and southern sections at t_0 as well as t_{10} . Erosion and deposition processes were clearly evident in the Chicken Creek catchment during the first years without plant cover. Substantial surface changes resulted from rill erosion, as aerial photographs (rill network) and a comparison of photogrammetry-based digital elevation models showed (Schneider et al., 2013). Inter-rill erosion did not lead to surface changes larger than about 20 cm during the first 5 years. Afterwards the establishment of an area-wide plant cover substantially reduces interrill erosion. Because all soil data at t_0 referred to a depth increment of 30 cm we reasonably assumed the same soil conditions for the sampled t_0 spots during the first years. Furthermore, we carefully selected sampling points at t_{10} to be not influenced by erosion, i.e., at spots with low surface roughness and outside rills. Soil samples for the determination of soil properties and plant samples were taken in five (western and southern section) and six (eastern section) field replicates at t_0 and t_{10} (Fig. 1). At every sampling point three undisturbed soil cores were taken with a core cutter (diameter = 3.4 cm, depth = 5 cm) and transferred into plastic bags. Bulk densities were calculated from dividing the weight of dried (105 °C) soil samples by their corresponding volumes.

2.3 Determination of basic soil properties

Soil samples were air dried and sieved and the fine earth fraction (<2 mm) was used for laboratory analyses. Soil pH was measured based on the DIN ISO method 10390 (1997) in 0.01 M CaCl_2 suspensions at a soil-to-solution ratio of 1 : 5 (w/v) after a 60 min equilibration period using a glass electrode. The total carbon content was analyzed by dry combustion using an elemental analyzer (Vario EL, Elementar Analysensysteme, Hanau, Germany). Carbonate (CaCO_3) was determined conductometrically using the Scheibler apparatus (Schlichting et al., 1995). Organic carbon (C_{org}) was computed as the difference between total carbon and carbonate carbon. Analyses of basic soil properties were performed in two lab replicates per sample.

2.3.1 Water-extractable Si ($\text{Si}_{\text{H}_2\text{O}}$)

Water-extractable Si was determined based on a method developed by Schachtschabel and Heinemann (1967). Ten grams of dry soil (<2 mm) was weighed and put into 80 mL centrifuge tubes, and 50 mL distilled water was added with

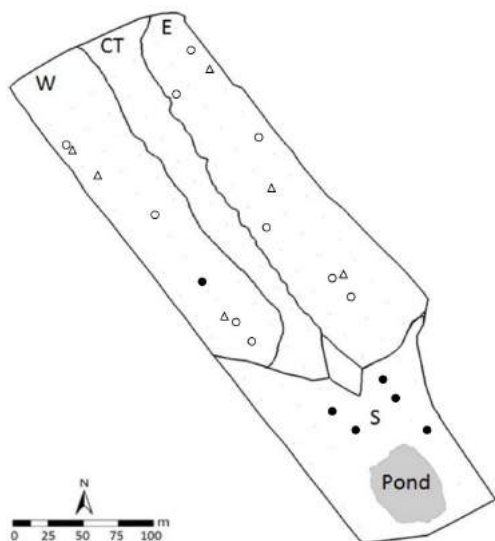


Figure 1. Map of Chicken Creek (W is the western section, CT is the central trench, E is the eastern section, S is the southern section with pond). Triangles indicate the sampling points used for BSi analyses at t_0 ($n = 6$). Circles indicate the sampling points used for measurements of soil parameters (at t_0 and t_{10}) and plant analyses (only at t_{10}) (W, $n = 5$; E, $n = 6$; S, $n = 5$). Empty and filled circles represent sampling points where *Calamagrostis epigejos* and *Phragmites australis* became dominant. Note that the size of sampling points is not to scale.

three drops of a 0.1 % NaN_3 solution to prevent microbial activity. Total extraction time was 7 days in which tubes were shaken by hand twice a day for 20 s. Mechanical (constant) shaking by using, e.g., a roll mixer, was avoided to prevent abrasion of mineral particles from colliding during shaking (McKeague and Cline, 1963). The solutions were centrifuged (4000 rpm, 20 min), filtrated (0.45 μm polyamide membrane filters) and Si was measured with ICP–OES (ICP–iCAP 6300 DUO, Thermo Fisher Scientific Inc). Analyses of water-extractable Si were performed in two lab replicates per sample.

2.3.2 Tiron-extractable Si (Si_{Tiron}), aluminum (Al_{Tiron}) and iron (Fe_{Tiron})

The Tiron ($\text{C}_6\text{H}_4\text{Na}_2\text{O}_8\text{S}_2 \cdot \text{H}_2\text{O}$) extraction followed the method developed by Biermans and Baert (1977) and modified by Kodama and Ross (1991). It has been used to quantify amorphous biogenic and pedogenic Si (Kendrick and Graham, 2004), although a partial dissolution of primary minerals is well known (Kodama and Ross, 1991; Sauer et al., 2006). The extraction solution was produced by dilution of 31.42 g Tiron with 800 mL of distilled water, followed by addition of 100 mL sodium carbonate solution (5.3 g Na_2CO_3 + 100 mL distilled water) under constant stirring. The final pH of 10.5 was reached by adding small volumes of a 4M NaOH solution. For the extraction, 30 mg of dry soil were

weighed into 80 mL centrifuge tubes and a 30 mL aliquot of the Tiron solution was added. The tubes were then heated at 80 °C in a water bath for 1 h. The extracted solutions were centrifuged at 4000 rpm for 30 min and filtrated (0.45 μm polyamide membrane filters, Whatman NL 17), and Si, Al and Fe were measured with ICP–OES. Analyses of Tiron-extractable Si, Al and Fe were performed in three lab replicates per sample.

2.4 Microscopical analyses of diatoms, sponge spicules and testate amoebae

Fresh soil samples were homogenized by gentle turning of the plastic bags before air drying. Afterwards 2 g of fresh soil was taken per sample and stored in 8 mL of formalin (4 %). Subsequently, biogenic siliceous structures, i.e., diatom frustules, testate amoeba shells and sponge spicules (Fig. 2a–d), were enumerated in soil suspensions (125 mg fresh mass – FM) received from serial dilution (1000–125 mg soil in 8 mL of water each) using an inverted microscope (OPTIKA XDS-2, objectives 20 : 1 and 40 : 1, equipped with a digital camera OPTIKAM B9).

2.5 Determination of phytoliths in soil samples

Ten grams of dry soil material (<2 mm) was processed in four steps (adapted from Alexandre et al., 1997). First organic matter was oxidized using H_2O_2 (30 Vol.%), HNO_3 (65 Vol.%) and HClO_4 (70 Vol.%) at 80 °C until the reaction subsided. Secondly, carbonates and Fe oxides were dissolved by boiling the sample in HCl (10 Vol.%) for 30 min. Thirdly, the <2 μm granulometric fraction was removed by dispersing the remaining solid phase of step 2 with 2 Vol.% sodium hexametaphosphate solution (6–12 h), centrifugation at 1000 rpm for 2–3 min and subsequent decantation. Finally, the phytoliths were separated by shaking the remaining solid phase of step 3 with 30 mL of sodium polytungstate ($\text{Na}_6(\text{H}_2\text{W}_{12}\text{O}_{40}) \cdot \text{H}_2\text{O}$) with a density of 2.3 g cm^{-3} and subsequent centrifugation at 3000 rpm for 10 min. Afterwards, the supernatant was carefully pipetted and filtered using 5 μm Teflon filters. This step was repeated three times. The filter residue was washed with water, bulked, dried at 105 °C and weighted.

2.6 Quantification of biogenic Si pools

In general, biogenic siliceous structures consist of hydrated amorphous silica ($\text{SiO}_2 \cdot n\text{H}_2\text{O}$). We assumed an average water content of about 10 % for these structures to avoid an overestimation of BSi pools (Mortlock and Froelich, 1989).

Protophytic Si pools (represented by diatom frustules) were quantified by multiplication of Si content per frustule with corresponding individual numbers (see Puppe et al., 2016). Protozoic Si pools (represented by testate amoebae) were quantified by multiplication of silica contents of diverse testate amoeba taxa (Aoki et al., 2007) with corresponding

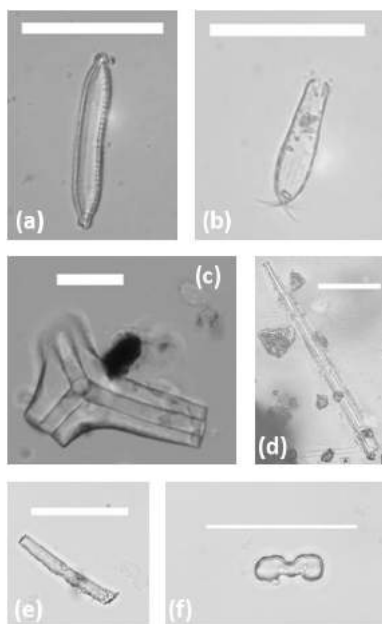


Figure 2. Micrographs (light microscope) of biogenic silica structures found at Chicken Creek. (a) Pennate diatom (valve view), (b) testate amoeba shell (*Euglypha cristata*), (c) and (d) sponge spicules (fragments), (e) elongate phytolith and (f) bilobate phytolith. All scale bars: 50 μm .

individual numbers (living plus dead individuals, for details see Puppe et al., 2014, 2015).

Zoogenic Si pools (represented by sponge spicule fragments) were calculated by multiplying volumes (μm^3) of the found spicule fragments with the density of biogenic Si (2.35 g cm^{-3}) and summing up the results. Volume measurements were conducted using a laser scanning microscope (Keyence VK-X110, magnification 200–2000 \times) (details in Puppe et al., 2016). For laser scanning microscopy spicule fragments were taken from soil suspensions by micromanipulation, washed in distilled H_2O and placed on clean object slides. Afterwards, air-drying images of spicule fragments were acquired (software Keyence VK-H1XVD) and analyzed (software Keyence VK-H1XAD).

Phytogenic Si pools were estimated by multiplying the numbers of found phytoliths with corresponding mean volumes (μm^3) of phytoliths, multiplying these results with the density of biogenic Si (2.35 g cm^{-3}) and summing up the results. Volume measurements with the laser scanning microscope of 30 typical elongate (Fig. 2e) and 30 typical bilobate phytoliths (Fig. 2f) resulted in mean volumes of $3765 \mu\text{m}^3$ and $707 \mu\text{m}^3$, respectively. For laser scanning microscopy extracted phytoliths were placed on clean object slides and images were acquired and analyzed analogous to sponge spicules. For bilobate phytoliths we measured the upper half per phytolith and doubled the result to obtain the corresponding total volume; thus we assumed bilobate phytoliths to be symmetric. We assumed phytoliths to consist of 95 % SiO_2

and 5 % other elements, e.g., carbon (Song et al., 2012) and elements like iron, aluminum or calcium (Buján, 2013).

BSi pools (mg m^{-2}) were calculated considering bulk density (g cm^{-3}), thickness (5 cm) and – for protistic and zoogenic Si pools – water content (% of fresh mass) per soil sample. Silica ($M = 60.08 \text{ g mol}^{-1}$) pools were converted to Si ($M = 28.085 \text{ g mol}^{-1}$) pools by multiplication with 28/60 (details in Puppe et al., 2014, 2015, 2016).

2.7 Plant analyses

Plant and litter samples of *C. epigejos* and *P. australis* were collected in the summer of 2015. In general, monomeric silicic acid (H_4SiO_4) enters the plant via its roots and is carried in the transpiration stream towards transpiration termini. When water evaporates, silicic acid becomes supersaturated and is precipitated as hydrated silica in the form of phytoliths. The vast majority of Si in plants is located at the transpiration termini (e.g., leaves) in the aerial plant parts, while considerably less Si can be found in other plant portions like stems, roots and rhizomes. Sangster (1983), for example, found no significant Si depositions in rhizomes of *P. australis*. Consequently, we only analyzed the aboveground vegetation (including transpiration termini and stems). The collected plant material was washed with distilled water to remove adhering soil minerals and oven-dried at 45°C for 48 h.

2.7.1 Total Si content in plant materials

Plant samples were milled using a knife mill (Grindomix GM 200, Retsch) in two steps: 4000 rpm for 1 min and then 10 000 rpm for 3 min. Sample aliquots of approximately 100 mg were digested under pressure in PFA digestion vessels using a mixture of 4 mL distilled water, 5 mL nitric acid (65 %) and 1 mL hydrofluoric acid (40 %) at 190°C using a microwave digestion system (Mars 6, CEM). A second digestion step was used to neutralize the hydrofluoric acid with 10 mL of a 4 % boric acid solution at 150°C . Silicon was measured with ICP–OES (ICP–iCAP 6300 Duo, Thermo Fisher Scientific Inc) with an internal standard. To avoid contamination, plastic equipment was used during the entire procedure. Analyses of total Si content were performed in three lab replicates per sample.

2.7.2 Determination of phytoliths in plants and litter

Plant material was washed with distilled water and oven-dried at 45°C for 48 h. Removal of organic matter was conducted by burning the samples in a muffle furnace at 450°C for 12 h. Next, the material was subject to additional oxidation using 30 % H_2O_2 for 12 h. The obtained material was filtered through a Teflon filter with a mesh size of $5 \mu\text{m}$. The isolated phytoliths and siliceous cast ($>5 \mu\text{m}$) were subject to analysis via polarized light microscopy (Nikon ECLIPSE LV100 microscope) for full characteristics. We used laser

Table 2. Measured soil parameters (upper 5 cm, means (\bar{x}) with standard deviation – SD) at the different sections of Chicken Creek.

Age	Section		Si _{H₂O}	Si _{Tiron}	Al _{Tiron}	Fe _{Tiron}	C _{org}	CaCO ₃	pH
			g m ⁻²						
t ₀	West	\bar{x}	0.70	524	312	249	237*	88	7.9
		SD	0.10	95	24	33	156	72	0.1
t ₁₀	West	\bar{x}	1.73	552	254	239	556*	101	7.4
		SD	0.22	300	154	104	167	93	0.1
t ₀	East	\bar{x}	0.87*	503	268	261	123	91	8.1
		SD	0.48	281	151	130	38	79	0.2
t ₁₀	East	\bar{x}	1.50*	196	122	151	396	30	7.1
		SD	0.57	49	27	29	54	18	0.2
t ₀	South	\bar{x}	0.84	399	232	238*	160*	174	8.3
		SD	0.06	154	112	65	131	109	0.1
t ₁₀	South	\bar{x}	2.24	317	147	157*	474*	126	7.4
		SD	0.33	149	62	57	258	40	0.1

Significant differences between t₀ and t₁₀ are each stated in bold (Mann–Whitney *U* test, *p* < 0.05) or marked with asterisks (*p* < 0.1) for the western, eastern and southern sections.

Table 3. Spearman's rank correlations between measured soil parameters and total BSi (upper 5 cm, *n* = 6) at Chicken Creek.

	Si _{H₂O}	Si _{Tiron}	Al _{Tiron}	Fe _{Tiron}	C _{org}	CaCO ₃	pH	BSi
Si _{H₂O}	1.000							
Si _{Tiron}	-0.257	1.000						
Al _{Tiron}	-0.600	0.829	1.000					
Fe _{Tiron}	-0.486	0.771	0.943	1.000				
C _{org}	0.714	0.086	-0.371	-0.486	1.000			
CaCO ₃	0.200	0.086	-0.086	-0.029	0.029	1.000		
pH	-0.600	0.200	0.486	0.543	-0.771	0.543	1.000	
BSi	0.941	-0.213	-0.577	-0.577	0.880	0.152	-0.698	1.000

Significant correlation coefficients are given in bold (*p* < 0.05).

scanning microscopy for measurements of the surface area (μm²) of the 30 typical bilobate and 30 typical elongated phytoliths used for volume measurements (see Sect. 2.6) and calculated corresponding surface-area-to-volume ratios (*A* / *V* ratios) as an indicator of the resistibility of these siliceous structures against dissolution. Higher *A* / *V* ratios indicate a bigger surface area available for dissolution processes.

2.8 Statistical analyses

Correlations were analyzed using Spearman's rank correlation (*r_s*). Significances in two-sample (*n* = 2) cases were verified with the Mann–Whitney *U* test. For *k*-sample (*n* > 2) cases the Kruskal–Wallis analysis of variance (ANOVA) was used followed by pairwise multiple comparisons (Dunn's post hoc test). Statistical analyses were performed using software package SPSS Statistics (version 19.0.0.1, IBM Corp.).

3 Results

3.1 Basic soil parameters

Soils at the initial state (t₀) showed organic carbon contents (C_{org}) in the upper 5 cm between 1.1 and 4.4 g kg⁻¹ in the western section, 0.8 and 1.8 g kg⁻¹ in the eastern section and 0.2 and 3.3 g kg⁻¹ in the southern section. This corresponded to mean carbon stocks of 237 g m⁻² (west), 123 g m⁻² (east) and 160 g m⁻² (south, Table 2). After 10 years (t₁₀) of ecosystem development the C_{org} stocks increased up to a factor of 3 (396–556 g m⁻² in the upper 5 cm) from corresponding values at t₀. This resulted in a surprisingly high mean annual CO₂-C sequestration rate of 27–32 g m⁻² (upper 5 cm). Hereby the largest C_{org} stock changes were found in the western section of the area followed by the eastern section and the southern section (Table 2).

The carbonate contents (CaCO₃) at t₀ varied between means of 1.0 g kg⁻¹ (west), 0.9 g kg⁻¹ (east) and 1.8 g kg⁻¹ (south). The corresponding stocks were 88 g m⁻² (west), 91 g m⁻² (east) and 174 g m⁻² (south, Table 2). The carbon-

Table 4. Surface areas, volumes and surface-to-volume ratios (A/V) of different biogenic siliceous structures found at Chicken Creek.

	Surface area (μm^2)		Volume (μm^3)		A/V ratio	
	Min.	Max.	Min.	Max.	Range	Mean (SD)
Bilobate phytoliths	216	3730	36	2046	0.7–9.8	2.8 (1.8)
Elongate phytoliths	2302	22203	390	14649	0.6–5.9	2.6 (1.1)
Diatom frustules*	351	9901	347	28024	0.3–3.3	0.9 (0.5)
TA shells*	1229	5085	900	15812	0.2–2.7	0.8 (0.7)
Sponge spicules*	305	16963	291	59744	0.3–1.6	0.8 (0.4)
Spicule fragments*	2828	17268	5255	34812	0.5–0.6	0.5 (0.03)

* Data taken from Puppe et al. (2016).

ate pools in the western and eastern section were very similar, while the high carbonate values in the southern section were due to the original soil properties. At t_{10} the distribution of carbonate was as follows: in the western section there was an increase of about 17 % (from 88 to 101 g m^{-2}), in the eastern part a distinct decrease of about 67 % (from 91 to 30 g m^{-2}) was detected and in the southern section again a decrease of about 28 % (from 174 to 126 g m^{-2}) was identified.

At t_0 the pH values of the soils showed a range between 7.9 and 8.3 (Table 2) with relatively low variation between the different sections. After 10 years the pH values decreased to 7.1–7.4 in all sections.

3.2 Water and Tiron extractions

The mean water-soluble Si ($\text{Si}_{\text{H}_2\text{O}}$) contents in the upper 5 cm showed low variation between the different sections at t_0 : 7.3 mg kg^{-1} (west), 7.2 mg kg^{-1} (east) and 8.6 mg kg^{-1} (south). The corresponding stock values were 0.7 g m^{-2} (west), 0.87 g m^{-2} (east) and 0.84 g m^{-2} (south) for all sections at t_0 (Table 2). After 10 years (t_{10}) an overall significant increase of $\text{Si}_{\text{H}_2\text{O}}$ from t_0 was found in each of the different sections. The corresponding stock values were 1.7 g m^{-2} (west), 1.5 g m^{-2} (east) and 2.2 g m^{-2} (south, Table 2).

At t_0 the mean Tiron-extractable Si contents in the upper 5 cm varied between 5.5 g kg^{-1} (west), 5.2 g kg^{-1} (east) and 4.1 g kg^{-1} (south). The related stock values were 524 g m^{-2} (west), 503 g m^{-2} (east) and 399 g m^{-2} (south, Table 2). After 10 years (t_{10}) the Tiron-extractable Si content showed a slight increase in the western section to 6.5 g kg^{-1} (552 g m^{-2}), while the concentration in the eastern section decreased significantly to 2.6 g kg^{-1} (196 g m^{-2} , Table 2). In the southern section only a slight decrease to 3.8 g kg^{-1} (317 g m^{-2}) was found. The Al and Fe-extractable Tiron contents followed the distribution of the Si concentrations with one exception in the western section, where contrary to Si the Al and the Fe contents slightly increased at t_{10} (Table 2). Si / Al ratios ranged between 1.6 and 2.2 at Chicken Creek. Tiron-extractable Si and Al fractions as well as Tiron-

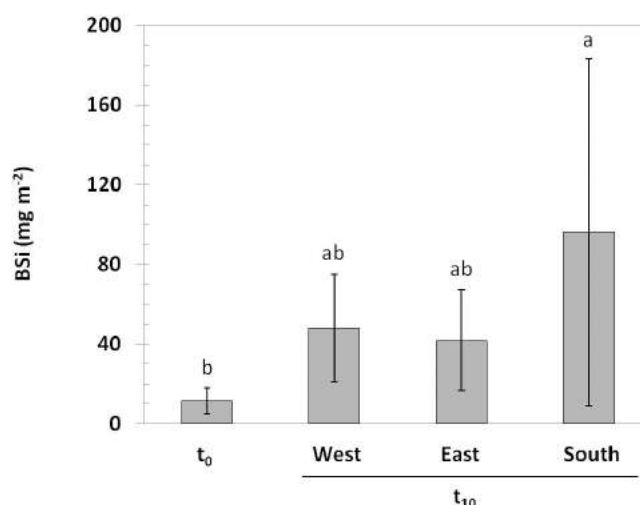


Figure 3. Total biogenic Si pools in soils (means \pm standard deviation, upper 5 cm) at Chicken Creek at the end of construction work (t_0) and after 10 years of ecosystem development (western, eastern and southern sections, t_{10}). Significant differences are indicated by different letters ($p < 0.05$, Kruskal–Wallis ANOVA with Dunn's post hoc test).

extractable Al and Fe fractions were strongly correlated (Table 3).

3.3 Biogenic Si pools in soils

In general, total biogenic Si pools increased in every section after 10 years of ecosystem development with statistically significant differences between t_0 ($11.6 \pm 6.5 \text{ mg Si m}^{-2}$) and the southern section at t_{10} ($96.0 \pm 87.2 \text{ mg Si m}^{-2}$) (Fig. 3). Total BSi showed strong positive and statistically significant correlations to water-soluble Si (Table 3). Phytogenic (phytoliths $> 5 \mu\text{m}$) Si pools ranged from 0 to 18 mg m^{-2} (mean: 6.6 mg m^{-2}) at t_0 and significantly increased to means of 20.7 mg m^{-2} (range: 7–52 mg m^{-2}) and 12.9 mg m^{-2} (range: 14–15 mg m^{-2}) at the eastern and southern sections over 10 years, respectively (Fig. 4a). Protophytic Si pools (diatom frustules) ranged from 0 to

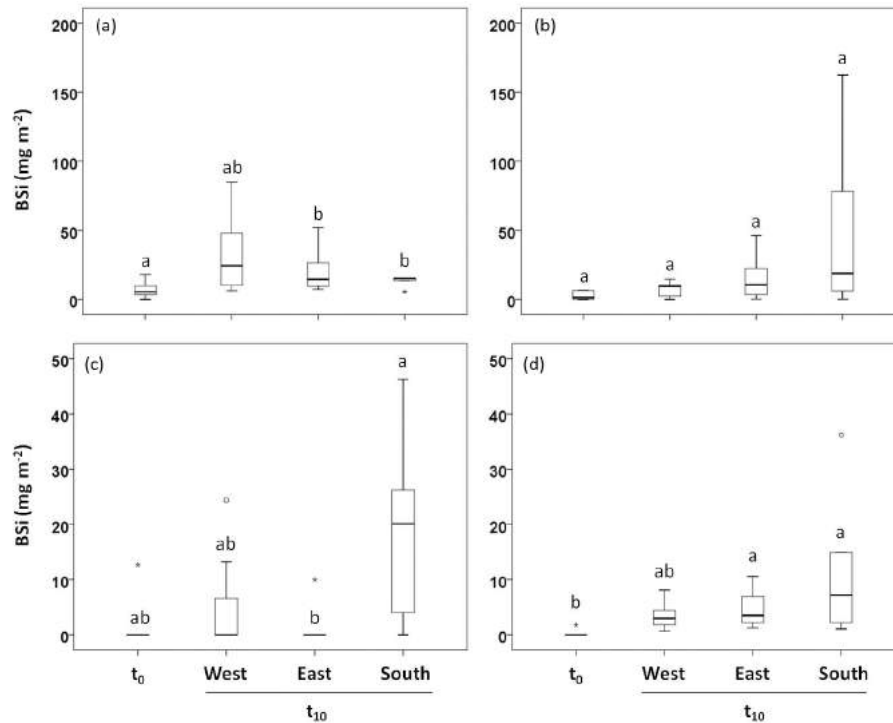


Figure 4. Box plots (top, middle and bottom lines of the boxes show the 25th, 50th and 75th percentiles and whiskers represent $1.5 \times$ the interquartile ranges) of biogenic Si pools in soils (upper 5 cm) at Chicken Creek at the end of construction work (t_0) and after 10 years of ecosystem development (western, eastern and southern sections, t_{10}). (a) Phylogenetic Si pools (phytoliths), (b) protophytic Si pools (diatom frustules), (c) zoogenic Si pools (sponge spicules) and (d) protozoic Si pools (testate amoeba shells). Significant differences are indicated by different letters ($p < 0.05$, Kruskal–Wallis ANOVA with Dunn’s post hoc test). Circles and asterisks indicate outliers and extreme values, respectively. Note different scales for diagrams (a) and (b) and (c) and (d).

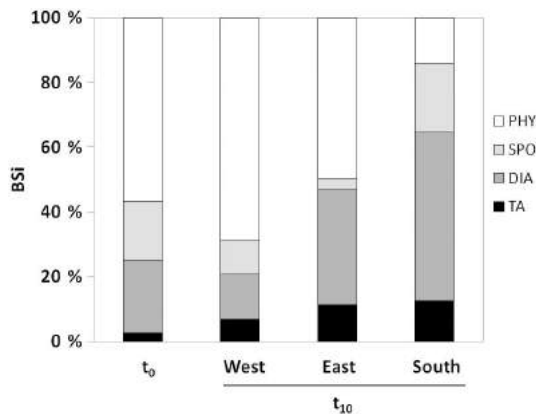


Figure 5. Proportions of phytoliths (PHY), sponge spicules (SPO), diatom frustules (DIA) and testate amoeba shells (TA) to total BSi in soils (upper 5 cm) at Chicken Creek at t_0 and t_{10} . Note that total BSi pools differ in size (see Fig. 3).

7 mg m^{-2} (mean: 2.6 mg m^{-2}) at t_0 and increased up to a mean of 47.4 mg m^{-2} (range: $0.1\text{--}162 \text{ mg m}^{-2}$) at t_{10} (southern section) (Fig. 4b). At t_0 no sponge spicules were found with one exception representing an extreme value

(12.7 mg m^{-2}). After one decade of ecosystem development zoogenic Si pools increased to a maximum of 46 mg m^{-2} in the southern section (t_{10}) (Fig. 4c). Protozoic Si pools were zero at t_0 , with one exception representing an extreme value (1.8 mg m^{-2}), and significantly increased to 4.6 mg m^{-2} (range: $1\text{--}11 \text{ mg m}^{-2}$) and 11.5 mg m^{-2} (range: $2\text{--}36 \text{ mg m}^{-2}$) in the eastern and the southern sections at t_{10} , respectively (Fig. 4d).

At t_0 most BSi ($> 50\%$) is represented by phytoliths $> 5 \mu\text{m}$ followed by diatom frustules, sponge spicules and testate amoeba shells (Fig. 5). After 10 years of ecosystem development the proportion of the different BSi pools to total BSi changed. While the proportion of protozoic Si pools increased in all sections at t_{10} , the other BSi pools showed more variable changes over time. The proportion of phylogenetic Si pools either increased (western section) or decreased (eastern and southern sections). In contrast, the proportion of protophytic Si pools decreased in the western section and increased in the eastern and southern sections. The proportion of zoogenic Si pools decreased in the western and eastern sections but increased slightly in the southern section at t_{10} .

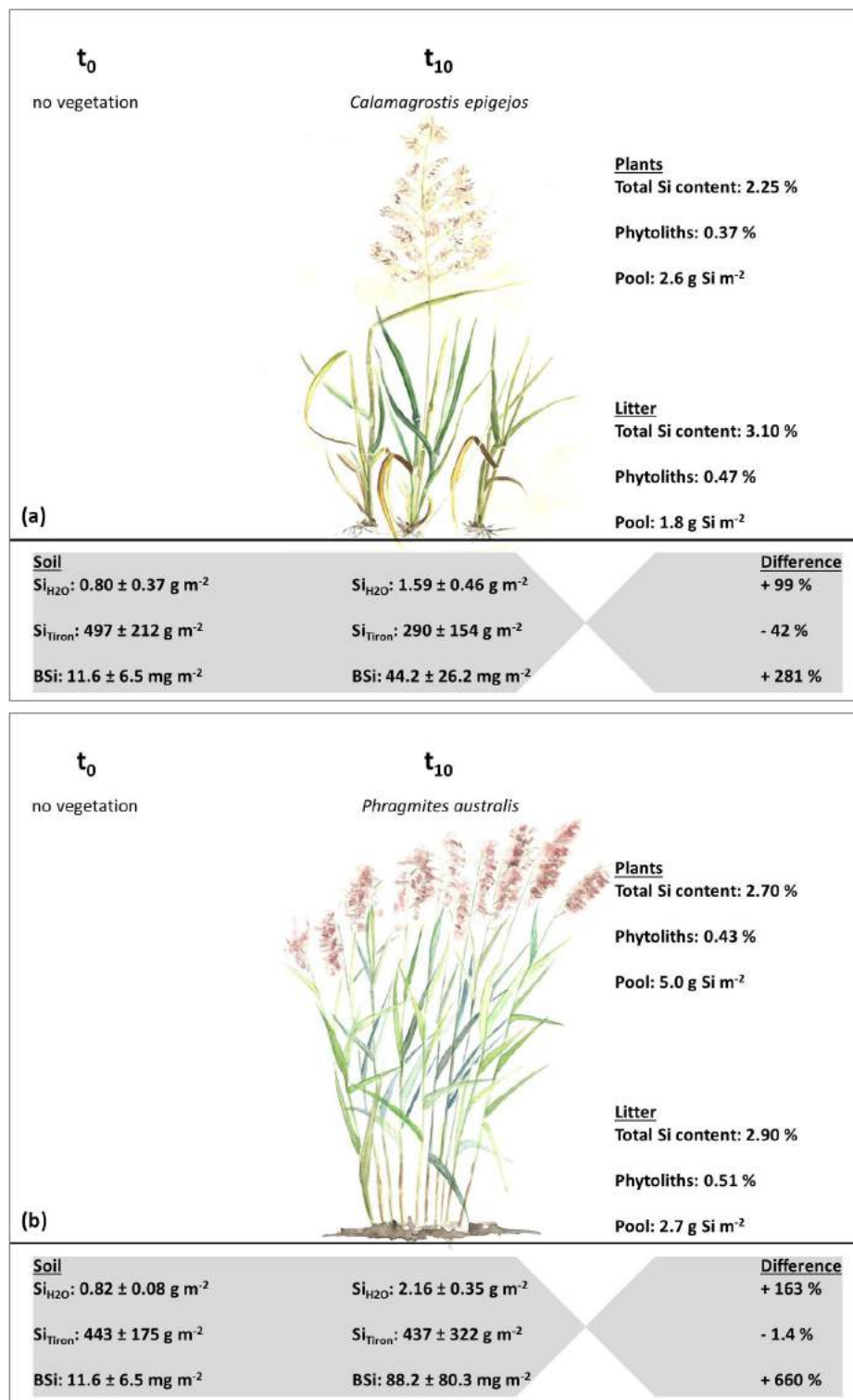


Figure 6. Comparison of water-soluble Si (Si_{H₂O}), amorphous Si (Si_{Tiron}) fractions and total BSi in soils (means ± standard deviation, upper 5 cm), where *Calamagrostis epigejos* (a) and *Phragmites australis* (b) became dominant. Data are given for t₀ (no vegetation) and t₁₀ (*C. epigejos*, *P. australis*). For t₁₀ total plant Si contents, extracted phytogenic Si (phytoliths) contents and Si pools for *C. epigejos* and *P. australis* (plants and litter) are stated in addition. Paintings are from Cornelia Höhn, Müncheberg.

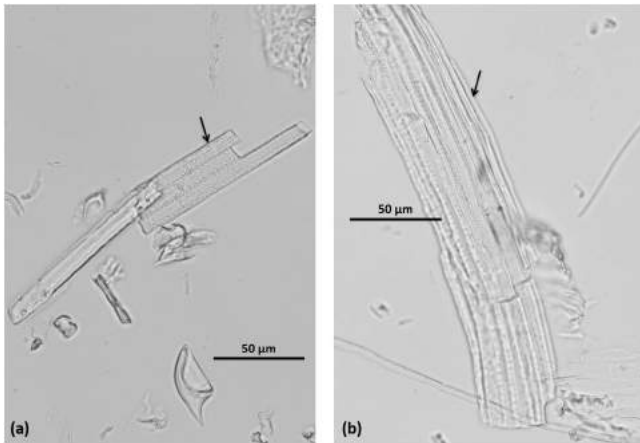


Figure 7. Micrographs of fragile phytogenic Si structures (arrows) of *C. epigejos* (a) and *P. australis* (b).

3.4 Phytoliths and total Si content in plant materials

The total content of Si was determined for two Si-accumulating plant species, *Calamagrostis epigejos* and *Phragmites australis*, which dominate distinct catchment sections. For *C. epigejos* the mean total content of Si was 2.25 % (range: 1.8–3.1 %), whereas for *P. australis* a mean total Si content of 2.70 % (range: 2.0–3.2 %) was determined (Fig. 6a, b). For litter we found mean total Si contents of 3.1 % (range: 2.8–3.3 %) and 2.9 % (range: 1.7–3.2 %) for *C. epigejos* and *P. australis*, respectively.

Phytoliths $>5\mu\text{m}$ were also isolated from both plants, showing mean phytolith contents of 0.37 % (range: 0.31–0.46 %) and 0.43 % (range: 0.37–0.50 %) for *C. epigejos* and *P. australis*, respectively (Fig. 6a, b). Regarding the total Si content of plants only about 16 % of phytogenic Si were represented by the extracted phytoliths. Thus, small-scale ($<5\mu\text{m}$) and/or fragile (siliceous structures mostly thinner than $5\mu\text{m}$, but up to several hundred micrometers long, Fig. 7) phytogenic Si represented about 84 % of total phytogenic Si in *C. epigejos* and *P. australis*, respectively. Mean extracted phytolith contents in plant litter were 0.47 % (range: 0.35–0.70 %) and 0.51 % (range: 0.41–0.59 %) for *C. epigejos* and *P. australis*.

Surface areas of 30 typical bilobate and 30 typical elongate phytoliths were in the ranges of 216 to $3730\mu\text{m}^2$ and 2302 to $22\,203\mu\text{m}^2$ (Table 4). The corresponding volumes of bilobate and elongate phytoliths were in the ranges of 36 to $2046\mu\text{m}^3$ and 390 to $14\,649\mu\text{m}^3$. Surface-to-volume ratios of bilobate and elongate phytoliths were in the ranges of 0.7 to 9.8 and 0.6 to 5.9 with means of 2.8 and 2.6 .

3.5 BSi and Si fractions under *Calamagrostis epigejos* and *Phragmites australis*

Water-soluble Si fractions increased by 99 and 163 % and total BSi by 281 and 660 % after 10 years of ecosystem devel-

opment in soils under *C. epigejos* and *P. australis* (Fig. 6a, b). In contrast, Si_{Tiron} decreased by 42 and 1.4 % from t_0 to t_{10} in soils under *C. epigejos* and *P. australis*. If we assume mean dry biomasses of 115 and 186g m^{-2} for *C. epigejos* and *P. australis* (M. Wehrhan, personal communication, 2017) about 2.6 and 5.0g Si m^{-2} are stored in the above-ground biomass at Chicken Creek at t_{10} . For *C. epigejos* and *P. australis* litter (mean dry biomasses of 59 and 94g m^{-2} at t_{10} ; M. Wehrhan, personal communication, 2017), we calculated corresponding pools of about 1.8 and 2.7g Si m^{-2} at t_{10} .

4 Discussion

4.1 Drivers of short-term changes in water-soluble Si at Chicken Creek

In general, weathering of silicates represents the ultimate source of $\text{Si}(\text{OH})_4$ in terrestrial biogeosystems in the long term (Berner, 2003). In this context, the long-term accumulation of BSi can influence the total amorphous (Tiron-extractable) Si as it is known from forested catchments or old chronosequence soils (Conley et al., 2008; Kendrick and Graham, 2004; Saccone et al., 2008). Contrary, short-term changes in BSi pools likely do not influence Tiron-extractable Si in initial soils (total BSi represents only 0.002–0.03 % of Tiron-extractable Si at Chicken Creek). Thus, the major proportion of Tiron-extractable Si at Chicken Creek seems to be of pedogenic origin (e.g., Si included in Al / Fe oxides / hydroxides). This is supported by relatively low Si / Al ratios (<5) indicating a minerogenic origin of Tiron-extractable Si instead of BSi as a source of Si_{Tiron} (Bartoli and Wilding, 1980). We further exclude changes in Tiron-extractable Si as the main driver of water-soluble Si at Chicken Creek in the short term, because (i) Si_{Tiron} and $\text{Si}_{\text{H}_2\text{O}}$ showed no statistical relationship at all and (ii) a significant change of the Tiron-extractable Si fraction occurred only in the eastern section, whereas in the western and southern section Si_{Tiron} did not change significantly over time. We assume that these changes in Si_{Tiron} in the eastern section are related to abiotic conditions (soil pH, conductivity, skeleton content, proportions of sand, silt and clay, concentration of organic and inorganic carbon), which were slightly different to the conditions of the western section at t_0 (Gerwin et al., 2010). Furthermore, we excluded atmospheric inputs as potential drivers of short-term changes in water-soluble Si at Chicken Creek. On the one hand, dust depositions (dry deposition) at Chicken Creek are very low (73 – $230\text{mg m}^{-2}\text{d}^{-1}$) and only slightly above the annual average (70 – $90\text{mg m}^{-2}\text{d}^{-1}$) measured in the state of Brandenburg (Wanner et al., 2015). On the other hand, the total input of Si (as a lithogenic element) from precipitation (wet deposition) is negligible as well ($<1\text{g Si ha}^{-1}\text{yr}^{-1}$, Sommer et al., 2013).

Our results indicate a strong relationship between water-soluble Si and total BSi. In this context, two different causal chains can be discussed: either SiO₂-synthesizing organisms are drivers of the amount of Si(OH)₄ in the soil or – vice versa – the amount of water-soluble Si in the soils is the main driver of SiO₂-synthesizing organisms as biosilicification is limited by Si(OH)₄. Laboratory studies revealed that SiO₂-synthesizing organisms, i.e., testate amoebae, can deplete the amount of Si(OH)₄ in culture media due to biosilicification (Aoki et al., 2007; Wanner et al., 2016). However, Wanner et al. (2016) also showed that culture growth of SiO₂-synthesizing testate amoebae was dependent on Si concentration in the culture media. Furthermore, in situ analyses showed that marine diatom blooms can deplete Si(OH)₄ concentrations in the oceans (Hildebrand, 2008). In forested biogeosystems Puppe et al. (2015) found high individual numbers of SiO₂-synthesizing testate amoebae at study sites with low amounts of Si(OH)₄ and vice versa. However, it is unlikely that testate amoebae depleted amounts of Si(OH)₄ at these sites, because corresponding protozoic Si pools are relatively small compared to phytogenic ones (Puppe et al., 2015; Sommer et al., 2013). Regarding vegetation and corresponding phytogenic Si pools, their influence on the amount of Si(OH)₄ in soils has been shown in several studies (e.g., Bartoli, 1983; Farmer et al., 2005; Sommer et al., 2013). On the other hand, phytolith production is probably more influenced by the phylogenetic position of a plant than by environmental factors like temperature or Si availability (Hodson et al., 2005; Cooke and Leishman, 2012).

From our results and the discussion above we conclude short-term changes in water-soluble Si to be mainly driven by BSi. However, total BSi represents only small proportions of water-soluble Si at t_0 (<2 %) and t_{10} (<4.5 %). From this result a question arises: where does the major part of the increase in water-soluble Si at Chicken Creek come from? We will discuss this question in Sect. 4.2 below.

4.2 Sources of water-soluble Si at Chicken Creek

From former results of BSi analyses in forested biogeosystems, we assumed the phytogenic Si pool to be the most prominent in size. In this context, results of Sommer et al. (2013) and Puppe et al. (2015) showed that phytogenic Si pools in soils of forested biogeosystems were up to several hundred times larger than protozoic Si pools. However, phytogenic Si pools in soils are surprisingly small compared to other BSi pools at Chicken Creek. Our findings can be attributed to at least two factors. Firstly, phytogenic Si is stored in a developing organic litter layer where it is temporarily protected against dissolution, and secondly, the used methods were not able to accurately quantify the total phytogenic Si pool, but only the larger (>5 µm) and more stable part.

Total Si and phytolith contents of litter samples at Chicken Creek did not differentiate from total Si and phytolith contents of plants. This fact indicates that litter decomposition

and related Si release into the subjacent soil are relatively slow processes and we interpret our findings as an indication of a developing compartment of dead plant tissue above the mineral soil surface. Esperschütz et al. (2013) showed in a field experiment in initial soils near Chicken Creek that after 30 weeks only 50 % of the *C. epigejos* litter was degraded, whereby degradation rates were highest in the first 4 weeks. Estimations of biomasses of *C. epigejos* and *P. australis* at Chicken Creek via remote sensing with an unmanned aerial system showed that the relation between phytogenic Si pools of plant biomass and litter biomass are almost the same for both plant species (factor about 1.5, based on the total area of Chicken Creek); i.e., Si in the plants was about one-third higher than in litter (M. Wehrhan, personal communication, 2017). At the sampling points about 1.8 and 2.7 g Si m⁻² were stored in the litter of *C. epigejos* and *P. australis* at t_{10} , respectively, which is in the range of published data for annual Si input through litterfall in a short grass steppe (2.2–2.6 g Si m⁻² yr⁻¹, Blecker et al., 2006).

Altogether, these results clearly underline our interpretation of a developing organic layer where litter accumulates and phytogenic Si is temporarily stored and protected against dissolution. Thus Si release is delayed and biologically controlled, as it can be observed at forested biogeosystems (Sommer et al., 2013). The Si pools in the aboveground biomass of *C. epigejos* (2.6 g Si m⁻²) and *P. australis* (5.0 g Si m⁻²) at Chicken Creek at t_{10} are comparable to reported values of Great Plains grasslands (2.2–6.7 g Si m⁻² in the aboveground biomass) (Blecker et al., 2006) and reach about 30 % (*C. epigejos*) or 59 % (*P. australis*) of published data for a beech forest (8.5 g Si m⁻² in the aboveground biomass of *Fagus sylvatica* trees) in northern Brandenburg, Germany (Sommer et al., 2013), after (only) 10 years of ecosystem development.

Regarding methodological shortcomings of the used phytolith extraction procedure there are several aspects to be discussed. Wilding and Drees (1971), for example, showed that about 72 % of leaf phytoliths of American beech (*Fagus grandifolia*) are smaller than 5 µm. This is in accordance with our findings. Phytoliths >5 µm only amounted to about 16 % of total Si contents of plant materials of *C. epigejos* and *P. australis*; thus about 84 % of phytogenic Si (<5 µm and/or fragile phytogenic Si structures) are not quantified by the used phytolith extraction method. Watteau and Villemin (2001) found even smaller (5–80 nm) spherical grains of pure silica in leaf residues in topsoil samples of a forested biogeosystem. In addition, silica depositions can be found in intercellular spaces or in an extracellular (cuticular) layer (Sangster et al., 2001), whereat no recognizable phytoliths are formed. These structures might be too fragile for preservation in soils and are likely lost to a great extent in the used phytolith extraction procedure due to dissolution. Meunier et al. (2017) analyzed different phytolith morphotypes, e.g. silica bodies originating from cells of the upper epidermis, silica casts of trichomes or parenchyma/collenchyma

cells and of durum wheat plant shoots. They found fragile subcuticular silica plates (2–4 µm thick, up to several hundred micrometers long and wide) to be the second most common phytolith morphotype. This is corroborated by our own findings as the biggest part (about 84 %) of total plant Si is represented by small-scale (<5 µm) and/or fragile phytogenic Si in *C. epigejos* and *P. australis*. If we assume that total Si contents of plants at Chicken Creek are one-to-one reflected by phytogenic Si pools in soils, we can easily calculate these small-scale and fragile pools resulting in about 130 and 100 mg m⁻² (84 % of total, i.e., 156 and 119 mg m⁻², phytogenic Si each) under *C. epigejos* and *P. australis*, respectively. These calculated phytogenic Si pools are about 13 (diatom frustules), 38 (testate amoeba shells) and 45 (sponge spicules) or 3 (diatom frustules) and 10 (testate amoeba shells, sponge spicules) times bigger than the other BSi pools at *C. epigejos* and *P. australis* sampling points. If we further assume an input of this phytogenic Si for at least 7 years (Zaplata et al., 2010) phytogenic Si might be the main driver of short-term changes in water-soluble Si at Chicken Creek. This is supported by relatively high surface-to-volume ratios of bilobate and elongate phytoliths. These ratios are about 3 times higher compared to ratios of other biogenic siliceous structures, i.e., testate amoeba shells, diatom frustules and sponge spicules.

In addition, Si pools represented by single siliceous platelets of testate amoeba shells have to be considered as well, as these platelets can be frequently found in freshwater sediments, for example (Douglas and Smol, 1987; Pienitz et al., 1995). Unfortunately, there is no available information on the quantity of such platelet pools in soils, but it can be assumed that these platelets can be frequently found in soils, as they are used by some testate amoeba genera (e.g., *Schoenbornia*, *Heleopera*) for shell construction (Meisterfeld, 2002; Schönborn et al., 1987). In general, it can be assumed that phytogenic Si structures <5 µm and single testate amoeba platelets (about 3–12 µm in diameter, Douglas and Smol, 1987) are highly reactive due to their relatively high surface-to-volume ratios. However, to the best of our knowledge there is no publication available dealing with corresponding physicochemical analyses or dissolution kinetics of these siliceous structures. In general, experiments with phytoliths (>5 µm) showed that surface areas and related dissolution susceptibilities are, for example, age-related due to changes in specific surface areas and the presence of organic matter bound to the surface of phytoliths (Frayse et al., 2006, 2009).

5 Conclusions

Decadal changes in water-soluble Si at Chicken Creek are mainly driven by BSi; thus Si cycling is already biologically controlled at the very beginning of ecosystem development. In this context, phytogenic Si plays a particularly prominent

role. However, a developing organic layer (L horizon) at the soil surface temporarily protects phytogenic Si against dissolution, because phytogenic Si is still incorporated into plant structural elements (tissues). As a consequence a delaying biogenic Si pool is built up and Si release into the soil is retarded. Furthermore, established phytolith extraction methods alone are not suitable to quantify total phytogenic Si pools, as phytoliths >5 µm seem to be only a minor part of this pool (about 16 % in the current study). In general, information on small-scale (<5 µm) and/or fragile phytogenic Si structures is urgently needed as they seem to represent the biggest and most reactive Si pool in soils and thus are the most important drivers of Si cycling in terrestrial biogeosystems. Future work should focus on (i) the quantification of this pool, (ii) physicochemical analyses of its components and (iii) their dissolution kinetics in lab experiments. The combination of modern microscopical (SEM-EDX, laser scanning microscopy) (this study; Puppe et al., 2016; Sommer et al., 2013) and spectroscopical (FTIR and micro-FTIR spectroscopy) (Liu et al., 2013; Loucaides et al., 2010; Rosén et al., 2010) methods might introduce new insights to this field.

Data availability. All relevant data are presented within the paper. Underlying data can be obtained on request from the corresponding author.

Competing interests. The authors declare that they have no conflict of interest.

Acknowledgements. This study has been financed by the DFG project “Spatiotemporal dynamics of biogenic Si pools in initial soils and their relevance for desilication” (SO 302/7-1). Many thanks to Christian Buhtz and René Ende for their excellent laboratory support. We would like to thank the members of the “Chicken Creek project” at BTU Cottbus-Senftenberg for providing soil samples from 2005 and organizational support. Vattenfall Europe Mining AG provided the research site. This study is a contribution to the Transregional Collaborative Research Centre 38 (SFB/TRR 38) financially supported by the German Research Council (DFG, Bonn) and the Brandenburg Ministry of Science, Research and Culture (MWFK, Potsdam). Last but not least we would like to thank the anonymous reviewers for their very helpful comments on our manuscript.

Edited by: Yakov Kuzyakov

Reviewed by: three anonymous referees

References

Alexandre, A., Meunier, J. D., Colin, F., and Koud, J. M.: Plant impact on the biogeochemical cycle of silicon and related weathering processes, *Geochim. Cosmochim. Ac.* 61, 677–682, 1997.

- Aoki, Y., Hoshino, M., and Matsubara, T.: Silica and testate amoebae in a soil under pine–oak forest, *Geoderma*, 142, 29–35, 2007.
- Barão, L., Clymans, W., Vandevenne, F., Meire, P., Conley, D. J., and Struyf, E.: Pedogenic and biogenic alkaline-extracted silicon distributions along a temperate land-use gradient, *Eur. J. Soil Sci.*, 65, 693–705, 2014.
- Bartoli, F.: The biogeochemical cycle of silicon in two temperate forest ecosystems, *Environ. Biogeochem. Ecol. Bull.*, 35, 469–476, 1983.
- Bartoli, F. and Wilding, L. P.: Dissolution of biogenic opal as a function of its physical and chemical properties, *Soil Sci. Soc. Am. J.*, 44, 873–878, 1980.
- Berner, R. A.: The long-term carbon cycle, fossil fuels and atmospheric composition, *Nature*, 426, 323–326, 2003.
- Biermans, V. and Baert, L.: Selective extraction of the amorphous Al, Fe and Si oxides using an alkaline Tiron solution, *Clay Miner.*, 12, 127–135, 1977.
- Blecker, S. W., McCulley, R. L., Chadwick, O. A., and Kelly, E. F.: Biologic cycling of silica across a grassland bioclimate sequence, *Global Biogeochem. Cy.*, 20, GB3023, <https://doi.org/10.1029/2006GB002690>, 2006.
- Buján, E.: Elemental composition of phytoliths in modern plants (Ericaceae), *Quatern. Int.*, 287, 114–120, 2013.
- Clarke, J.: The occurrence and significance of biogenic opal in the regolith, *Earth-Sci. Rev.*, 60, 175–194, 2003.
- Clymans, W., Struyf, E., Govers, G., Vandevenne, F., and Conley, D. J.: Anthropogenic impact on amorphous silica pools in temperate soils, *Biogeosciences*, 8, 2281–2293, <https://doi.org/10.5194/bg-8-2281-2011>, 2011.
- Conley, D. J., Likens, G. E., Buso, D. C., Saccone, L., Bailey, S. W., and Johnson, C. E.: Deforestation causes increased dissolved silicate losses in the Hubbard Brook Experimental Forest, *Global Change Biol.* 14, 2548–2554, 2008.
- Cooke, J. and Leishman, M. R.: Tradeoffs between foliar silicon and carbon-based defences: evidence from vegetation communities of contrasting soil types, *Oikos*, 121, 2052–2060, 2012.
- Creevy, A. L., Fisher, J., Puppe, D., and Wilkinson, D. M.: Protist diversity on a nature reserve in NW England – with particular reference to their role in soil biogenic silicon pools, *Pedobiologia*, 59, 51–59, 2016.
- DIN ISO 1039: Bodenbeschaffenheit: Bestimmung des pH-Wertes, Deutsches Institut für Normung, Beuth, Berlin, 1997.
- Douglas, M. S. and Smol, J. P.: Siliceous protozoan plates in lake sediments, *Hydrobiologia*, 154, 13–23, 1987.
- Dürr, H. H., Meybeck, M., Hartmann, J., Laruelle, G. G., and Roubeix, V.: Global spatial distribution of natural riverine silica inputs to the coastal zone, *Biogeosciences*, 8, 597–620, <https://doi.org/10.5194/bg-8-597-2011>, 2011.
- Ehrlich, H., Demadis, K. D., Pokrovsky, O. S., and Koutsoukos, P. G.: Modern views on desilicification: biosilica and abiotic silica dissolution in natural and artificial environments, *Chem. Rev.*, 110, 4656–4689, 2010.
- Epstein, E.: Silicon: its manifold roles in plants, *Ann. Appl. Biol.* 155, 155–160, 2009.
- Esperschütz, J., Zimmermann, C., Dümig, A., Welzl, G., Buegger, F., Elmer, M., Munch, J. C., and Schloter, M.: Dynamics of microbial communities during decomposition of litter from pioneering plants in initial soil ecosystems, *Biogeosciences*, 10, 5115–5124, <https://doi.org/10.5194/bg-10-5115-2013>, 2013.
- Farmer, V. C., Delbos, E., and Miller, J. D.: The role of phytolith formation and dissolution in controlling concentrations of silica in soil solutions and streams, *Geoderma*, 127, 71–79, 2005.
- Fraysse, F., Pokrovsky, O. S., Schott, J., and Meunier, J. D.: Surface properties, solubility and dissolution kinetics of bamboo phytoliths, *Geochim. Cosmochim. Ac.*, 70, 1939–1951, 2006.
- Fraysse, F., Pokrovsky, O. S., Schott, J., and Meunier, J. D.: Surface chemistry and reactivity of plant phytoliths in aqueous solutions, *Chem. Geol.*, 258, 197–206, 2009.
- Frings, P. J., Clymans, W., Jeppesen, E., Lauridsen, T. L., Struyf, E., and Conley, D. J.: Lack of steady-state in the global biogeochemical Si cycle: emerging evidence from lake Si sequestration, *Biogeochemistry*, 117, 255–277, 2014.
- Gerwin, W., Schaaf, W., Biemelt, D., Fischer, A., Winter, S., and Hüttl, R. F.: The artificial catchment ‘Chicken Creek’ (Lusatia, Germany) – A landscape laboratory for interdisciplinary studies of initial ecosystem development, *Ecol. Eng.*, 35, 1786–1796, 2009.
- Gerwin, W., Schaaf, W., Biemelt, D., Elmer, M., Maurer, T., and Schneider, A.: The Artificial catchment ‘Hühnerwasser’ (Chicken Creek): construction and initial properties, in: *Ecosystem Development I*, edited by: Hüttl, R. F., Schaaf, W., Biemelt, D., and Gerwin, W., Brandenburg University of Technology Cottbus–Senftenberg, Germany, 1–58, 2010.
- Hildebrand, M.: Diatoms, biomineralization processes, and genomics, *Chem. Rev.*, 108, 4855–4874, 2008.
- Hodson, M. J., White, P. J., Mead, A., and Broadley, M. R.: Phylogenetic variation in the silicon composition of plants, *Ann. Bot. London*, 96, 1027–1046, 2005.
- Keller, C., Guntzer, F., Barboni, D., Labreuche, J., and Meunier, J. D.: Impact of agriculture on the Si biogeochemical cycle: input from phytolith studies, *C. R. Geosci.*, 344, 739–746, 2012.
- Kendrick, K. J. and Graham, R. C.: Pedogenic silica accumulation in chronosequence soils, Southern California, *Soil Sci. Soc. Am. J.*, 68, 1295–1303, 2004.
- Kendzia, G., Reißmann, R., and Neumann, T.: Targeted development of wetland habitats for nature conservation fed by natural inflow in the post-mining landscape of Lusatia, *World Min.*, 60, 88–95, 2008.
- Kodama, H. and Ross, G. J.: Tiron dissolution method used to remove and characterize inorganic components in soils, *Soil Sci. Soc. Am. J.*, 55, 1180–1187, 1991.
- Liu, X., Colman, S. M., Brown, E. T., Minor, E. C., and Li, H.: Estimation of carbonate, total organic carbon, and biogenic silica content by FTIR and XRF techniques in lacustrine sediments, *J. Paleolimnol.* 50, 387–398, 2013.
- Loucaides, S., Behrends, T., and Van Cappellen, P.: Reactivity of biogenic silica: Surface versus bulk charge density, *Geochim. Cosmochim. Ac.* 74, 517–530, 2010.
- Ma, J. F. and Yamaji, N.: Functions and transport of silicon in plants, *Cell. Mol. Life Sci.*, 65, 3049–3057, 2008.
- McKeague, J. A. and Cline, M. G.: Silica in soil solutions I. The form and concentration of dissolved silica in aqueous extracts of some soils, *Can. J. Soil Sci.*, 43, 70–82, 1963.
- Meisterfeld, R.: Order Arcellinida Kent, 1880, in: *The illustrated guide to the Protozoa*, edited by: Lee, J. J., Leedale, G. F., and Bradbury, P., 827–860, Society of Protozoologists, Lawrence, KS, USA, 2002.

- Meunier, J. D., Colin, F., and Alarcon, C.: Biogenic silica storage in soils, *Geology*, 27, 835–838, 1999.
- Meunier, J. D., Barboni, D., Anwar-ul-Haq, M., Levard, C., Chau-rand, P., Vidal, V., Grauby, O., Huc, R., Laffont-Schwob, I., Rabier, J., and Keller, C.: Effect of phytoliths for mitigating water stress in durum wheat, *New Phytol.*, 215, 229–239, <https://doi.org/10.1111/nph.14554>, 2017.
- Mortlock, R. A. and Froelich, P. N.: A simple method for the rapid determination of biogenic opal in pelagic marine sediments, *Deep-Sea Res.*, 36, 1415–1426, 1989.
- Pienitz, R., Douglas, M. S., Smol, J. P., Huttunen, P., and Meriläinen, J.: Diatom, chrysophyte and protozoan distributions along a latitudinal transect in Fennoscandia, *Ecography*, 18, 429–439, 1995.
- Puppe, D., Kaczorek, D., Wanner, M., and Sommer, M.: Dynamics and drivers of the protozoic Si pool along a 10-year chronosequence of initial ecosystem states, *Ecol. Eng.*, 70, 477–482, 2014.
- Puppe, D., Ehrmann, O., Kaczorek, D., Wanner, M., and Sommer, M.: The protozoic Si pool in temperate forest ecosystems – Quantification, abiotic controls and interactions with earthworms, *Geoderma*, 243–244, 196–204, 2015.
- Puppe, D., Höhn, A., Kaczorek, D., Wanner, M., and Sommer, M.: As Time Goes By – Spatiotemporal Changes of Biogenic Si Pools in Initial Soils of an Artificial Catchment in NE Germany, *Appl. Soil Ecol.*, 105, 9–16, 2016.
- Rosén, P., Vogel, H., Cunningham, L., Reuss, N., Conley, D. J., and Persson, P.: Fourier transform infrared spectroscopy, a new method for rapid determination of total organic and inorganic carbon and biogenic silica concentration in lake sediments, *J. Paleolimnol.*, 43, 247–259, 2010.
- Russell, D. J., Hohberg, K., and Elmer, M.: Primary colonisation of newly formed soils by actinedid mites, *Soil Org.* 82, 237–251, 2010.
- Saccone, L., Conley, D. J., Likens, G. E., Bailey, S. W., Buso, D. C., and Johnson, C. E.: Factors that control the range and variability of amorphous silica in soils in the Hubbard Brook Experimental Forest, *Soil Sci. Soc. Am. J.*, 72, 1637–1644, 2008.
- Sangster, A. G.: Anatomical features and silica depositional patterns in the rhizomes of the grasses *Sorghastrum nutans* and *Phragmites australis*, *Can. J. Botany*, 61, 752–761, 1983.
- Sangster, A. G., Hodson, M. J., and Tubb, H. J.: Silicon deposition in higher plants, 85–113, in: *Silicon in agriculture* (Vol. 8), edited by: Datnoff, L. E., Snyder, G. H., and Korndörfer, G. H., Elsevier, Amsterdam, The Netherlands, 2001.
- Sauer, D., Saccone, L., Conley, D. J., Herrmann, L., and Sommer, M.: Review of methodologies for extracting plant-available and amorphous Si from soils and aquatic sediments, *Biogeochemistry*, 80, 89–108, 2006.
- Schaaf, W., Biemelt, D., and Hüttl, R. F.: Initial development of the artificial catchment ‘Chicken Creek’ – monitoring program and survey 2005–2008. *Ecosystem Development 2*, edited by: Hüttl, R. F., Schaaf, W., Biemelt, D., and Gerwin, W., 194 pp., 2010.
- Schachtschabel, P. and Heinemann, C. G.: Wasserlösliche Kieselsäure in Lössböden, *Z. Pflanzenern. Bodenkd.*, 118, 22–35, 1967.
- Schlichting, E., Blume, H. P., and Stahr, K.: *Soils Practical*, Blackwell, Berlin, Wien, Germany, Austria, 295 pp., 1995.
- Schneider, A., Gerke, H. H., Maurer, T., and Nenov, R.: Initial hydro-geomorphic development and rill network evolution in an artificial catchment, *Earth Surf. Proc. Land.*, 38, 1496–1512, 2013.
- Schönborn, W., Petz, W., Wanner, M., and Foissner, W.: Observations on the Morphology and Ecology of the Soil-Inhabiting Testate Amoeba *Schoenbornia humicola* (Schönborn, 1964) De-cloitre, 1964 (Protozoa, Rhizopoda), *Arch. Protistenkd.*, 134, 315–330, 1987.
- Sommer, M., Kaczorek, D., Kuzyakov, Y., and Breuer, J.: Silicon pools and fluxes in soils and landscapes – a review, *J. Plant Nutr. Soil Sci.*, 169, 310–329, 2006.
- Sommer, M., Jochheim, H., Höhn, A., Breuer, J., Zagorski, Z., Busse, J., Barkusky, D., Meier, K., Puppe, D., Wanner, M., and Kaczorek, D.: Si cycling in a forest biogeosystem – the importance of transient state biogenic Si pools, *Biogeosciences*, 10, 4991–5007, <https://doi.org/10.5194/bg-10-4991-2013>, 2013.
- Song, Z., Wang, H., Strong, P. J., Li, Z., and Jiang, P.: Plant impact on the coupled terrestrial biogeochemical cycles of silicon and carbon: implications for biogeochemical carbon sequestration, *Earth-Sci. Rev.*, 115, 319–331, 2012.
- Street-Perrott, F. A., and Barker, P. A.: Biogenic silica: a neglected component of the coupled global continental biogeochemical cycles of carbon and silicon, *Earth Surf. Proc. Land.* 33, 1436–1457, 2008.
- Struyf, E. and Conley, D. J.: Emerging understanding of the ecosystem silica filter, *Biogeochemistry*, 107, 9–18, 2012.
- Struyf, E., Smis, A., Van Damme, S., Garnier, J., Govers, G., Van Wesemael, B., Conley, D. J., Batelaan, O., Frot, E., Clymans, W., Vandevenne, F., Lancelot, C., Goos, P., and Meire, P.: Historical land use change has lowered terrestrial silica mobilization, *Nat. Commun.* 1, 129, <https://doi.org/10.1038/ncomms1128>, 2010.
- Tréguer, P. J. and De La Rocha, C. L.: The world ocean silica cycle, *Ann. Rev. Mar. Sci.*, 5, 477–501, 2013.
- Tréguer, P. and Pondaven, P.: Global change: silica control of carbon dioxide, *Nature*, 406, 358–359, 2000.
- Vandevenne, F. I., Barão, L., Ronchi, B., Govers, G., Meire, P., Kelly, E. F., and Struyf, E.: Silicon pools in human impacted soils of temperate zones, *Global Biogeochem. Cy.*, 29, 1439–1450, 2015.
- Wanner, M. and Elmer, M.: “Hot spots” on a new soil surface – how do testate amoebae settle down?, *Acta Protozool.*, 48, 281–289, 2009.
- Wanner, M., Elmer, M., Sommer, M., Funk, R., and Puppe, D.: Testate amoebae colonizing a newly exposed land surface are of airborne origin, *Ecol. Indic.*, 48, 55–62, 2015.
- Wanner, M., Seidl-Lampa, B., Höhn, A., Puppe, D., Meisterfeld, R., and Sommer, M.: Culture growth of testate amoebae under different silicon concentrations, *Eur. J. Protistol.*, 56, 171–179, 2016.
- Watteau, F. and Villemin, G.: Ultrastructural study of the biogeochemical cycle of silicon in the soil and litter of a temperate forest, *Eur. J. Soil Sci.*, 52, 385–396, 2001.
- Wilding, L. P. and Drees, L. R.: Biogenic opal in Ohio soils, *Soil Sci. Soc. Am. J.*, 35, 1004–1010, 1971.
- Zaplata, M. K., Fischer, A., and Winter, S.: Vegetation dynamics, in: *Ecosystem development 2*, edited by: Schaaf, W., Biemelt, D., Hüttl, R. F., Brandenburg University of Technology Cottbus-Senftenberg, Germany, 2010.